UNIVERSITY OF VENDA
SCHOOL OF ENVIRONMENTAL SCIENCES
DEPARTMENT OF MINING AND ENVIRONMENTAL GEOLOGY

MASTERS RESEARCH

VARIATION OF THE COAL STRATIGRAPHY AND CHARACTERISATION OF THE SOUTPANSBERG COALFIELD, LIMPOPO PROVINCE, SOUTH AFRICA

BY
MAWILA EDITH ELIZABETH TINTSWALO
STUDENT NO: 11550595

A DISSERTATION SUBMITTED TO THE DEPARTMENT OF MINING AND ENVIRONMENTAL GEOLOGY, SCHOOL OF ENVIRONMENTAL SCIENCES, UNIVERSITY OF VENDA, IN FULFILMENT OF THE REQUIREMENTS FOR THE DEGREE OF MASTER OF EARTH SCIENCES IN MINING AND ENVIRONMENTAL GEOLOGY

SUPERVISOR: PROF. J.S. OGOLA
DEPARTMENT OF MINING AND ENVIRONMENTAL GEOLOGY
UNIVERSITY OF VENDA

C0-SUPERVISOR: DR. J.K. KIRUI
DEPARTMENT OF PHYSICS
SCHOOL OF MATHEMATICS AND NATURAL SCIENCE

MARCH 2019

DEDICATION

This research is dedicated to my children Farai and Farianne Phiri, I am grateful and blessed for your being on this earth as this has propelled my determination and passion for academic studies and completion of this research.

Thank you my kids and you're dearly loved.

DECLARATION

I Edith Elizabeth Tintswalo Mawila, student No: 11550595, hereby declare that this Dissertation for Master of Earth Sciences in Mining and Environmental Geology (MESMEG) Degree at the University of Venda, submitted by me has not been previously submitted at this or any other institution of higher learning, that this is my own work in design and execution, and that all reference material contained herein have been duly acknowledged

Signature (Student) **Date**

…….. …….

Signature (Supervisor) **Date**

…….. ……..

Signature (Co-Supervisor) **Date**

…… ……

ACKNOWLEDGEMENT

First of all I would like to thank the Almighty God for blessing me with the ability, perseverance and wisdom to undertake this research to its completion. Thank you Heavenly Father for the gift of life and for favouring me.

Professor J. S. Ogola thank you for being the fountain of knowledge and wisdom, for being the kind academic father that strives for perfection in everything I touch and produce. Your positive criticism, support and encouragement whenever I lose hope never goes unnoticed. Dr. Kirui you not only the co-supervisor but a father too who boost my morale when the academic space feels congested. Your support, determinism and wisdom had paved the way for me to work against my difficult odds and failures. Thank you Prof. Ogola and Dr. Kirui for walking this path with me, I have not only completed my research but I have gathered an ocean of knowledge and practical experience.

Dr. John Sparrow, and the Coal of Africa team (Mulalo, Spinner and the rest) thank you for welcoming me with open arms to your premises, making this research to have a foundation to start from. I am highly indebted to your kindness, generosity and warmth throughout my period of undertaking this research project. I would also like to thank my sponsors Eskom (Gas Emission Funds) and Merseta for lifting the financial burden from me. Your funds have greatly assisted me in many ways and made this journey memorable and less stressful.

Dr. Kataka, I am grateful that you were my mentor, your positive energy, straight talk, outlook on matters and wisdom has shaped me to be a creative hard core decision making woman, and very enthusiastic about the prospects of academic life. Dr. Dacosta and the MEG Department (Mr Mhlongo, Mr Muzerengi, Mr Mahlaule, Mr Nengovhela, Ms. Mundalamo and Ms. Rembuluwane), thank you for the support and guidance throughout my postgraduate journey at the University of Venda, your warmth and kindness is highly appreciated.

Dearest Mom and Dad thank you for your countless sacrifices, your unconditional love and for fuelling my energy and positivity to tackle anything brought before me. I thank you for not giving up on me and for being humble people. My siblings (Franklin, Priscilla, Gail and Louis Mawila) thank you for walking this journey with me your presence has channelled my hunger to always succeed. Mr Nemapate I thank you for being a ray of sunlight reminding me of life with laughter whenever things got difficult and unbearable.

Thank you my wonderful children Farai and Farianne Phiri for always making me smile, for understanding my absence from home when taking this academic path, I hope one day you will read this research and understand why I spent so much time away. My loving partner Allen Phiri, thank you for nourishing my mind and soul with love and support, making me to beam with love whenever your name comes to mind. I thank you for the life prospects, warmth and blessings we share together during our trying and happy times. Your positive life approach has instilled a lot of courage and determination in my life to conquer and enjoy life. Lastly to everyone who has contributed positively to this journey, I say thank you from the bottom of heart and cheers to many more beautiful academic journeys.

ABSTRACT

The future of energy in South Africa depends on coal as it is one of the cheapest and most affordable sources of energy; however, some of the coal is uneconomical to mine due to the thickness and depth of the coal seams. For many years the coal resources of the Soutpansberg Coalfield remained untapped and limitedly researched and with the coal resources running out in the other coalfields, the Soutpansberg Coalfield remained the bright coalfield of tomorrow in South Africa. Coal seams in the Soutpansberg Coalfield occur within the Madzaringwe Formation. Three coal basins have been identified in this coalfield, are the Venda-Pafuri, Tshipise and Mopane.

Sedimentological basin analysis of the coal stratigraphy and characterisation of the Soutpansberg Coalfield in the Makhado area, Limpopo Province was investigated within the farms of Rissik, Fannie, Duel, and Lurkin. The main purpose of the study was to establish the variation of the coal stratigraphy and how coal influenced the stratigraphy within the area.

Fieldwork involved core logging and core sampling from the different farms within the Makhado coal area, while laboratory work included petrographic studies, investigation of the physical and chemical properties of coal. Core logging revealed the occurrence of coal zones where coal seams were intercalating with mudstones, but rarely with siltstone that formed the footwall of coal. Rarely was coal intruded by dolerite dyke as was the case along borehole W6610001. Core logging further revealed the sedimentary structures in the lithologies and the depth at which different lithologies were intersected. From these sedimentary structures, the environment of coal deposition was deduced supported by the geochemical analysis of major oxides and trace elements. Correlation of boreholes along the strike showed that the shale and mudrock were the predominant rocks within the coal horizon leading to the conclusion that these were the coal host rocks.

Whole rock geochemical analysis was undertaken, using X-Ray Fluorescence Spectroscopy in order to establish the rock types and their trace element contents. The collected samples were analysed at the University of Venda, Department of Mining and Environmental Geology Laboratory, Siza Coal Services in Secunda and Council for Geoscience.

The study indicated that the coal seams of the Soutpansberg Coalfield were deposited within the floodplain of a mixed-load fluvio-deltaic (fluvial and braided) systems. This sedimentary channel has been the major influence on the development of the coal seams. Locational changes in sedimentary facies above and below the coal seams within the study area has caused variations in the rates of compaction and subsidence which influenced the coal basin morphology and the coalification pattern. These two parameters (variations in the rates of compaction and subsidence) controlled the coal quality parameters, and coal seam thickness as well as the coal composition.

The study confirmed that coal quality and thickness vary markedly from place to place in this coalfield due to varying local depositional environments. Most of the drill holes intersected mainly 3 coal seams, although in some cases either 2 or 5 seams were intersected. The thickest coal seam (borehole F578002) was 8 m.

It was concluded that the coal was sub-bituminous to bituminous coal rank class (medium-volatile bituminous coal rank class). The coal had low moisture content ranging from 0.7-0.8%, and ash content ranging from 21.4-32%. The fixed carbon and volatile matter values of the coal samples ranged from 42.5 to 50.4% and from 25.2 to 27.4% respectively. The carbon and hydrogen were the main principal combustible elements in coal, however; carbon is the predominant one based on weight, constituting about 5.3% (the lowest) to 70.3% (highest) of the total. Due to the nature and thickness of the coal seams we conclude that this coal was economical to be mined and can be used for electricity generation and in cement grinding plants.

A graph of coal gas concentrations over combustion time showed that methane (CH_4) and carbon dioxide (CO_2) had high gas concentrations, amounting to 1.75% and 1.70% respectively.

Keywords: local variation, Soutpansberg Coalfield, coal stratigraphy, Makhado coal area, coal quality.

TABLE OF CONTENT

CHAPTER 1: INTRODUCTION

CHAPTER 2: LITERATURE REVIEW

CHAPTER 3: MATERIALS AND METHODS

CHAPTER 4: DATA ANALYSIS AND INTERPRETATION

CHAPTER 5: DISCUSSION, CONCLUSIONS AND RECOMMENDATIONS

LIST OF FIGURES

LIST OF PLATES

LIST OF TABLES

LIST OF ACRONYMS

AIDS	Acquired Immunodeficiency Syndrome
ASTM	American Society for Testing Materials
CBM	Coal Bed Methane
EoH	End of Hole
GC	Gas Chromatography
GPS	Global Positioning System
HIV	Human Immunodeficiency Virus
IPCC	Intergovernmental Panel on Climate Change
ITB	Interburden
SACS	South African Committee for Stratigraphy
USCOR	United States Office of Coal Research
XRF	X-Ray Fluorescence Spectroscopy
OVB	Overburden
WHO	World Health Organisation
UNFCCC	United Nations Framework Convention on Climate Change
PPM	Parts Per Million
MEG	Mining Environmental Geology

GLOSSARY

The definitions below were extracted from the book called Glossary of Geology by Neuendorf (2005):

Coalfield is a region in which coal deposits of known or possible economic value occur and may be mined.

Coal Basin is a coalfield with a basinal structure for example the Carboniferous coal

Coal Sub-Basin is a structural geologic feature where a larger coal basin is divided into a series of small basins with intervening intrabasinal highs

Coal Seam is the stratum or bed of coal

Coal Classification is the analysis or grouping of coals according to a particular property, such as the degree of metamorphism (rank), constituent plant material (type) or degree of impurity (grade). It can be further defined as the grouping or analysis of coal according to the percentage of volatile matter and coking properties.

CHAPTER 1: INTRODUCTION

1.1 **Background**

South Africa has approximately 242 billion tons in-situ coal resources and reserves that are deemed to be recoverable (Wagner and Hlatshwayo, 2005). Globally it is ranked as the 6th largest coal producer in the world, and 5th largest exporter of coal. Coal basins in South Africa are located within the Karoo Basin. However, 25% of this coal is uneconomical to mine by means of conventional mining methods due to the depth of the coal seams (Feris, 2015).

The Main Karoo Basin is a retroarc foreland basin which formed north of the Cape Fold Belt and is part of a series of other Gondwana basins which formed between the late Palaeozoic era to early Mesozoic era (Catuneanu *et al*., 2005). The basin was bound to the north by the Cargonian Highlands and to the south by the Cape Fold Belt (Isbell *et al*., 2008). The sedimentary sequence which fills the Main Karoo Basin is known as the Karoo Supergroup and is split into four main groups; Dwyka, Ecca, Beaufort, Stormberg, which were deposited over a period of approximately 120 million years from the late Carboniferous period to the middle Jurassic period and terminated with the eruption of the Drakensburg basaltic lavas.

The Karoo Supergroup rocks host the most important natural resources dominated by coal, including coalbed methane natural gas, in addition to clay and groundwater resources. It is without doubt that the Main Karoo basin holds great potential as a major contributor to build the South African economy anchored on mineral resources (Williamson, 1996; Modie, 2008). Coal in South Africa acts as a primary source of energy for homes and industry, as well as being the feedstock for the production of substantial percentage of the country's liquid coal fuels. It is mined with varying degrees of sophistication, from local individuals to some of the world's largest opencast and underground collieries (Cairncross, 2001).

The Karoo Supergroup of South Africa represents a fairly complete stratigraphic section of the Upper Palaeozoic and Lower Mesozoic sedimentary rocks and for this reason it has been studied extensively for various purposes. Many of the coalfields in South Africa have been extensively explored and exploited, however, those in the

north of the country, in Limpopo Province of South Africa, have until recently received much less attention, and Sparrow (2012) referred to them as the forgotten basins.

Four coalfields occur partly or wholly within the Limpopo Province of South Africa and they may contain about 70% of the country's remaining coal resources (Sparrow, 2012). These coalfields, namely; the Waterberg, Springbok Flats, Tuli and Soutpansberg, have been the focus of recent exploration due to the presence of large coking and thermal coal resources, including their potential for coalbed methane. Thus these resources need to be unlocked with regards to creating maximum benefit and environmental protection (Hancox and Goetz, 2014).

The nature of coal deposits in the Soutpansberg Coalfield gradually changes from a multi-seam coal mudstone association, which is about 40 m thick in the west and comprising up to 7 discrete coal seams. This is evident in the Mopane Coal basin in the Waterpoort area. Two individual seams in the east (Pafuri Coal basin in the Tshikondeni area), have a 3 m thick upper seam and a 2 m thick lower seam that is approximately 100 m deep. The transition from multi-seam to discrete is quite sudden and adjacent to the farm Gaandrik 162MT, with argillaceous rocks that occur to the west and arenaceous lithologies to the east of the coalfields (Sparrow, pers. Comm., 2012).

Jurassic aged igneous intrusions (dykes and sills) are common, being associated with volcanism in the Main Karoo Basin (Cadle *et al*., 1993). These intrusions caused local metamorphism in the northern part of the basin, producing meta-anthracites and might have been responsible for destroying oil and gas deposits in the south (Cadle *et al*., 1993; Wheeler, 2015).

Coal from Limpopo (Tuli) coalfields has never been utilized in any application except during bulk testing carried out by Anglo American during 1970 when a prospecting shaft was sunk. The results from these tests indicate that the quality of the washed product is high and there is potential for this washed coal to be a good blend coking coal. The coal has high ash content (Barker, 1999; Jeffrey, 2005).

Coalfields have been thoroughly explored in South Africa except for the Soutpansberg Coalfield and for this reason, the focus has shifted to the Soutpansberg coalfield due to recent exploration and the presence of large coal resources. Furthermore, the

characteristics of coal in the Soutpansberg coalfield have not been determined and evaluated, hence this study is aimed at evaluating the variation of coal stratigraphy in the eastern side of the Limpopo Coal Basin, and to determine the characteristic features of such coal resources to warrant future exploitation.

1.2 **Study Area**

1.2.1 **Location**

The study area is located in the Vhembe District, Limpopo Province of South Africa (Fig. 1.1). Limpopo is South Africa's northernmost province, lying within the great curve of the Limpopo River. This Province borders the North West province, Gauteng and Mpumalanga provinces, as well as Botswana to the west, Zimbabwe to the north and Mozambique to the east. The Soutpansberg Coalfield is situated northeast direction of Musina and has a strike length that extends for approximately 80 km.

The Soutpansberg together with the Tuli coalfields are situated to the Northern part of South Africa. The former comprises Pafuri, Tshipise and Mopani coal basins (Fig. 1.1).

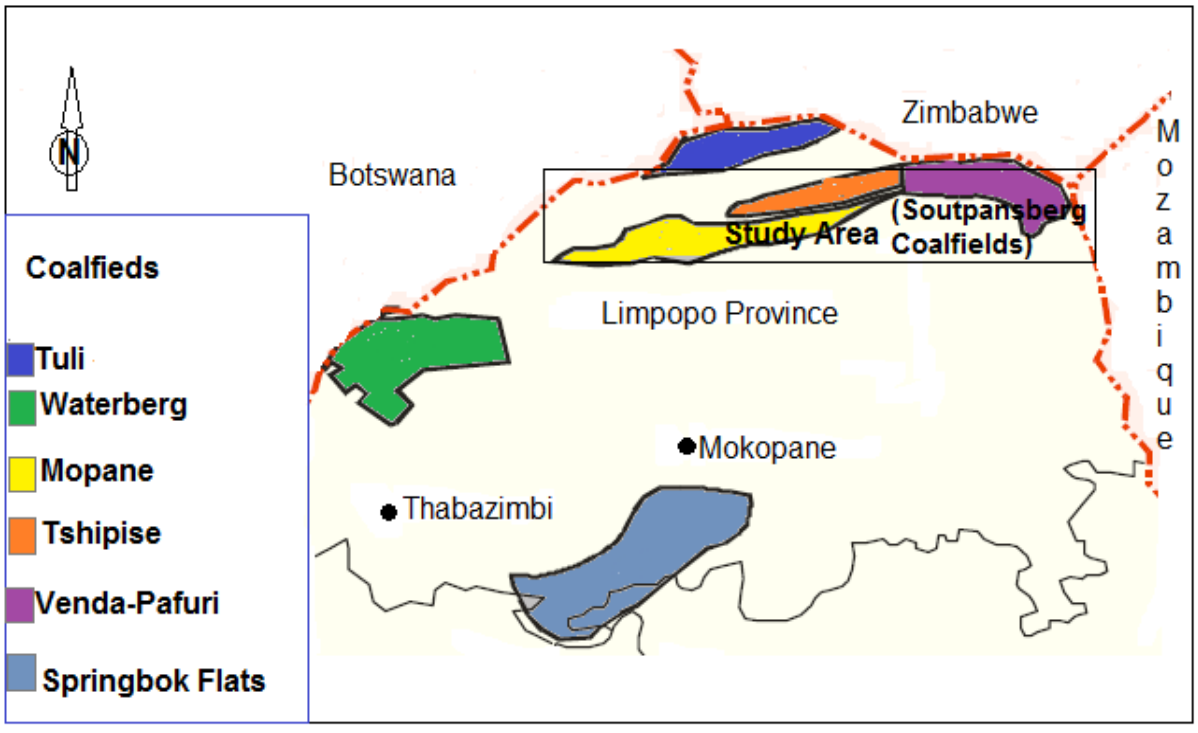

Figure 1.1: Map showing the location of the study area, the Soutpansberg Coalfields in South Africa (Eberhard, 2011).

1.2.2 **Climate**

The Limpopo Province is characterised by summer rainfall. The northern and eastern areas are sub-tropical with hot and humid summers, and mist in the mountains. Winter is mild and mostly frost-free. The province has two distinct climatic regions: the lowveld region, middle and highveld are characterised by a semi-arid climate, while the escarpment experiences sub-humid climate (South African Weather Service, 2008).

In summer the Province can get quite hot with average temperatures of 27^0C, while in winter it is about 20^0C. The bulk of the precipitation occurs in summer and annual rainfall ranges between 400-600 mm over most of the province.

1.2.3 **Topography and Drainage**

The Limpopo Province can be split into several topographic zones. In the east the topography is flat to gently undulating lowveld plain, at an altitude of 300 to 600 m, bounded in the west by the Northern Drakensberg escarpment and Soutpansberg, with steep slopes and peaks up to 2000 m (Naledzani, 1992; Tshikhudo, 2005).

The almost level Springbok Flats in the south lie at an altitude of 900 m, while the Waterberg and Blouberg to the north, with undulating to very steep terrain, reach 2000 m. The north-western zone is a flat to undulating plain, which slopes down to the north and west at 800 to 1000 m.

The Limpopo Province is drained by two main rivers, namely; Mokolo running north-south, and the Limpopo River running roughly south/west-north. Both rivers can be classified as non-perennial. The Limpopo River is an international water course within which drains Botswana, South Africa, Zimbabwe and Mozambique. There are other small rivers in Limpopo Province (Tshikhudo, 2005).

1.2.4 **Soil and Vegetation**

The study area is covered predominately by sandy soils, but shallow, stony soils are found on the higher-lying areas and the clayey soils occur in the valleys. There is a direct relationship between the soil and type of vegetation that grows in the area. The area is situated in a dry savannah region, characterised by open grasslands with scattered trees (generally known as Bushveld) and bushes (Tshikhudo, 2005).

1.3 **Problem Statement**

Previous work has been done on Limpopo Coalfields. However, the coal characteristics and the variation of the coal stratigraphy in the Soutpansberg coalfield has not been established. This left knowledge gaps that are crucial for the evaluation of coal within the coalfields for future exploitation.

1.4 **Justification**

- The Soutpansberg Coalfield had in the past received less attention in terms of research and exploration when compared to other coalfields in South Africa, hence Sparrow (2012) has referred to them as the forgotten basins.
- With the Mpumalanga and Kwazulu Natal Coals nearing depletion, much focus has been shifted to the Springbok Flats and Waterberg Coalfields for exploitation and production, and this is currently taking place in these coalfields.
- With the growing need for power supply and liquid fuels in South Africa, the demand for coal has increased; accordingly the focus has shifted to the Soutpansberg Coalfield for exploration.
- Variations in the coal stratigraphy due to geological factors have not been investigated hence this research will provide an understanding of the regional setting and depositional environment of coal within the Soutpansberg Coalfield.

This research will also help in determining the coal rank along with the variation of the coal stratigraphy.

1.5 **Research Questions**

- What influences the variation of coal stratigraphy in the Soutpansberg Coalfield?
- What is the coal depositional environments?
- What are the petrological characteristics of coal and how do they assist in determination of depositional environments?
- What is the relationship between the host rock and depositional environment?
- What are the coal characteristics of the Soutpansberg coal?

1.6 **Objectives**

The main objective of this study was to determine the variation of coal stratigraphy and coal characteristics in the Soutpansberg Coalfield.

Specific Objectives were to:

a) Investigate the coal depositional environment

This was achieved through studying the sedimentary facies and lithological features along boreholes through core logging, sampling and analysis. Characterization comprised petrographic study and whole rock geochemical analysis, using X-Ray Fluorescence Spectrometry.

b) Determine the coalbed stratigraphy

This objective was achieved through detailed core logging, correlation of core logs and petrographic study of the lithologies.

c) Establish coal-bearing rocks

This was achieved by core logging, whole rock geochemical analysis and by analysis of major oxides and associated trace elements

d) Establish the physical and chemical properties of coal

This was achieved through the physical and chemical analysis of coal using gas chromatography and x-ray diffractometry.

CHAPTER 2: LITERATURE REVIEW

2.1 **Main Karoo Basin**

South Africa has one major sedimentary basin, the Karoo Basin that contains thick, organic-rich shales (Fig. 2.1). The basin is large, extending across nearly two-thirds of the country, with the southern portion of the basin potentially favourable for shale gas. At the same time, the basin contains significant areas of igneous intrusions that apparently impact on the quality of shale resources, limit the use of seismic imaging, and increase the risks of shale exploration (Aarnes *et al*., 2010; and Du Plessis, 2008).

The Main Karoo Basin covers more than 50% of the surface of South Africa, and can be sub-divided into the Dwyka, Ecca and Beaufort Groups (Fig. 2.1). The layers overlying the Beaufort Group can further be sub-divided into the Molteno, Elliot and Clarens Formations which are in turn overlain by the Drakensberg Basalts (Johnson *et al*., 1996).

In Limpopo Province, the Karoo-aged rocks occur mainly in two areas, namely; the Tuli and Tshipise Basins with minor outliers between them. The basal Karoo sediments in the Tuli Basin, known as the Tshidzi Formation (Dwyka Group equivalent), consists of angular blocks and fragments derived mainly from much older underlying strata imbedded in coarse sand and grit (Brandl, 2002). These diamictite deposits are overlain by channel deposits in the form of coarse reddish micaceous grits which pass upward into laminated shale of the Madzaringwe Formation (Ecca Group equivalent).

The Karoo Supergroup is world famous for its terrestrial vertebrate fossils, distinctive plant assemblages, thick glacial deposits and extensive flood basalts with their associated dolerite dykes and sills (Brandl, 2002). The Karoo Supergroup ranges in age from late Carboniferous to Middle Jurassic periods and attains a total cumulative thickness of approximately 12 km in the south-eastern portion of the Main Karoo Basin towards the eastern end of the Karoo Trough (Johnson *et al*., 2006). The bulk of the Karoo strata occur in the main basin, which covers an area of approximately 700 000 km² but was much more extensive during the Permian periods. Significant deposits are also present in the smaller Springbok Flats, Ellisras, Tshipise and Tuli Basins to the north of the Main Basin, while an easterly dipping monoclonal downwarp

has resulted in the preservation of a narrow strip of Karoo rocks in a linear belt along the eastern margin of South Africa.

2.2 Geology of the Coalfields

2.2.1 Geology of the Soutpansberg

The Soutpansberg Coalfield is situated to the north of the Soutpansberg Mountain Range in Limpopo Province and forms part of the Tshipise Basin. Rocks that fall into this group of the Limpopo Province occupy a wedge-shaped mountainous area that extends from the Kruger National Park in the east to the Blouberg in the west and towards the north the rocks pinch-out against a fault (SACS, 1980).

According to Sparrow (2012), the Soutpansberg is sometimes referred to as the forgotten basin with only one active colliery, the Tshipise mine, which has now closed down. It had become the focus of significant exploration for both thermal and coking coal as well as for coalbed methane (CBM). The coal bearing strata in the Soutpansberg Coalfield are inconsistently developed with coal occurrences being that of typical bright coal/ carbonaceous mudstone associations, forming composite coal zones.

The coalfield is characterised by intensive faulting with the result that the original depositional basin has been sliced up into a number of discrete structural blocks, the tendency of coal quality and thickness vary markedly from place to place in this coalfield due to varying local depositional environments (Brandl, 2002).

Brandl and McCourt (1980) recognised that the location and shape of the Soutpansberg Coalfield were controlled by east-northwest and west-southwest orientated faults that follow the trend of the Limpopo Mobile Belt. The coal bearing Karoo Supergroup rocks dip between 3° and 20° northwards, terminating against east-west trending strike faults on the northern margin (Brandl, 1981).

Visser (1989) noted that the rocks are jointed, a feature related to the intrusion of dolerite dykes and sills. Intrusive dykes and sills occur at Sibasa with smaller occurrences near Nzhelele Dam and Blouberg. This has resulted in coal seams striking in an east-west direction between major faults. There are two main coal seams, namely the upper or main seam and the lower seam that are separated by a

vertical distance of 95 m. According to Barker (1976), there is an absence of marine sedimentation in this trough.

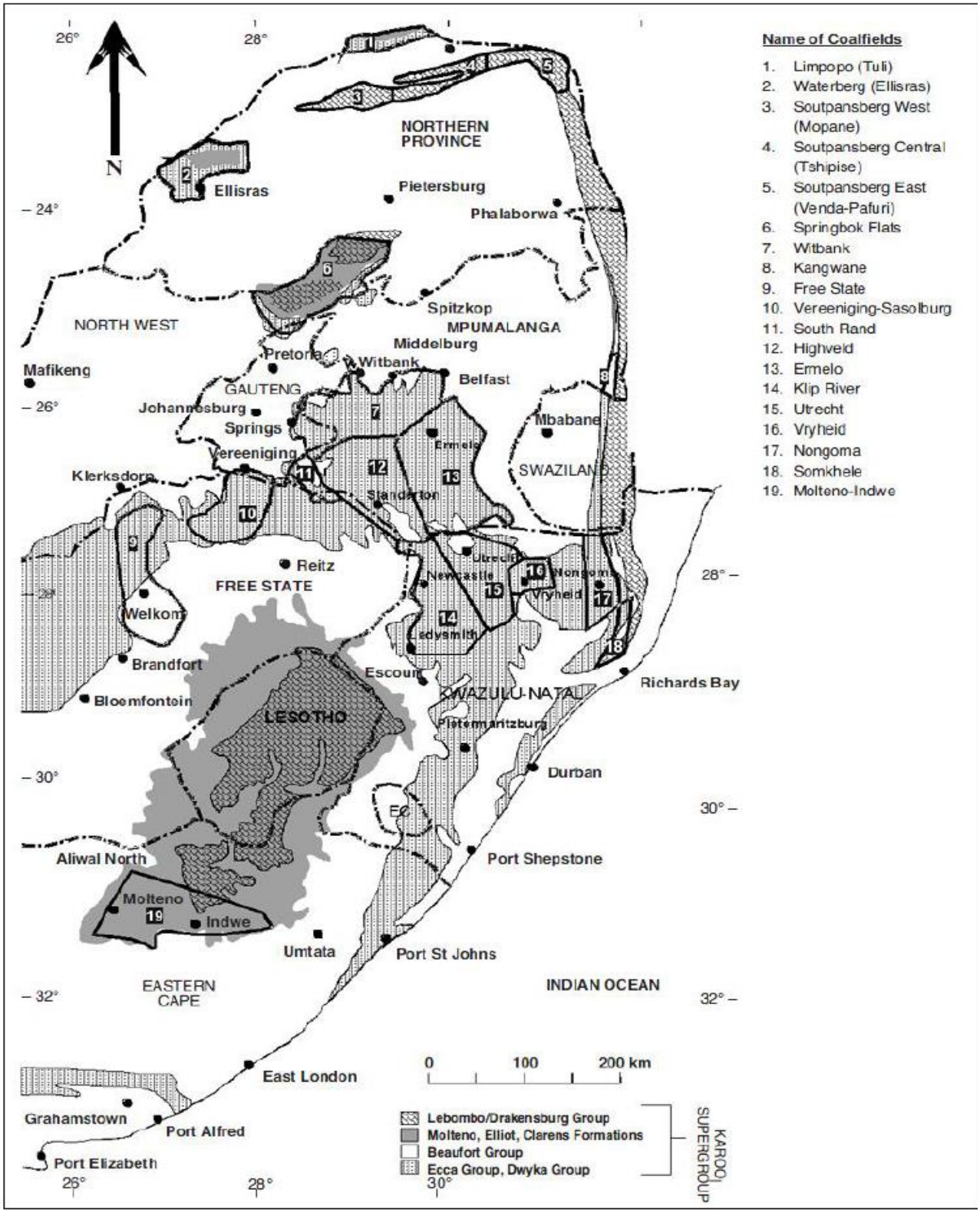

Figure 2.1: Map of the Main Karoo Basin and the coalfields of South Africa (Jeffrey, 2005).

The basin has been extensively faulted into a series of horst and graben blocks as a result of post-Karoo tectonics. The faulting was caused by extensional tectonism and occurred over a short period of time, after the deposition of the Karoo sediments and prior to the intrusion of dykes (McCourt and Brandl, 1980). This area was tectonically active during various geologic periods and overlies the previously active Proterozoic Limpopo Mobile Belt. This faulting continued during the deposition of the Karoo sediments and was reactivated in post-Karoo times and resulted in a very complex structural setting (Tshikondeni Mine Report, 1993). Excessive lateral and vertical pressure which occurred during this activity has faulted and fractured the strata including the coal seams.

Three major faults can be recognised in the Soutpansberg Coalfield, namely the Bosbokpoort, Tshipise and Klein Tshipise Faults. The faults trend east-north-east parallel to the regional strike, and they delineate major host and graben structures. All the faults which affect the Coalfield appear to be normal and probably of post-Karoo age (Brandl, 1981). However, minor faulting also took place and are recognisable in some areas. They are believed to be prior to the deposition of the Karoo rocks. It is believed that the dip of the Karoo strata in the Soutpansberg Coalfield is generally to the north and varies between 5° and 15° (Brandl, 1981).

In the Main Karoo Supergroup, coal occurs in the sandstone-rich Madzaringwe Formation and overlying Mikambeni Formation (Brandl and McCourt, 1980). The main seam is up to 3.5 m thick and is a composite seam made up of several coal band interbedded with carbonaceous shales. At the base is the Tshidzi Formation which comprises diamictite interbedded with typical coarse-grained sandstones.

The Soutpansberg Coalfield is sub-divided into 3 separate smaller basins, namely the Pafuri (Eastern Soutpansberg), Tshipise (Central Soutpansberg) and Mopane (Western Soutpansberg) basins (Barker, 1999). However, Sparrow (2012) defines seven sub-basins for this Coalfield from west to east, namely the Waterpoort, Mopane, Sand River, Mphefu, Tshipise South, Tshipise North and Pafuri.

Lithology

The Karoo Supergroup in this area is largely covered by younger quartzite boulder beds of the Malvernia Formation that lie in a sandy argillaceous matrix locally cemented by calcrete and have only recently been deposited (Brandl, 1981).

According to the Tshikondeni Mine Report (1993), the Fripp Sandstone Formation overlies the coal-bearing strata in the Tshikondeni area and the thickness of the layers varies between 100 and 120 m. This Formation occurs throughout the whole area and forms prominent ridges that strike north-northeast. Colour varies from white to greenish in places and is fine to coarse-grained with various conglomerate bands. Pebbles up to 4 cm are angular to sub-angular in shape (Tshikondeni Mine Report., 1993).

The Soutpansberg Group floor rocks consist of pink quartzite, but volcanic rocks can also occur. These rocks are coarse to fine crystalline and are green to brown in colour. Brandl (1981), found that the Nzhelele Formation quartzite was predominatly argillaceous and in outcrop shows thin bedding and ripple marks. The sedimentary and volcanic rocks of the Soutpansberg Group were deposited in an elongated fault-bounded depression which developed by rifting along a major zone of weakness between the central and southern marginal zones (Brandl, 1981).

The Tshidizi Formation forms the base of the Karoo Supergroup in the Soutpansberg area and consists of diamictites, thin bands of medium-grained sandstone, varved shales and thin matrix-supported conglomerate layers. These facies do alternate but the diamictite usually occurs at the bottom of the succession below the sandstone and conglomerate layers.

The Madzaringwe and Mikambeni Formations are predominantly arenaceous but due to changes in facies in the west, these rocks become more argillaceous and were deposited under relatively shallow fluviatile conditions. The number of coal bands in the coal-bearing zones also increase in response to the change in facies from east to west (Tshikondeni Mine Report, 1993).

Tshipise-Pafuri Coalfield

This coal basin falls within the Soutpansberg coalfield that is located in Limpopo Province (Figure 1.1; De Jager, 1976).

Structure

According to previous studies by De Jager, (1976) this coalfield begins about 20 km west of Tshipise and extends eastward for 40 km and then changes to a north easterly direction for another 40 km into the Kruger National Park. Along this 100 km strike the Karoo strata dip to the north and to the east.

Lithology

In the Alldays-Tshipise-Pafuri area, the Tshidizi Formation forms the base of the Karoo Supergroup and because of its poor sorting and argillaceous matrix it may in places be regarded as a diamictite which could be correlated with Dwyka Formation (SACS, 1980). The Madzaringwe Formation is the equivalent to the Vryheid Formation and overlies the Tshidizi Formation. It consists of alternating black shale, micaceous sandstone, siltstone and interbedded coal seams (SACS, 1980; Tshikondeni Mine Report, 1993).

The Fripp Sandstone Formation consists of up to 60 m of white coarse-grained feldspathic sandstone. The Solitude Formation overlies the Fripp Sandstone Formation and consists of a lower grey shale unit with occasional bands of coal and a thicker upper of alternating purple and grey mudstone with intercalations of sandstone and siltstone (SACS, 1980). The Fripp Sandstone and Solitude Formations are the Limpopo Province's equivalent to the Beaufort Group. The Pafuri Crocodile River sector covers 300 km² and falls entirely within the Kruger National Park.

2.2.2 Geology of theTuli Coalfield

The Tuli Coalfield is the northernmost Coalfield in South Africa and forms part of the great Tuli Coalfield (greater Tuli block/ Bubye River Coalfield) that extends northwards from South Africa into Zimbabwe and Botswana (Fig. 2.1). In South Africa this Coalfield is represented by a relatively narrow deposit of the Karoo Supergroup rocks on the right hand bank of the Limpopo River (Malaza *et al*., 2013).

The pre-Karoo basement of the Tuli Coalfield consists of the metamorphic and meta-sedimentary rocks of the Limpopo Mobile Belt. Deposition of the Karoo sediments occurred with concurrent movement on the pre-existing fault planes (Bordy, 2000). The sedimentary sequence is thinner (estimated thickness of 450-500 m) and less continuous than the late Carboniferous to middle Jurassic Karoo Supergroup (Catunaenu *et al*., 1998).

Bordy (2000) noted that on the South African part of the Tuli Basin, the Karoo sedimentary rocks occupy an area of about 1000 km², a relatively small area with an east-west-trending in which sedimentation was fault controlled and consists of various terrigenous clastic and chemical deposits. However, in the Tuli Basin there are no major faults but minor faulting trends east-northeast, these faults are believed to be normal.

The Limpopo Coalfields host a higher grade of coal than the Coalfields of the Main Karoo Basin, containing a valuable percentage of South Africa's coking coal which is essential for the steel and metallurgical industry (Hancox and Goetz, 2014). The coal seams tend to sub-outcrop under a thick layer of superficial deposits and the presence of coal was first detected in water boreholes. The coal zone is estimated to be up to 150 m thick, consisting of 22 thin coal bands alternating with mudstone, to form composite seams.

2.3 Regional Stratigraphy

The South African basins containing the Karoo Supergroup strata appear in different tectonic settings, but the overall climatic overprinting resulted in similar vertical lithological profiles (Groenewald *et al*., 1991; Johnson *et al*.,1996). The early formations of the Karoo Supergroup in the Main Karoo Basin reflect marine/deltaic rather than lacustrine/fluvial conditions. Other dissimilarities are due to the fact that some of the basins were subjected to tectonism, leading to considerable thickness variation and intra-strata unconformities (Johnson *et al*., 1996).

The sedimentary rocks contained in the Main Karoo Basin were deposited in a foreland basin (Visser, 1989) that was deeper in the south and shallower northward. The rocks contained in the Karoo Basin can be divided into the following lithostratigraphic subdivisions (SACS, 1980): Dwyka, Ecca, Beaufort and Drakensberg Groups.

Dwyka Group

After the deposition of the Cape Supergroup, increasingly colder conditions initiated the onset of the Permo-Carboniferous glaciation in the Southern Hemisphere (Stratten, 1968). The Dwyka Formation is the lowermost stratigraphic unit of the Karoo Supergroup and attains a maximum thickness of 1100 m in the Cape-Karoo trough, but thins northwards to 60 m (Visser and Kingsley, 1982). The Dwyka lithologies vary, but consist mainly of massive to stratified diamictite deposited by continental and marine ice sheets during the Late Carboniferous age (Johnson *et al*., 2006) as well as conglomerate, pebbly sandstone, black gritty mudstone, dark-grey shale and dropstones. The sediments comprising this group are considered to be glacial in origin and were deposited during the Late Carboniferous to Early Permian (Cadle *et al*., 1990).

Ecca Group

The transition from the Dwyka Group to the overlying Ecca Group for the most part is presented by an abrupt but diachronous contact representing an environmental change, from melt water influenced alluvial fans issuing into an euxinic lake to more stable lower energy fluvial systems building out fine-grained deltas into a sea (Smith *et al*., 1993; Van der Walt, 2012). The early Permian-late Permian Ecca Group consists of two contrasting units where in the northern part of the basin differs in character from the units in the southern part of the basin.

In the northern part of the Karoo Basin, the Ecca Group is divided into 3 Formations, namely, the Pietermaritzburg Formation, the Vryheid Formation and the Volksrust Formation (Fig. 2.2). Alluvial strata are present only in the north eastern part of the basin (Part of Vryheid Formation) (Cadle *et al*., 1993); in the rest of the basin, the group was formed in marine environment (Johnson, 1994).

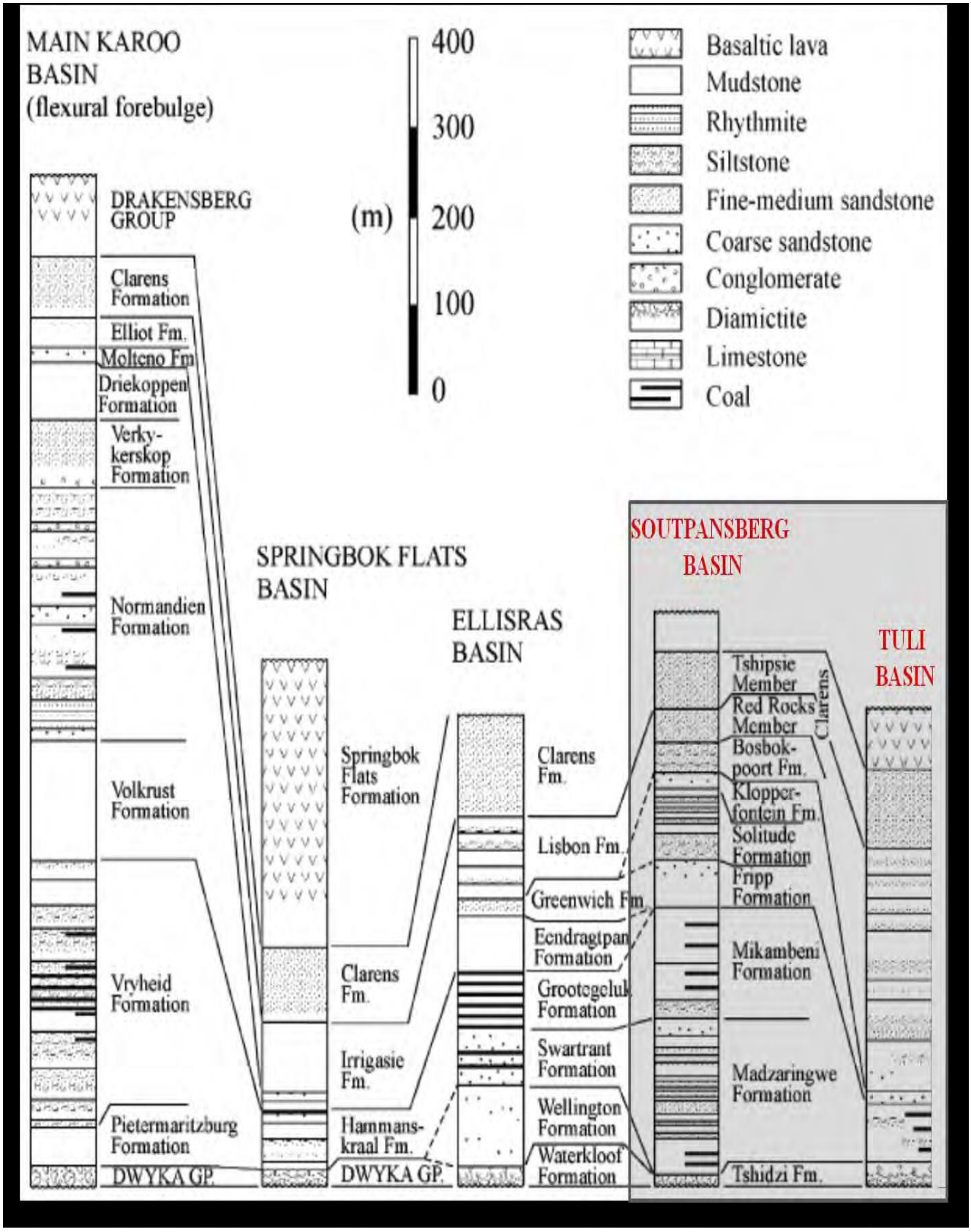

Figure 2.2: Stratigraphy of the Main Karoo Basin and the northern sub-basins. Highlighted are the Soutpansberg and Tuli Basin (Johnson *et al*., 1996).

The lower part of the group was laid down in deep marine environment characterized by submarine fan depositories. These rocks consist of greywacke, siltstones and mudstones forming Bouma sequences (Visser and Lock, 1978; Catuneanu *et al*., 1998), characteristic of turbidites. The upper part of the group is identified by the increasing dominance of arenaceous deposits formed in open shelf and then on shore face and deltaic environments (Johnson, 1976; Kingsley, 1985).

Beaufort Group

The Beaufort Group of the Karoo Supergroup diachronously overlies the Ecca Group and was deposited on vast alluvial plain (Johnson, 1976; Groenewald *et al*., 1991; Catuneanu *et al*., 1998) from the Late Permian to early Mid-Triassic times. According to work done by Visser (1989) the Beaufort Group covers the greatest surface in the region of 200 000 km² within the Karoo Basin and it reaches a maximum thickness of 6000 m in the Eastern Cape Province (Johnson, 1976). The Beaufort Group stratum contains a rich and diverse collection of fossils, including fauna and flora with therapsids being abundant (Johnson *et al*., 2006; McCarthy and Rubidge, 2005; Van der Walt, 2012).

The Beaufort Group is overlain by the Late Triassic-early Middle Jurassic Stormberg Group. Starting with a coarse sediment wedge of a braided river system (Moltene Formation), this group also comprises laterally continuous floodplain mudstones and associated fluvial sandstones (Elliot Formation), as well as Aeolian sandstones (Clarens Formation) (Johnson, 1976; Groenewald *et al*., 1991; Cairncross *et al*., 1995; Catuneanu *et al*., 1998).

Drakensberg Group

The Drakensberg Group forms the uppermost succession of the Karoo Supergroup and consists of layers of volcanic flows up to 1400 m thick which extruded during the middle Jurassic (Haskins *et al*., 1995; Duncan and Marsh, 2006; Van der Walt, 2012). The main volcanic episode occurred roughly 200 Ma, with acid volcanism continuing until approximately 140 Ma (Fitch and Miller, 1971).

This episode was initially explosive as seen by the tuff and volcanic vent remnants and was followed by a succession of balsatic lava flows that are traceable for kilometres (Fig. 2.2). Outside of the main Karoo Basin, the Drakensberg Group is

correlated with the Lebombo Group, which also consists chiefly of basic and acid volcanic rocks (Johnson *et al*., 1996).

2.4 Limpopo Coalfields

There are 19 coalfields in South Africa, covering an area of 9,7 million hectares. The distinguishing characteristics between the coalfields are based on geographic considerations and variations in the mode of sedimentation, origin, formation, distribution and quality of coal. These variations are related to specific conditions of deposition and local tectonic history of the area (Hancox and Gotz, 2014). The Soutpansberg Coalfield is Limpopo's 2nd biggest coalfield and can be divided into 3 sub-basins namely, Mopane, Tshipise and Venda-Pafuri.

South Africa's Limpopo coal deposits in the north host the vast majority of the country's remaining largely undeveloped coal resources. Four coal basins have been identified as the major coal deposits in Limpopo (Jeffrey, 2005). These are in the Waterberg, Soutpansberg, Tuli and Springbok Flats region (Fig. 2.1). These Coalfields are currently considered the future of coal in South Africa.

Soutpansberg Coalfield Stratigraphy

Sullivan *et al*. (1994) noted that the coal seams in the Soutpansberg coalfield are intensely disturbed by faults and dolerite intrusions; more so the coal is predominately bright and high in vitrinite. Dull coal occurs at the base of the multi-seam coal-mudstone association in the Waterpoort area as well as in the upper part of the lower seam at Tshikondeni (Fig. 2.3). The coal rank increases from the west to the east, however, the volatile matter in the west is about 35% and decreases to about 25% in the east.

Through studying the stratigraphy and geology of rock units, it is possible to outline the formations of rocks, structural patterns and depositional environments. Brandl and McCourt (1980) considered two stratigraphic periods namely, the Permian and Triassic Periods. The Permian Period consists of four formations namely; Tshidzi, Madzaringwe, Mikambeni and Fripp Formations; while the Triassic Period consists of four formations namely; The Solitude, Klopperfontein, Bosbokpoort and Clarens Formation.

In order to understand the regional variation of the coal stratigraphy in the Soutpansberg Coalfield, the borehole cores within the Soutpansberg Coalfield were studied and examined in detail. The lithostratigraphy of the Karoo Basin showing the position of the Soutpansberg and Tuli Basins is shown in figure 2.2 as adapted and defined by Johnson *et al*. (1996).

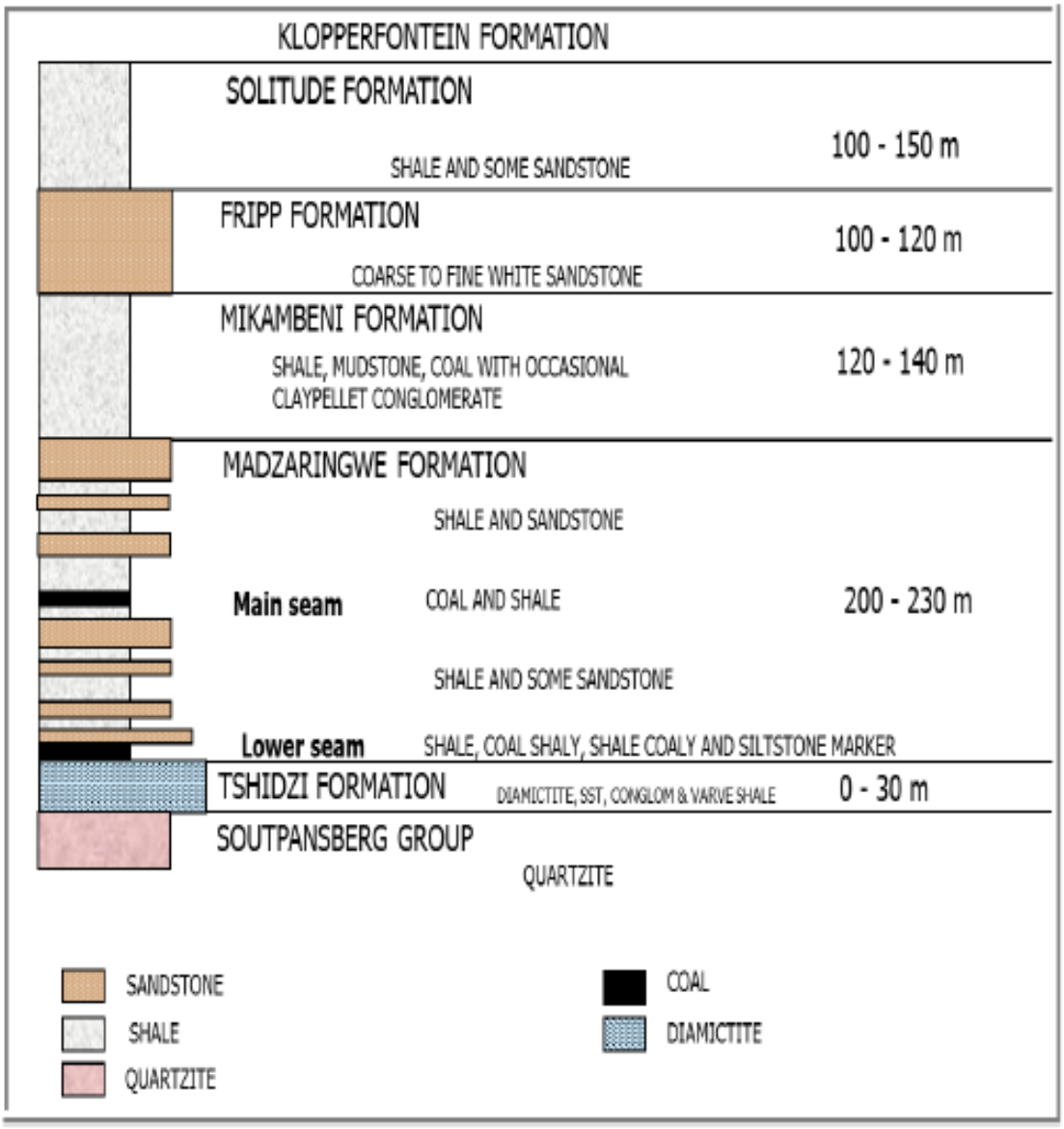

Figure 2.3: A general simplified stratigraphic column of the Mopane, Tshipise and Pafuri Coalfields/Soutpansberg Coalfield (Sullivan *et al*., 1994).

Tuli Coalfield

The Limpopo Coalfield which is also known as the Tuli Coalfield is located on the northern part of South Africa, and forms part of the Vryheid Formation consisting of

top and bottom seams that are flat lying and dip at an angle of 2° to the north and northwest (Jeffrey, 2005; Chabedi, 2013). This coalfield is characterised mostly by dykes and by soft rocks such as shales, siltstones and interlaminated mudstones (Fig. 2.4). Currently no mining activity is taking place due to poor geological factors.

The main coal zone is about 210 m thick, three coal zones were identified; bottom coal with numerous coal layers/bands intercalating with mudstone having an approximate thickness of 40 m. furthermore, the middle coal zone comprised a single layer of about 20 m in thickness; while the top coal zone was about 35 m thick with a mudstone layer in between.

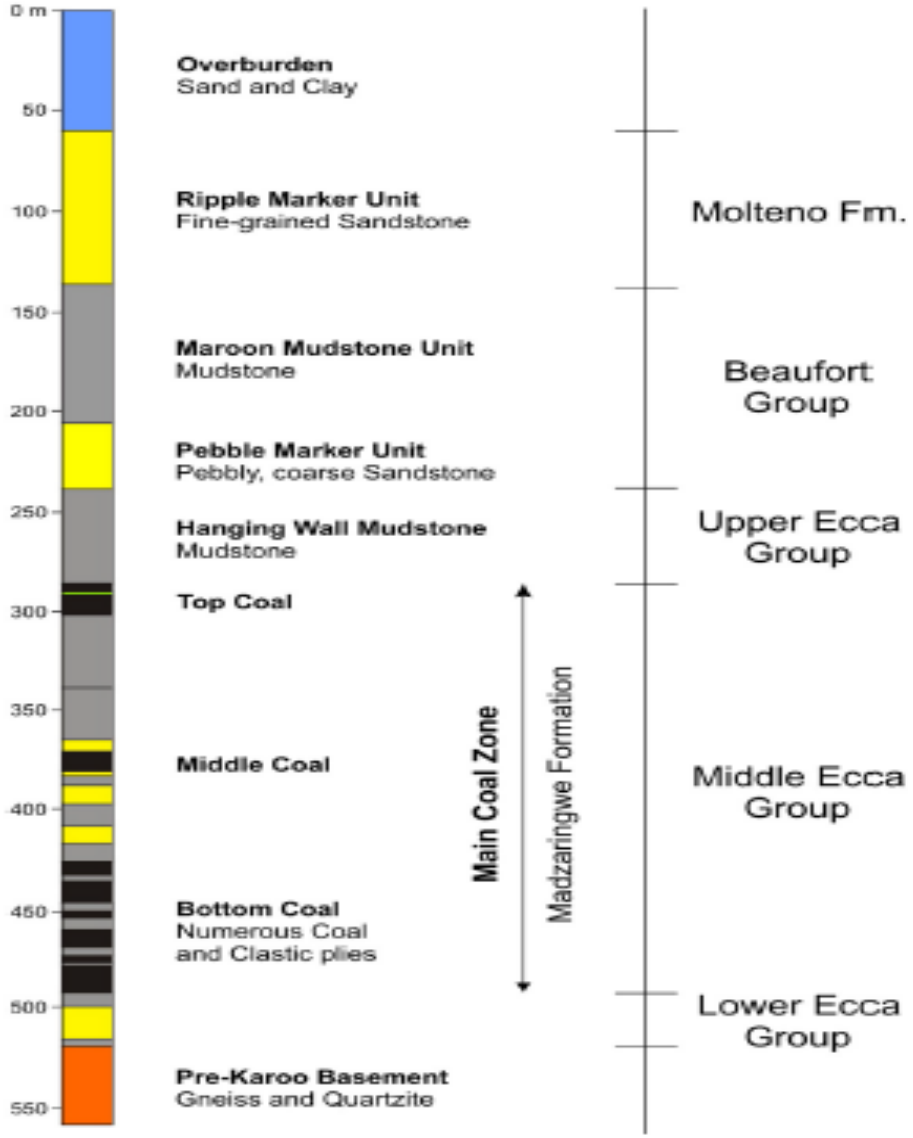

Figure 2.4: A generalised stratigraphic profile of the Karoo Supergroup in the Limpopo Coalfield (Sparrow, 2006).

Waterberg Coalfield

The Waterberg Coalfield is situated in the western part of Limpopo Province, about 25 km west of Lephalale town. This coalfield has a strike length of about 88 km east-west and a width of approximately 40 km north-south, with a total seam thickness of 110 m making the Waterberg in-situ reserves large (Chabedi, 2013). A stratigraphic column of the Waterberg Coalfield showing all the 11 coal zones being mined is shown in Figure 2.5.

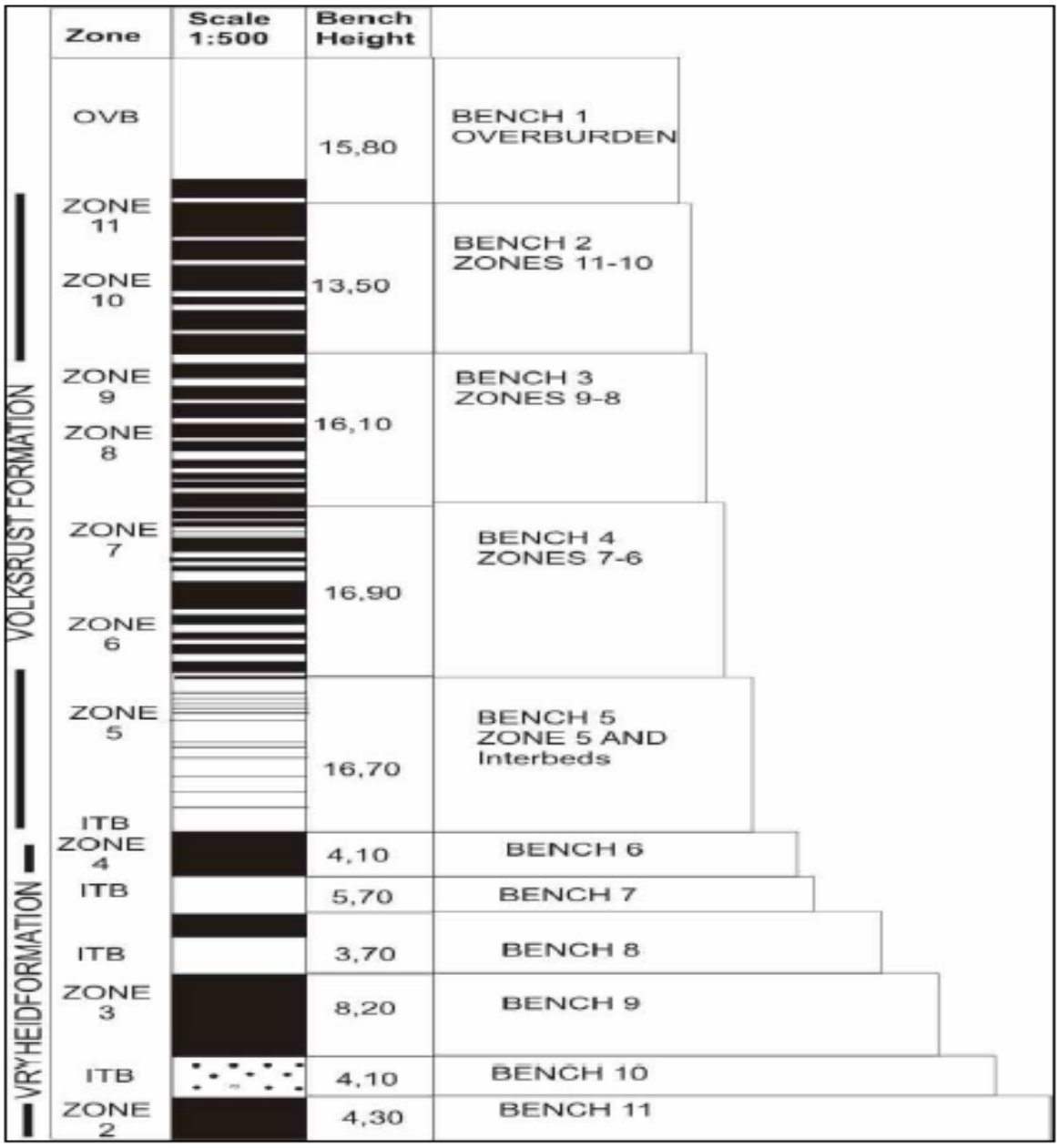

Figure 2.5: Stratigraphic column of the lithological units of the Grootegeluk Formation in the Waterberg Coalfield: OVB- overburden and ITB- interburden (Dreyer, 1999).

The Waterberg Coalfield is characterised by two main coal-bearing formations, the upper Grootegeluk Formation (known previously as the Volksrust Formation) which ranges in depth from 60 m to 110 m in the south and the lower Vryheid Formation, which is a more carbonaceous and interbedded sequence at approximately 55 m in thickness (Jeffrey, 2005).

The Waterberg Coalfield has been identified as a valuable potential coal resource which will take over from the Witbank and Highveld Coalfields as South Africa's most important coal producing basin later in the 21st century (Fourie *et al*., 2014).

Hancox and Geotz (2014), have described this Coalfield as being characterised by a fault basin with various dimensions, as well as the depositional and preservation characteristics of the coal occurrences in the area being a result of faulting.

Springbok Flats Coalfield

The Springbok Flats Coalfield is characterised by a half-graben, bordered to the north by a normal fault, and covers an area of approximately 180 by 40 km. The sediments of this coalfield dip towards the centre of the basin and northwards towards the northern boundary fault (Roberts, 1992).

The coal seams are best developed in the central part of the Springbok Flats Coalfield and is characterised by a single coal zone which is 3 m to 7 m in thickness in the upper zone (Fig. 2.6). De Jager (1983) further recognised that the coal zone is located stratigraphically between the mudstone of the Beaufort Group and the siltstone of the Vryheid Formation of the Karoo Sequence. The coal seams are shale and mudstone bounded lying very deep at depths between 200 m and 1000 m (Barker, 2012). Currently, no mining is taking place due to the complicated structure and geology of the area owing to the presence of several faults and igneous intrusions.

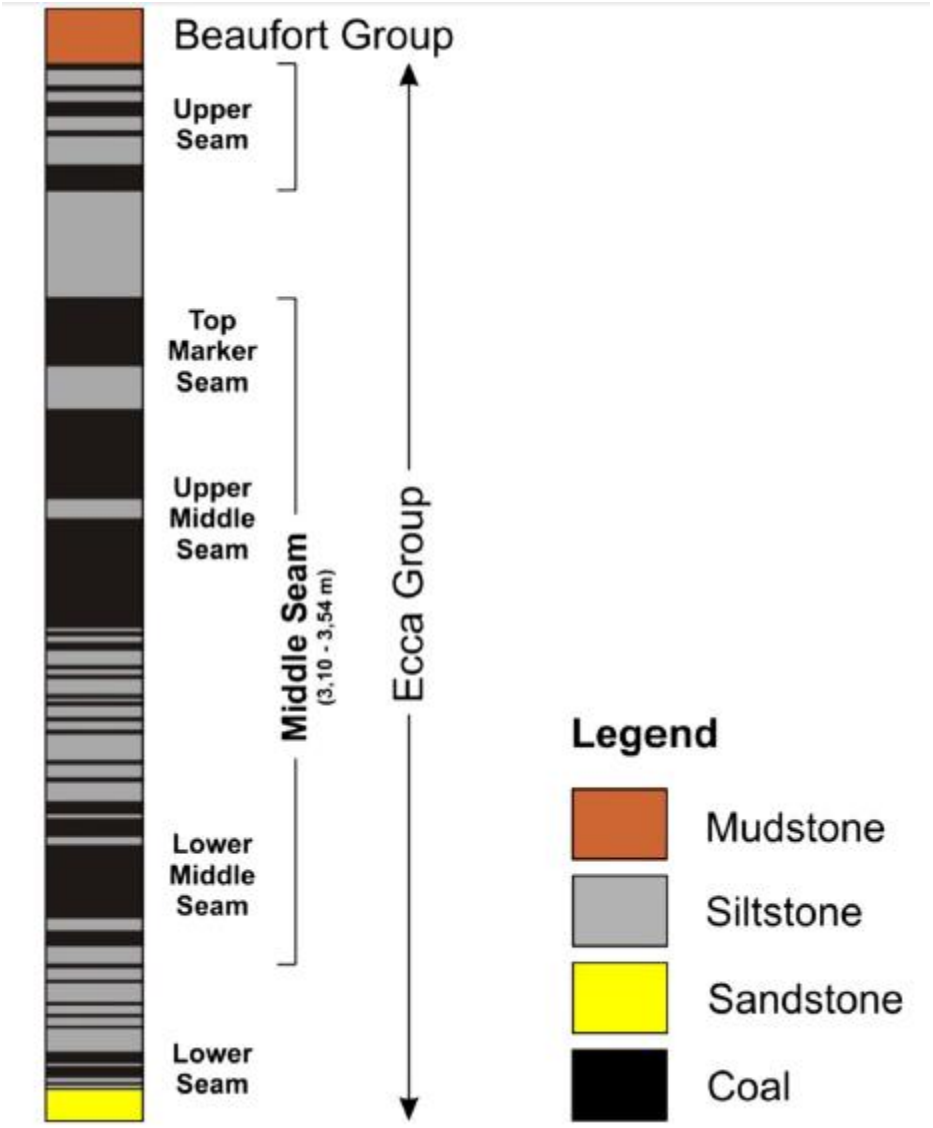

Figure 2.6: A generalised stratigraphic column of the coal-bearing succession in the Tuinplaats Area of the Springbok Flats Coalfield (Mybury, 2012).

2.5 Coal Formation and Characteristics

2.5.1 Coal Formation

In the late Palaeozoic times, collision of the crustal plates caused an area of the Gondwanaland super continent to steadily subside. This created the Karoo Basin, where peat swamps developed on the margins of the glaciated valleys and lakes (Catuneanu et al., 2005; Johnson et al., 2006). Coal formation begins when plants are deposited in swamps, then submerged rapidly enough to limit oxidation but to allow microbial decomposition to occur (Fig. 2.7).

The peat forming environments of coal are poorly drained, have high water table and contain stagnant anoxic water that inhibits microscopic organisms from decomposing the plant materials. Coal is a fossil fuel composed of carbonaceous material, furthermore a combustible sedimentary rock that formed from prehistoric organic remains that were buried and altered through geological time (Cairncross, 2005).

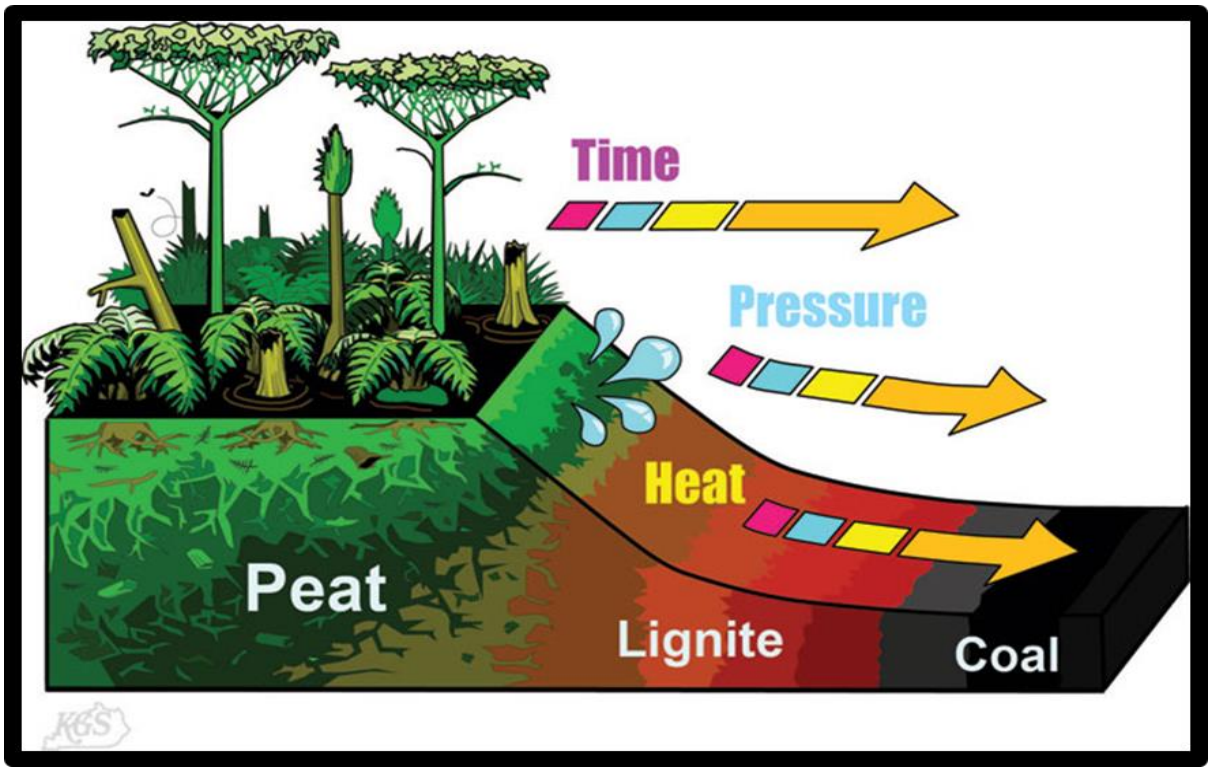

Figure 2.7: Stages and Processes of Coal Formation (www.uky.edu).

The greatest coal-forming time in geological history was during the 354 to 290 million years ago (Ma), called Carbonaceous Period (Falcon and Ham, 1988; and Mintek Report, 2007). In addition some large coal deposits are found in the Permian Age (290 to 248 Ma). During coal-forming periods most of this region on earth was covered in swamps, with plants growing within these swamps. Coal formation is two-fold: the first stage is peat formation (humification), followed by putrefication (Mintek Report, 2007). When plants die, their biomass is deposited in layers within the aquatic environment, where conditions are anaerobic (Fig. 2.7). The lack of oxygen prevents complete decay of the organic material by oxidation and decomposition is slow. Interaction from bacteria converts the material to peat, which is then compacted by sediment loading, squeezing the interstitial water out of the peat (Falcon and Ham, 1988).

Burial of the material increases the pressure (increased overburden stress), while temperature is affected by burial depth, the presence of intrusive bodies, and geothermal influences in regions of crustal weakness. Increasingly deeper burial and heat gradually converts the organic material to coal (Mintek Report, 2007). The factors controlling the rate and degree of degradation (coalification) include sedimentary environments and tectonic control, prevailing climatic conditions, plant communities and geochemical conditions such as water level and salinity (Falcon and Ham, 1988).

The changes in maturity of coal are controlled by pressure, temperature and the passage of time (Fig. 2.7). Eventually due to the onset of the initial tectonic events, the coal forming environment comes to an end. However, this ending is characterised by an abrupt behaviour (coal forming processes) resulting in coal seams having a sharp upper contact with the overlying strata (Falcon and Ham, 1988).

A prolonged stable environment is essential for the formation of economic coal and the water feeding the peat swamps must remain free of sediment and this is only possible when erosion is minimal in the uplands of the rivers which feed the coal swamps and efficient trapping of the sediments exists (Mintek Report, 2007).

Falcon and Ham (1988) noted that the Southern Hemisphere coals formed in the Permian Period have been found to be characteristically rich in minerals, highly variable in rank and organic matter composition; and are different from the Carboniferous coals of the Northern Hemisphere. Swamps in the Northern Hemisphere were set in a hot, humid, equatorial climate and coal-bearing basins were set in uncompacted deep, actively and rapidly subsiding geosynclines within the Laurasian Supercontinent. Plant growth was rapid with long, continuous growing seasons. The rate of plant degradation was also rapid.

The Gondwanaland Supercontinent lay in the Southern Hemisphere. The Permian swamps existed in a cool temperate climate associated with waning of a massive ice age induced by the drifting of the supercontinent away from the South Pole. Peat was deposited within relatively stable continental depressions. The flora that dominated was significantly different from that which flourished in the considerably warmer Northern Hemisphere. Plant growth was only moderate with short growing seasons, and degradation was slow to moderately rapid (Mintek Report, 2007).

South African coals are all hosted within the Karoo Supergroup (Catuneanu *et al.,* 2005). The major period of coal formation began at about 260 Ma and lasted for about 30 Ma. In the southern and eastern Mpumalanga and northern KwaZulu-Natal in the Middle Permian, from this central region in the Main Karoo Basin, coal development proceeded outwards in all directions over the ensuing period, finally ending during the Upper Permian Period (Mintek Report, 2007; Johnson *et al.,* 2006). Deposits are found within two major tectonic settings, namely; stable cratonic platforms and fault-bounded rift basins. Coal rank in the Main Karoo Basin normally increases in an easterly direction and the coal in the northern basins varies from low to high ranks (Falcon and Ham, 1988).

2.5.2 Coal Characteristics

Maceral Composition

Macerals are the organic components of coal and are divided into 3 groups namely, vitrinite, liptinite and inertinite. Furthermore, each maceral is characterised by its own specific physical and chemical properties and can be distinguished under the microscope from one another by differences in colour, shape, reflectance, morphology, size polishing hardness and fluorescence. The maceral composition of coal can be used to study the transformation of the carbonaceous structure because each maceral group reacts differently (Sharma *et al*., 2000; Van Niekerk *et al*., 2008).

Coal Composition and Rank

Coal is classified by rank according to their percentage of fixed carbon and heating value. Fixed carbon is the carbon residue that remains when coal is heated without combustion to drive off volatile matter, while volatile matter includes gases and vapours released by coal when heated. Coals heating value and carbon percentage, except in the case of anthracite, have an inverse relationship with the moisture and volatile matter content (Akinyemi *et al*., 2011).

Coal rank refers to the degree of maturation of the coals in the coalification process, and this is often accompanied by structural changes. There are four types of coals which vary in terms of the heating value, chemical composition, ash content and geological origin. The coal types are lignite, sub-bituminous, bituminous and anthracite

being the highest rank of coal and considered a metamorphic rock due to the degree of metamorphism that it underwent (Hendrikson, 1975).

Lignite is the lowest rank of coal, formed from peat that was compacted and altered, having colour that ranges from brown to black, has fibrous earthy texture and commonly has high moisture content and low heating value. Lignite is composed of recognizable woody materials imbedded in macerated and partially decomposed vegetable matter.

Sub-bituminous coal is dull, black band and has developed bedding planes while it shows little woody materials. This type of coal is characterised by heating values that ranges from 8,300 to 11,500 Btus (British Thermal Units) and has less moisture content compared to lignite.

Liu *et al.* (2005), noted that bituminous coal is dense, compacted, banded, brittle and displays columnar cleavage; and has a dark black colour. This type of coal is resistant to disintegration in air when compared to sub-bituminous and lignite coals. It has low moisture and sulphur (S) content, carbon content that ranges from 69 to 86%, volatile matter content ranged from 15 to 50%, and its heating value ranges from 10,500 to 15,500 Btus. The principal components of bituminous coal fly ash are silica, alumina, iron oxide and calcium with varying amounts of carbon (Adriano *et al.*, 1980)

Anthracite is the highly metamorphosed coal, characterised by a jet black colour, being hard and brittle, breaks with a conchoidal fracture and displays a high lustre. Anthracite has a carbon content that ranges from 86 to 98% and has a slightly lower heating value than bituminous coal due to the low volatile matter content.

Mineral Matter Content

The mineral matter associated with coal cover a wide range of minerals, the most abundant being clays, quartz, pyrites, carbonates and oxides. The decomposition of clays such as kaolinite, montmorillonite, illite and chamosite produces the amorphous aluminiosilicate phase (Kosminski *et al.,* 2006). According to Gaigher, (1980), the dominant mineral matter in South African coals is reported to be clays kaolinite and illite, with an estimated average clay composition of 54.1% and 29.2% respectively.

During coal utilisation the mineral matter undergoes structural and chemical changes, for example, the oxidation of pyrite and/or siderite would be expected to form hematite at similar or even lower temperatures, but only if abundant oxygen is available. However, with more reducing conditions (limited oxygen) magnetite would be expected to form instead. Likewise pyrrhotite would also be expected to form from pyrite in limited oxygen conditions (Bryers, 1996; Kerkkonan, 1997).

2.6 Igneous Intrusions (Dolerite Dykes and Sills)

Dolerite intrusions are a common feature within the Karoo Basin (Duncan and Marsh, 2006). The intrusions have been linked to the breakup of Gondwana from Pangaea in the Early Jurassic period. In the main basin, in South Africa, the intrusions have manifested themselves as extensive cross cutting dykes or displacing sills. Where the intrusions interfere and interact with the country rock, thermal contact metamorphism occurs. The intrusions not only affect the quality and characteristics of coal (Van Alphen, 2012), but they also have direct influence on mining processes (Du Plessis, 2008).

According to Mussett and Khan (2000) the contact metamorphic effect of an igneous intrusion at a specific temperature and composition is thought to be directly related to the volume of the intrusive material which passes through the conduit at the time of emplacement and the nature of the surrounding material. Thus the greater the volume of magma passing through the dolerite conduit the larger the metamorphic aureole that is produced.

Furthermore, Van Alphen (2012) and Melenevsky *et al.* (2008) argue that the intrusions do not only cause transformation of the coal, they also have an influence on the physical characteristics of the coal as well as the combustion characteristics. Analytically coal maybe devolatilised; that is, the volatile matter original present has been driven off by high temperatures. If the temperatures are high enough the coal maybe converted to a higher ranking such as anthracite and coke (Falcon, 2012; Melenevsky *et al.,* 2008).

Many studies have been undertaken in order to understand the influence of sills on the surrounding country rock, with much interest in the coal and organic-matter-rich sedimentary rocks. Crelling and Dutcher (1968) discovered that coal can be thermally

altered and this was concluded by noting the highly contorted bed, the natural coke and the prismatic fracturing of the coal zone.

It was also deduced that the sulphur content of coal was not influenced by the sill and had no relation to the sill. However, volatile matter was found to have been influenced by the sills and varies in the coal seams from low to high as the distance between the coal seam and the sill decreases (Crelling and Dutcher, 1968). This was attributed to the release and re-absorption of the volatile matter, or the volatile matter was never released initially during heating.

Saghafi *et al.* (2008) concluded that the bituminous and sub-bituminous coal of the Highveld Coalfield had been adversely affected by the dolerite intrusions. The coal had been devolutised and displaced as a result of the intrusions. Nevertheless metamorphism of the coal had increased the coal's gas storage capacity and that the dolerites were capable of trapping and storing gas. Furthermore, an investigation by Melenevsky *et al.* (2008) showed that a thick dolerite dyke which intruded a sheet of coal altered the bituminous coal to anthracite and that most of the volatile matter in the coal was released during the first stage of contact metamorphism.

Studies conducted on the metamorphic effect of dolerite intrusions have indicated various outcomes. Aarnes *et al*. (2010) noted that when a sill interacted with the Ecca Group, the organic matter was converted to hydrocarbons and dehydration reactions were observed. Yao *et al. (*2011) concluded that the intrusions affected the coal quality, rank and adsorption capacity.

2.7 Climate Change and Carbon Emissions

2.7.1 Science of Climate Change

Climate change is one of the defining issues of the 21st century, and climate is defined as the mean condition of the atmosphere in terms of elements such as solar radiation, temperature, pressure, precipitation, humidity and wind, and their variations at a given locality over a long period of time (Ogola and Awuor, 1997). Climate change, however, is defined by the United Nations Framework Convention on Climate Change (UNFCCC) as a change of climate which is attributed directly or indirectly to human

activity that alters the composition of the global atmosphere and which is in addition to natural variability observed over comparable time periods (UNFCCC, 2007).

The climate of the earth is determined by the incoming energy from the sun, the outgoing energy radiated from the earth, and the exchanges of energy among the atmosphere, land, oceans, ice and living things (IPCC, 2007). The composition of the atmosphere is important because some gases and aerosols affect the flow of incoming solar radiation and outgoing infrared radiation (Fig. 2.8).

There are two different sources of greenhouse gases namely, natural and anthropogenic. In natural sources the greenhouse gases causing climatic variations are emitted primarily from natural processes such as geological and meteorological processes, wherein geological processes include volcanic eruptions, earthquakes and weathering emitting different concentrations of gases such as CO_2, CO, N_2 and CH_4, thereby weakening the flux of solar radiation to the Earth (Ogola *et al*, 1997; IPCC, 2007).

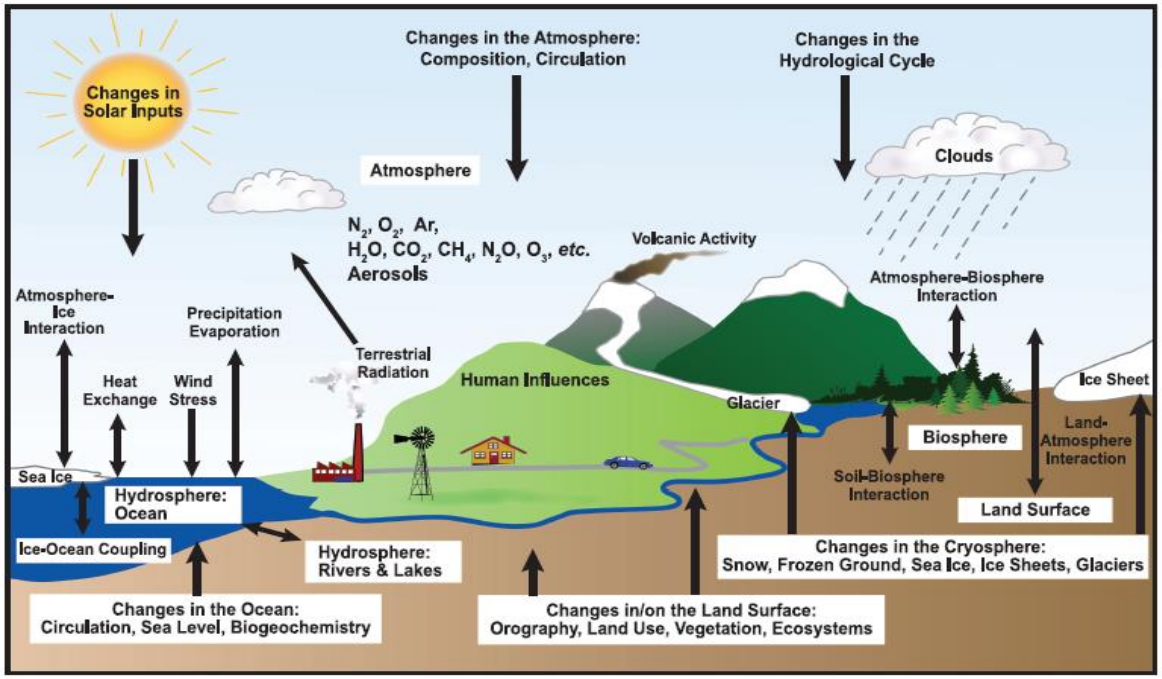

Figure 2.8: Components of climate system, their processes and interactions (Le Truet *et al*., 2007).

Chemical and biochemical weathering are responsible for the release of greenhouse gases such as CH_4, CO_2, and N_2O as a result of organic decay. However, the

weathering of organic matter which results in the release of CO_2 into the atmosphere is balanced by the organic carbon of buried sedimentary rocks (Ogola, 1997).

Worldwide the main source of anthropogenic greenhouse gas emissions is energy use, as a result of energy production, industrial non-energy activities, deforestation and clearing of land for agriculture (Ogola, 1997), energy is obtained from renewable and non-renewable sources (Johansson *et al*., 1992). The most important anthropogenic sources of greenhouse gases are fossil fuels which emit gases into the atmosphere at different stages namely, during production, transportation and consumption. The burning of oil, coal and natural gas releases large quantities of CO_2, CH_4 and NO_2 to the atmosphere (Ogola, 1997).

Human activities especially the burning of fossil fuels since the start of the Industrial Revolution and the increasing changes in land-use has contributed to the amount of emissions and these activities are still continuing to emit gases, thereby increasing the quantities of greenhouse gases into the Earth's atmosphere (UNFCCC, 2007). Greenhouse gases include nitrogen dioxide (N_2O), carbon dioxide (CO_2), and methane (CH_4) to mention a few, and an increase in these gases has caused a rise in the amount of heat from the sun withheld in the earth's atmosphere, heat that would be radiated back into space (Ogola and Awuor, 1997). This increase in heat has led to the greenhouse gas effect which results in global warming.

The main characteristics of climate change are increases in average global surface temperature (global warming), changes in cloud cover and precipitation particularly over land, melting of ice caps, glaciers and reduced snow cover; and increases in ocean temperatures and ocean acidity due to seawater absorbing heat and carbon dioxide from the atmosphere (UNFCCC, 2007). Coal mining produces negative externalities primarily in the form of air pollution, global warming from greenhouse gases emissions, biodiversity impacts and water pollution (Goldblatt *et al*., 2002).

Carbon Dioxide (CO_2)

Carbon dioxide is a colourless, odourless and non-combustible gas with a faint acid taste (Budavari *et a*l., 1989), it is produced by combustion of all carbonaceous fuels and is a product of animal metabolism. The burning of fossil fuels produces carbon dioxide, with coal production and mining releasing twice as much of the gas as

petroleum, fossil fuels generate 85% of the electricity; industrial manufacturing such as that of steel & iron and cement production releases large amounts of carbon dioxide due to industries consuming large quantities of heat to convert raw materials into construction products. Biomass burning associated with deforestation is the most common human activity producing carbon dioxide especially in poor countries (Ogola *et al*., 1997)

Carbon Monoxide (CO)

Carbon monoxide is a highly toxic, colourless, odourless, tasteless gas produced by the incomplete combustion of carbon containing material (hydrocarbons), and in coal mines it can be produced by the low temperature oxidation of coal. Ambient levels of carbon monoxide in the atmosphere vary depending on the characteristics of the coal (Prockop and Chichkova, 2007).

Methane (CH_4)

Methane is a gas formed as part of the process of coal formation; when coal is mined methane is released from the coal seam and the surrounding disturbed rock strata; moreover methane can be released as a result of natural erosion and faulting. The methane content in coal seams increases with depth and age of the seam (as depth of the coal seam increases, so does the pressure level), thereby reducing the level of permeability causing methane to be tightly bounded to the coal and surrounding rock strata (www.worldcoal.org, February 2017). Underground mining amounts to higher methane gas concentration emissions when compared to surface mining (approximately 90%). Methane is highly combustible and its poses serious implications to the environment and also as a potent greenhouse gas.

Ozone (O_3)

A stable climate is one of the key requirements for the complex life forms that populate the Earth today. Different organisms require steady supply of oxygen for respiration; furthermore, oxygen is a highly reactive gas that combines readily with other elements such as hydrogen, carbon and iron. Many metals react directly with oxygen in the air to form metal oxides (Annenberg Foundation, 2016). Climate, volcanism and plate tectonics all played a crucial role in regulating the oxygen levels during various time periods.

Nitrous Oxide (N_2O)

Nitrous oxide is one of the most common greenhouse gases occurring in high concentrations in the atmosphere, and has the ability to deplete the ozone layer. Nitrous oxide is a result of both natural and anthropogenic sources; however, the man-made sources are increasing at an alarming rate when compared to natural sources of N_2O. The burning of fossil fuel (coal) for electricity generation is the major source of nitrous oxide (Hayhurst and Lawrence, 1992).

2.7.2 Impacts of Climate Change

Africa is a continent under pressure from climate stresses and is highly vulnerable to the impacts of climate change. Different areas in Africa have variable climatic time scales over time. Floods and droughts can occur in the same area within months of each other, and these events can lead to famine and widespread distribution of socio-economic well-being (UNFCCC, 2007).

Many factors contribute and compound the impacts of current climate variability in Africa and will have negative effects on the continent's ability to cope with climate change. These include poverty, illiteracy and lack of skills, weak institutions, limited infrastructure, lack of technology and information, low levels of primary education and health care, poor access to resources, low management capabilities and armed conflicts. The over-exploitation of land resources including forests, increase in population, desertification and land degradation pose additional threats (UNDP, 2006).

Climate change will affect many sectors such as water resources, agriculture and food security, ecosystems and biodiversity, human health and coastal zones. Cruz *et al* (2007) noted that land and ecosystems are being degraded, threatening to undermine food security. In addition water and air quality are deteriorating while continued increase in consumption and associated waste have contributed to the exponential growth in existing environmental problems.

Africa will face increasing water scarcity and stress with a subsequent potential increase of water conflicts as almost all of the 50 river basins in Africa are transboundary (Ashton, 2002; De Wit and Jacek, 2006). Agricultural production relies heavily on rainfall and will be severely undermined, particularly for subsistence farmers in Sub-Saharan Africa. Fischer *et al.* (2002) recognized that under climate change

most agricultural land will be lost, with shorter growing seasons and lower yields. This will cumulatively result in more people at risk of hunger due to climate change.

Due to climate change various regions in Africa will be vulnerable to a number of climate sensitive diseases such as malaria, tuberculosis and diarrhoea (Guernier *et al*., 2004). The rising temperatures due to climate change are altering the geographical distribution of disease vectors which are migrating to new areas and higher altitudes (Boko *et al*., 2007). According to Harris and Baneth (2005), future climate variability will also interact with other stresses and vulnerabilities such as HIV/AIDS which is already reducing the life expectancy, and conflict and war, resulting in increased susceptibility and risk to infectious diseases (cholera and diarrhoea) and malnutrition for adults and children (WHO, 2004).

Climate change is an added stress to already threatened habitat's, ecosystems and species in Africa, and it is likely to trigger species migration which will lead to habitat destruction and reduction. Over 50% of the total biodiversity is at risk due to reduced habitat and other human-induced pressures (Boko *et al*., 2007). The rise in sea levels has the potential to cause impacts on the African coastlines by threatening the lagoons, mangrove forests and the already degraded coral reefs; furthermore, it is likely to impact the urban centres and ports of Africa such as Cape Town and Maputo.

2.7.3 Mitigation of Climate Change

Human responses to climate change falls into two categories namely adaptation and mitigation strategies. Mitigation strategies of climate change is the human ability to intervene in order to reduce or stop the sources or enhance the sinks of greenhouse gases. The main objective of mitigation is to reduce the harmful effects of climate change especially from man-made activities (Ogola and Auwour., 1997).

Mitigation and adaptation of climate change can work concurrently to stabilize greenhouse gas concentrations in the atmosphere at a level to prevent dangerous anthropogenic interference with the climate system. This can happen within a time frame sufficient to allow ecosystems to adapt to ensure that food production is not threatened and to enable economic development to proceed in a sustainable manner.

Reducing and limiting the emissions of greenhouse gases in the atmosphere, requires considerable examination and control of individual greenhouse gases. Energy use

efficiency is the answer to controlling anthropogenic emissions of greenhouse gases and this requires the following measures (Ogola, 1997):

- Changes in lifestyles, mobility patterns and transport systems;
- Improving the efficiency of energy supply and use;
- Strong policy measures calculated to reduce greenhouse gas emissions, however improvements in energy efficiency requires strong policy measures to offset growth in energy demand; and
- Moving from fossil fuel use to more energy friendly sources such as renewable sources of energy.

Fossil fuel could be avoided completely by switching to solar, wind, biomass, hydropower and geothermal energy generating technologies (Ogola, 1997). These energy systems may account for about 20% of the world energy consumption.

Emissions of CO_2 to the atmosphere can be reduced by:

- Implementing better technologies for the removal or disposal of CO_2;
- Increasing the use of low CO_2 emitting fuels; and
- Imposing tough penalties and high taxes.

2.7.4 Adaptation of Climate Change

Adaptation is a process through which societies make themselves better able to cope with an uncertain future. Adapting to climate change involves taking the right measures to reduce the negative effects of climate change by making the appropriate adjustments and changes (UNFCCC, 2007). However, Ogola (1997) argues that adaptation can either be anticipatory or forced and its strategies require the adjustment of the environment or human ways of using it to reduce the consequences of a changing climate.

Anticipatory adaptation requires large financial boosts to accommodate some environmental modification measures such as changes in coastal defences and fresh water supply systems that require large investments in infrastructure. At individual level, adjustments in lifestyle and behavioural changes would be required (Ogola *et al*., 1997).

Global warming threats and impacts are widespread as a result the type, frequency and intensity of extreme events such as tropical cyclones (hurricanes and typhoons), floods, drought and heavy precipitation events that are expected to rise even with relatively small average temperature increases (Meehl *et al*. 2007). Human activities in terms of carbon dioxide have increased the atmospheric concentrations from a pre-industrial value of 278 ppm to 379 ppm by 2005, and the average global temperature rose by 0.74 ^{o}C. With this in mind it is evident that global warming due to greenhouse gases especially carbon dioxide will require measures for adaptation (UNFCCC, 2007).

Adaptation to climate change in developing countries is important, however, the limitations that exist in capacity, both human and financial resources, makes adaptation difficult. Adaptation in developing countries will be best suited when adaptation approaches address the various environmental stresses and factors such as poverty alleviation, enhancement of food security and water availability, combating land degradation and reducing loss of biological diversity and ecosystem services, as well as improving adaptive capacity.

CHAPTER 3: MATERIALS AND METHODS

In order to accomplish the objectives of this research work, the following field, and laboratory methods and procedures were adopted (Fig. 3.1).

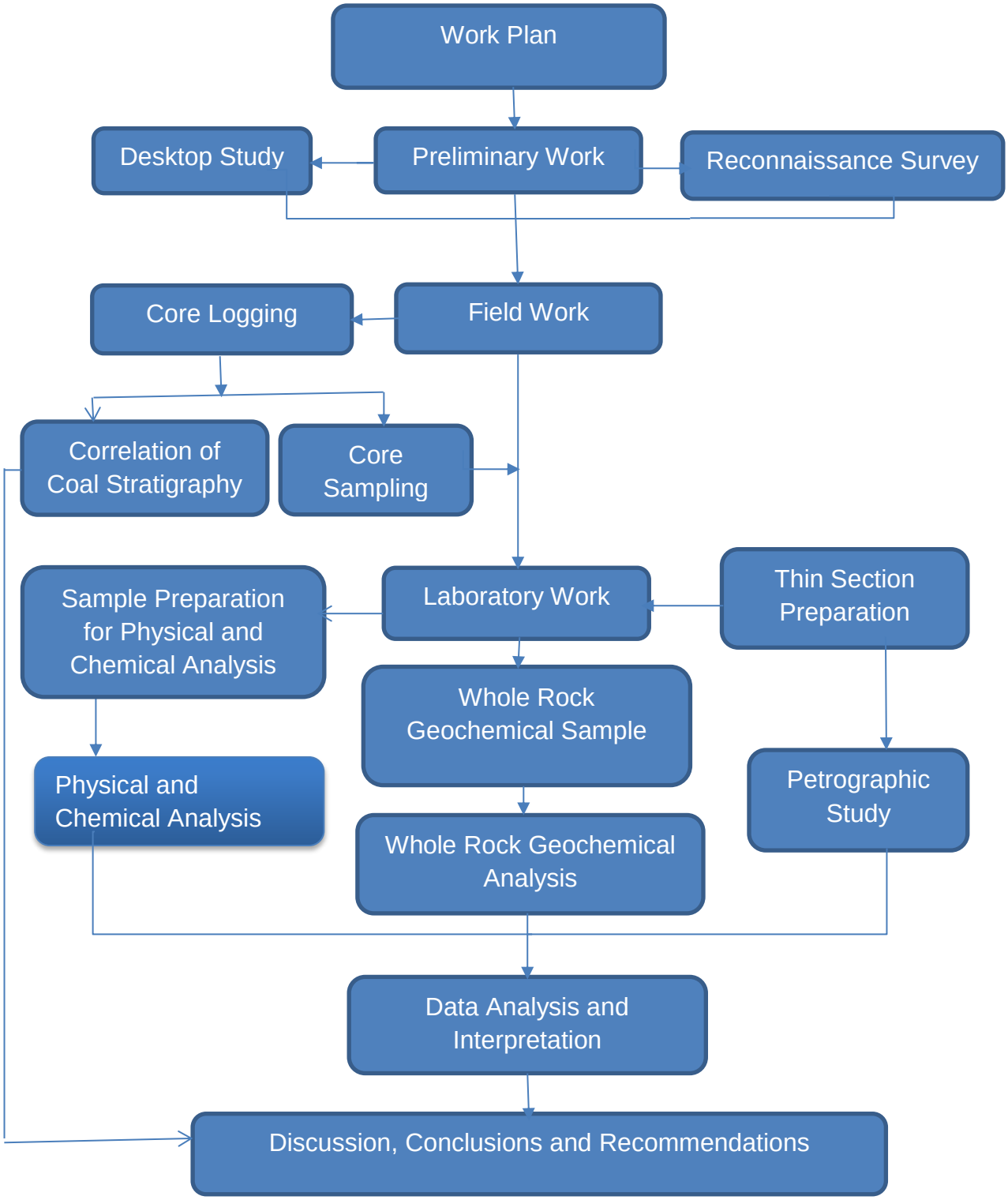

Figure 3.1: Flow chart showing the methods and procedures that were applied in the study.

3.1 Preliminary Work

Preliminary work for this research was carried out in two stages namely: desktop study and reconnaissance survey (Fig. 3.1).

3.1.1 Desktop study

Desktop study was undertaken in order to acquire information about the study area before fieldwork. During desktop study, various sources of information about the study area were used in order to ascertain the geology of the Karoo Basin, and especially the geology of the Limpopo Coalfields. This includes the review of previous technical reports, geological maps, internet information, books, topographical maps, journals and aerial photographs.

3.1.2 Reconnaissance Survey

Reconnaissance survey was undertaken by going to the field with the objective of familiarizing oneself with the surrounding environment of the study area. This helped to identify areas of significant interest for the study and to be aware of the surroundings. During this stage, the geological setting, topography, drainage, soil type and sedimentary facies were investigated.

3.2 Fieldwork

Fieldwork involved collecting information about the distribution of rock units, identifying coal deposits and coal characteristics, within the study area, geological structures which helped establish an understanding of the geological history of the area. Core logging and sampling of the rocks was carried out in the field. The purpose of conducting core logging was to ascertain the stratigraphic position of coal. Photographs of sections of core that were logged and samples were taken. The samples were clearly marked in the field using a permanent marker and later separated and selected for laboratory work, for example, sample preparation for thin sections and laboratory analysis.

Tools that were used during fieldwork included the following; tape measure, geological hammer, hand lens, sample bags, clino-ruler, GPS, note book and marking pens.

The Makhado Coal found within the Soutpansberg Coalfield has been the centre of recent exploration in Limpopo Province. Several boreholes were drilled in the area, followed by core logging. Out of these, only 3 boreholes, namely; F578001, F578007 and R637002 were correlated because they occurred along the same strike line (Fig 3.2). This project consisted of boreholes from various farms which have various rock types such as calcrete, sandstone, coal, mudstones that were predominant in the area.

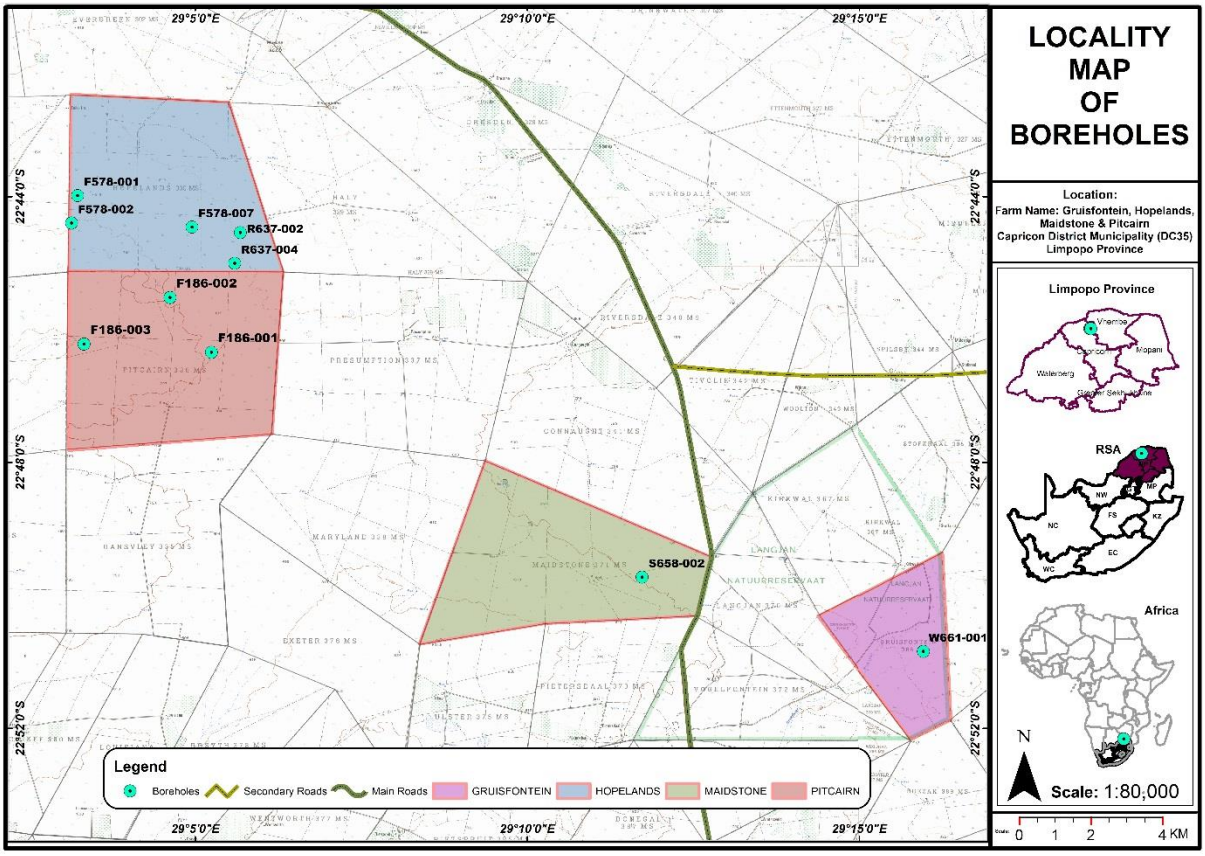

Figure 3.2: Map showing locations of boreholes that were logged in the Soutpansberg Coalfield (Google Maps, 2016; Modified by Phoenix Consultants; 04 December 2016).

3.2.1 Core Logging

Drilling of the boreholes in the study area was accompanied by core logging. A total of 10 boreholes were drilled and logged. Core logging involved the identification and description of rock forming minerals, rock types; their grain size, texture, thickness, structure and coal occurrence. Core logging was done to establish the regional variation of the coal stratigraphy of the Soutpansberg Coalfield. The tape measure was used to measure the rock intervals and the distances within the hanging wall, coal horizon and footwall. The GPS was used to precisely locate the boreholes and any

outcrops, and a clino-ruler was used to measure the geological/sedimentary structures and thickness of grain sizes in the field.

Field outcrops were studied in order to understand the sedimentary structures within the rocks, thus assisting in understanding the depositional environment under which these rocks were formed. All this information was recorded in a logbook. Out of the logged boreholes, four namely, F578001, F578002, R637002 and R637004 intersected the hanging wall, coal seams, and footwall lithologies. These boreholes were logged in detail to give a full stratigraphic profile of the Soutpansberg Coalfield.

Summary logs were done on boreholes F578007, S658002, W661001, F186001, F186002 and F186003 in order to ascertain the boundaries (contacts), variations and type of coal between the hanging wall and coal seam. The following tools were used during core logging: water spray, permanent marker, hand lens, magnetic pencil, and a clino-ruler. The following steps were followed during core logging:

- Spraying the cores with water using a water spray in order to remove dust and to enhance visibility of minerals, contacts and geological structures as a result the cores are easily documented when they are wet.
- The contacts and geological structures were marked with a marker, the depth was measured with a clino-ruler and the measurements were recorded on a log sheet as well as the grain size and rock textures. These were identified using a hand lens. A magnetic pencil was also used to identify lithologies that have magnetic properties.

Borehole R637002

The Rissik 637002 borehole was drilled to a depth of 221.58 m and logging was done from 1.32 m due to surface weathering (Fig. 3.2). The borehole intersected the hanging wall, coal seams and footwall lithologies. Borehole R637002 has 3 coal seams, namely; coal seam 1, coal seam 2 and coal seam 3 (Fig. 3.3).

Coal Seam 1

Coal seam 1 along borehole R637002 occurred at a depth interval of 216.88-211.88 m and consisted of a tillite which was grey in colour, comprising of consolidated masses of unweathered blocks (large angular rock bodies) and glacial till (unsorted

and unstratified rock material) in the rock floor. The matrix which comprised a large percentage of the rock had a dark grey to greenish colour and consisted of angular quartz and feldspar grains; and rock fragments in a fine-grained paste.

Coal seam 1 was embedded within the mudstone with a thin coal layer being separated by an intercalating band of mudstone, about 2.6 m thick. The entire coal seam was about 6 m thick with the main coal layer being 3 m; and was characterised by a black to dark black colour with vitreous lustre on cleat surfaces.

Coal seam 2

Coal seam 2 was embedded within the mudstone and occurred at a depth of 203.29 – 187.22 m, having a maximum thickness of 16.07 m; with intercalations of mudstone. The footwall of coal seam 2 was characterised by mudstone with a very thin layer of carbonaceous shale that was about 0.58 m thick. The mudstone consisted of a mixture of clay and silt size particles (very fine-grained), having a light black to dark grey colour indicating the degree of maturity; as well as the degree of carbonaceous content.

The mudstone was not competent and had pyrite, the colour of mudstone made the contact between coal seam 2 and underlying mudstone footwall lithology not to be very clear. Carbonaceous shale consisted of silt size particles and a dull black colour. The hanging wall of coal seam 2 consisted of mudstone and carbonaceous shale, making this coal seam to be the thickest seam in this borehole.

Coal Seam 3

Coal seam 3 occurred at a depth interval of 170-160.77 m. Coal seam 3 was embedded within the mudstone with a thin carbonaceous shale layer on the footwall of the seam being separated by an intercalating band of mudstone; that is about 1.37 m thick. The entire coal seam 3 was about 9.23 m thick (Fig. 3.3).

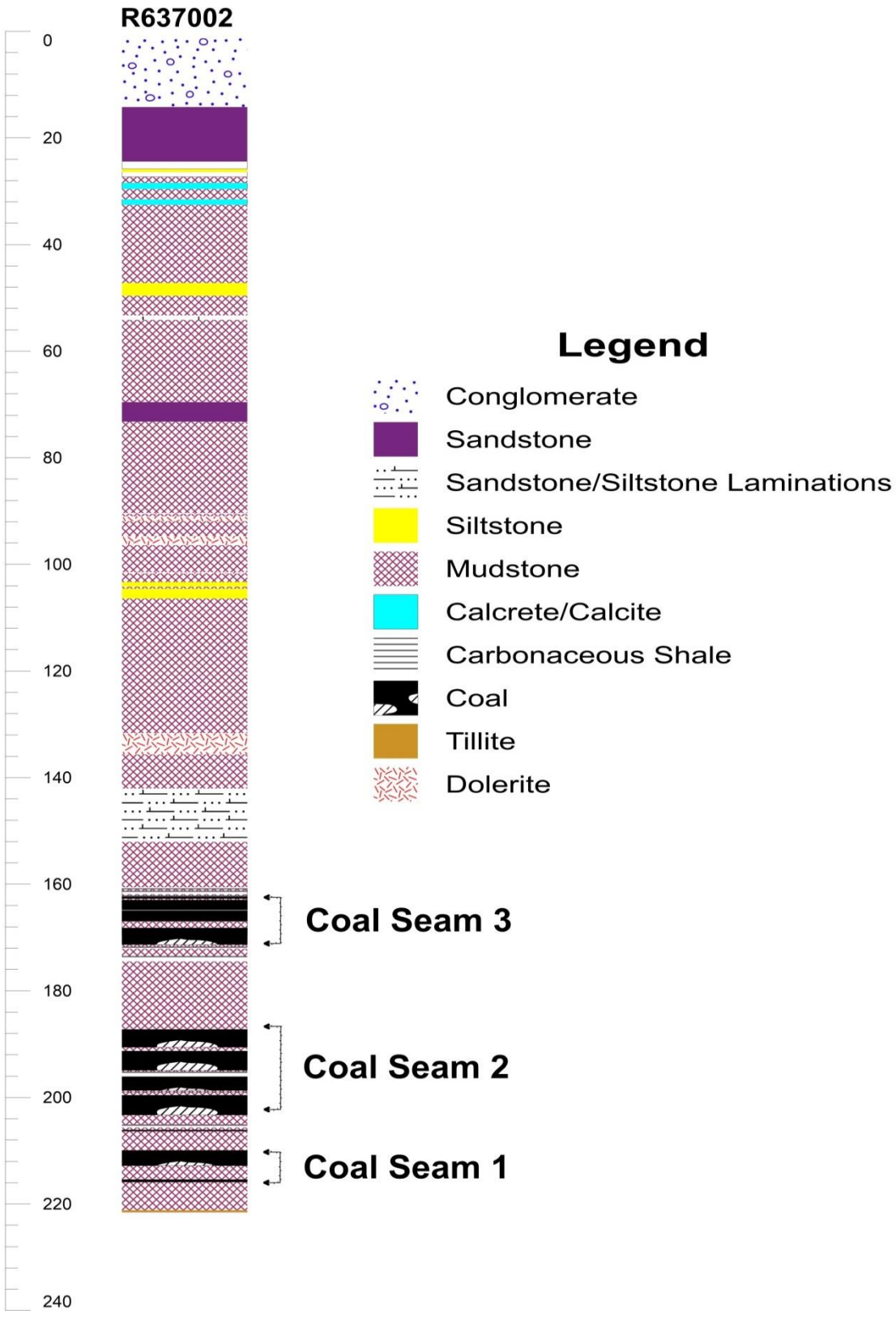

Figure 3.3: Borehole R637002 showing different lithologies and coal seams on Rissik Farm.

Borehole R637004

Borehole R637004 was drilled at Rissik Farm, attaining a total thickness of 59.43 m and had intersected the coal seam zones at 35.60 m below the surface. Borehole R637004 has 3 coal seams, namely; coal seam 1, coal seam 2 and coal seam 3 (Fig. 3.4).

Coal Seam 1

The footwall of coal seam 1 along borehole R637004 occurred at a depth interval of 59.43-46.95 m (12.48 m thick) and consisted of a tillite and siltstone. Coal seam 1 was embedded within the mudstone and siltstone; with the mudstone having a thickness of about 1 m, while the siltstone was characterised by a grey colour and silt size particles. The entire coal seam 1 was about 3.36 m thick.

Coal Seam 2

Coal seam 2 is embedded within the mudstone with the main coal seam layer having a maximum thickness of 2.15 m. The mudstone has a thickness of 0.96 m and was characterised by silt size particles.

Coal Seam 3

Coal seam 3 occurred at a depth of 39.85 m, and was embedded within the mudstone with a thin coal layer being separated by an intercalating band of mudstone, that is about 0.33 m thick. The maximum thickness of the entire coal seam 3 was about 4.25 m thick, with the main coal layer being 2.17 m thick. From the 3 coal seams in borehole R637004, coal seam 3 is the thickest seam.

The hanging wall of coal seam 3 consisted of an isolated thin layer of coal that was about 0.17 m thick and a carbonaceous shale that was having a thickness of 0.32 m thick; embedded and being separated by intercalating bands of mudstone, about 0.68 m thick.

The occurrence of mudstone above and below the coal seams as well as intercalations of mudstone was interpreted as the deposition by clay settling out of suspension in low energy transporting mode. The silt size particles within the mudstone were due to

periods of increased flow and sediment supply, displaying a series of cyclicity on the environment of deposition.

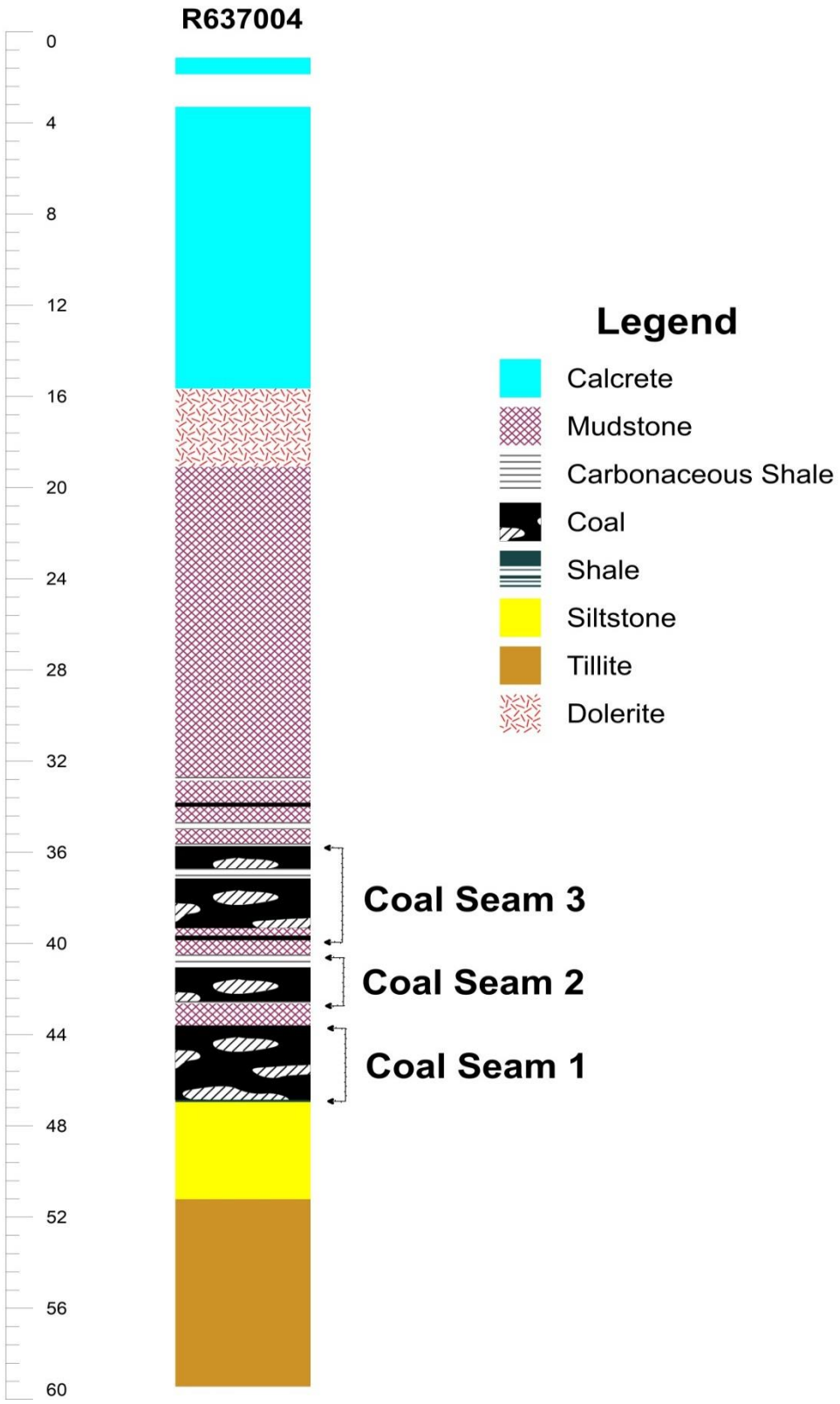

Figure 3.4: Borehole log of R637004 showing lithological variations through the hanging wall, coal seams and footwall.

Borehole F578001

The Fannie 578001 borehole was drilled to a depth of 197.67 m and logging was done from 2 m due to surface weathering (Fig. 3.5). The borehole intersected the coal seam zone at 146.75 m below the surface. The coal seam zones in this borehole comprised 4 coal seams, namely; coal seam 1, coal seam 2, coal seam 3 and coal seam 4.

Coal Seam 1

Coal seam 1 was embedded within the mudstone and the coal seam layer was about 2.51 m thick.

Coal Seam 2

Coal seam 2 was embedded within the mudstone and the coal seam layer was about 3.38 m thick. The mudstone and carbonaceous shale were characterised by a very dark black colour; furthermore the contact between the carbonaceous shale and coal was gradational.

Coal Seam 3

Coal seam 3 was embedded within the mudstone and dolerite dyke intrusion of about 1.38 m thick (Fig. 3.5). This coal seam occurred at a depth range of 167.58-166.03 m (1.55 m thick). The dolerite dyke intrusion was characterised by a greenish grey colour with fine to medium grains.

Coal Seam 4

Coal seam 4 was embedded within the mudstone and sandstone/siltstone laminations with a thin layer of coal being separated by an intercalating band of mudstone, about 0.91 m thick. The maximum thickness of the entire coal seam 4 was about 4 m thick with the main coal layer being 2.41 m thick.

From this study it was observed that the sandstone/siltstone laminations occurred at the upper part of the fining-upward sequences where sandstone, mudstone and coal were present. The rocks were characterised by very fine grained, thin fining upward sequences that indicated lithologies deposited in floodplain conditions that were formed by unidirectional flow under fluvial conditions.

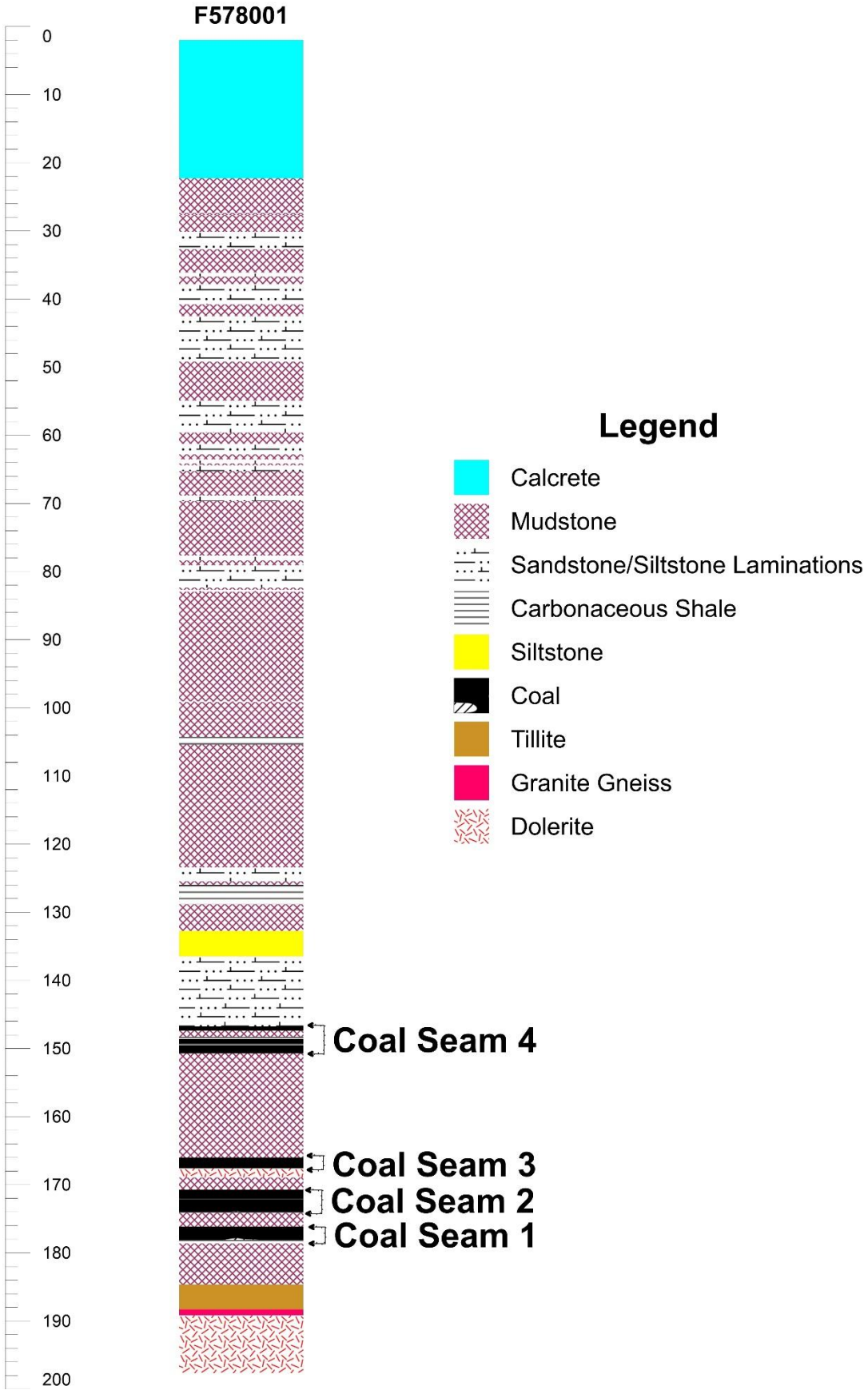

Figure 3.5: Borehole F578001 showing lithological variations and the occurrence of coal seams.

Borehole F578002

Borehole F578002 was drilled to a depth of 74.65 m and had intercepted the hanging wall, coal seams and footwall lithologies (Fig. 3.6). The borehole had 3 coal seams, namely; coal seam 1, coal seam 2 and coal seam 3. Furthermore this borehole comprised of various lithologies such as calcite, dolerite, sandstone which had siltstone laminations, mudstone, carbonaceous shale, coal, siltstone and tillite.

Coal Seam 1

Coal seam 1 occurred at a depth interval of 65.45 – 63.13 m and is embedded within the siltstone footwall and a mudstone hanging wall. The maximum thickness of this coal seam was about 2.32 m thick and has a clear contact with the footwall lithology. The siltstone was about 3.54 m thick and characterised by a greyish colour with very fine grained particles (silt size particles).

Coal Seam 2

Coal seam 2 was embedded within the mudstone with 2 separate coal layers of different thickness ranging from 1.78 to 0.45 m thick being separated by an intercalating band of mudstone, about 0.46 m thick. The entire coal seam 2 was about 8 m thick with the main coal layer being 5.61 m thick; this makes coal seam 2 in this borehole to be the thickest coal seam.

The coal was characterised by glittering vitreous lustre and was dark black in colour, while mudstone was composed of a mixture of clay and silt size particles (very fine grained), having a light black to dark grey colour indicating the degree of maturity as well as the degree of carbonaceous content within the mudstone.

Coal Seam 3

Coal seam 3 was embedded within the mudstone and characterised by thin intercalating layers of carbonaceous shale. The footwall of coal seam 3 was characterised by mudstone with a dolerite dyke intercalation occurring at a depth interval of 49.28. This coal seam occurred at a depth interval of 45.35 - 48.21 m (2.86 m thick). The carbonaceous shale consisted of silt size particles and a dull black colour while the dolerite intrusions were characterised by medium (intermediate) grain sizes

with a greenish black colour which indicated that it had been influenced by the dark minerals in mudstone.

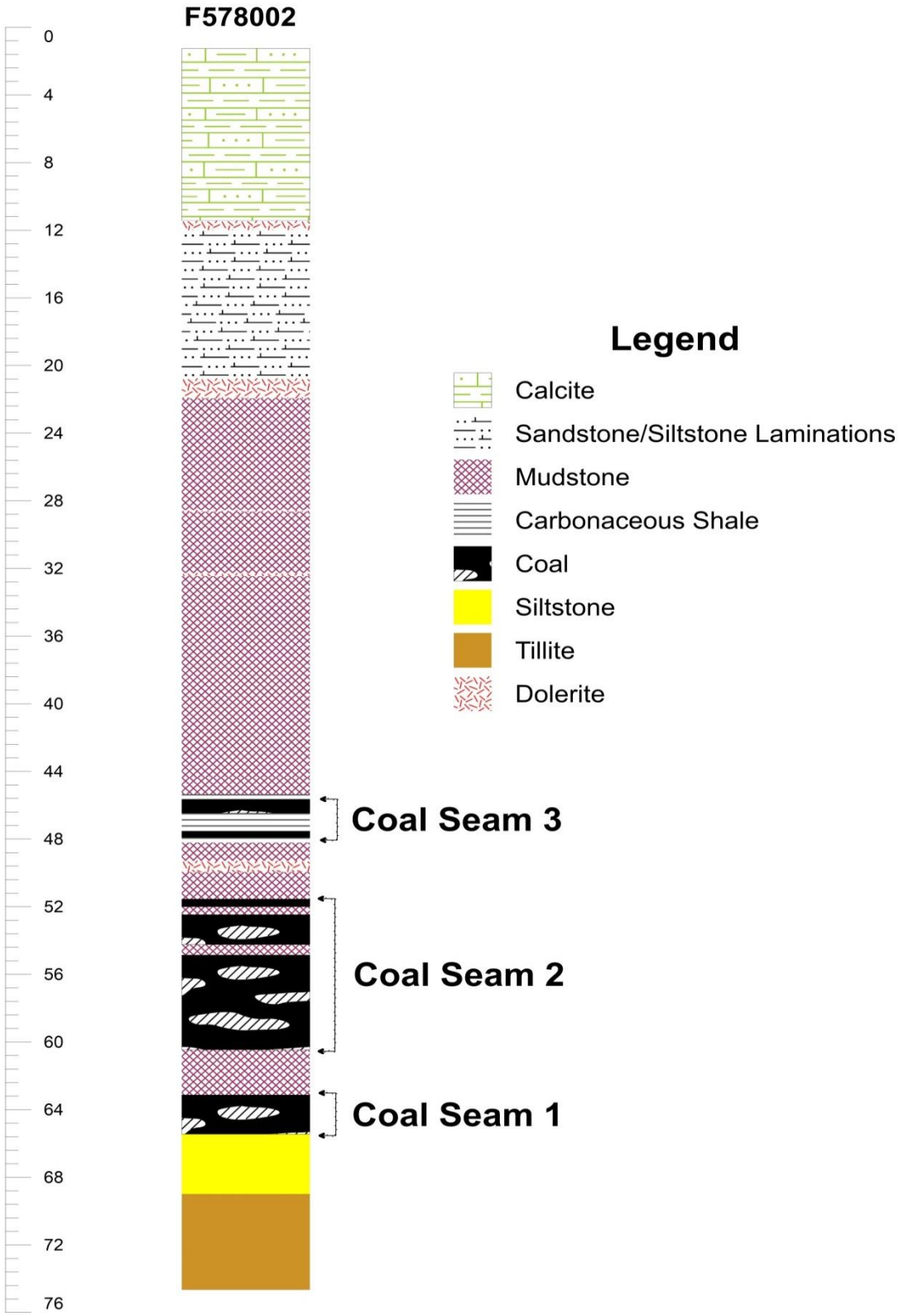

Figure 3.6: Borehole F578002 intersected the hanging wall, coal seams and footwall lithologies, showing three coal seams.

Borehole F578007

A summary log was done for borehole F578007 which was drilled to a depth of 176.69 m and intersected the hanging wall and coal seams. The coal seam zone comprises 5 coal seams (Fig. 3.7).

Coal Seam 1

Coal seam 1 was intersected at depth interval of 168.60 - 166.36 m and was embedded with a siltstone footwall and a mudstone hanging wall that was about 2.8 m thick. The maximum thickness of the entire coal seam was about 2.24 m thick. The siltstone was having a grey colour with silt size particles and the carbonaceous shale had a vitreous lustre with a dark black colour together with coal. The association between the mudstone, coal and carbonaceous shale can be interpreted as an increasing order of facies maturity with depth.

Coal Seam 2

Coal seam 2 was embedded within the mudstone with moderate to thin coal layers being separated by intercalating bands of mudstones ranging in thickness from 0.83 to 0.58 m thick. The entire coal seam had a maximum thickness of about 6.61 m thick; this was the thickest coal seam within the borehole and the coal was characterised by a very dark black colour and rich organic matter.

Coal Seam 3 and 4

Coal seam 3 was embedded within the mudstone and the coal seam layer attained a maximum thickness of about 2.76 m. Coal seam 4 was embedded within the mudstone with a thin layer of coal being separated by an intercalating band of mudstone that was about 1 m thick. The entire coal seam has a maximum thickness of 4.87 m, making coal seam 4 to be the second thickest seam within this borehole F578007.

Coal Seam 2

Coal seam 5 was embedded with a mudstone footwall and a sandstone/siltstone laminations hanging wall, with a moderately thick layer of coal being separated by an intercalating band of mudstone. The entire coal seam was about 3.39 m thick, the

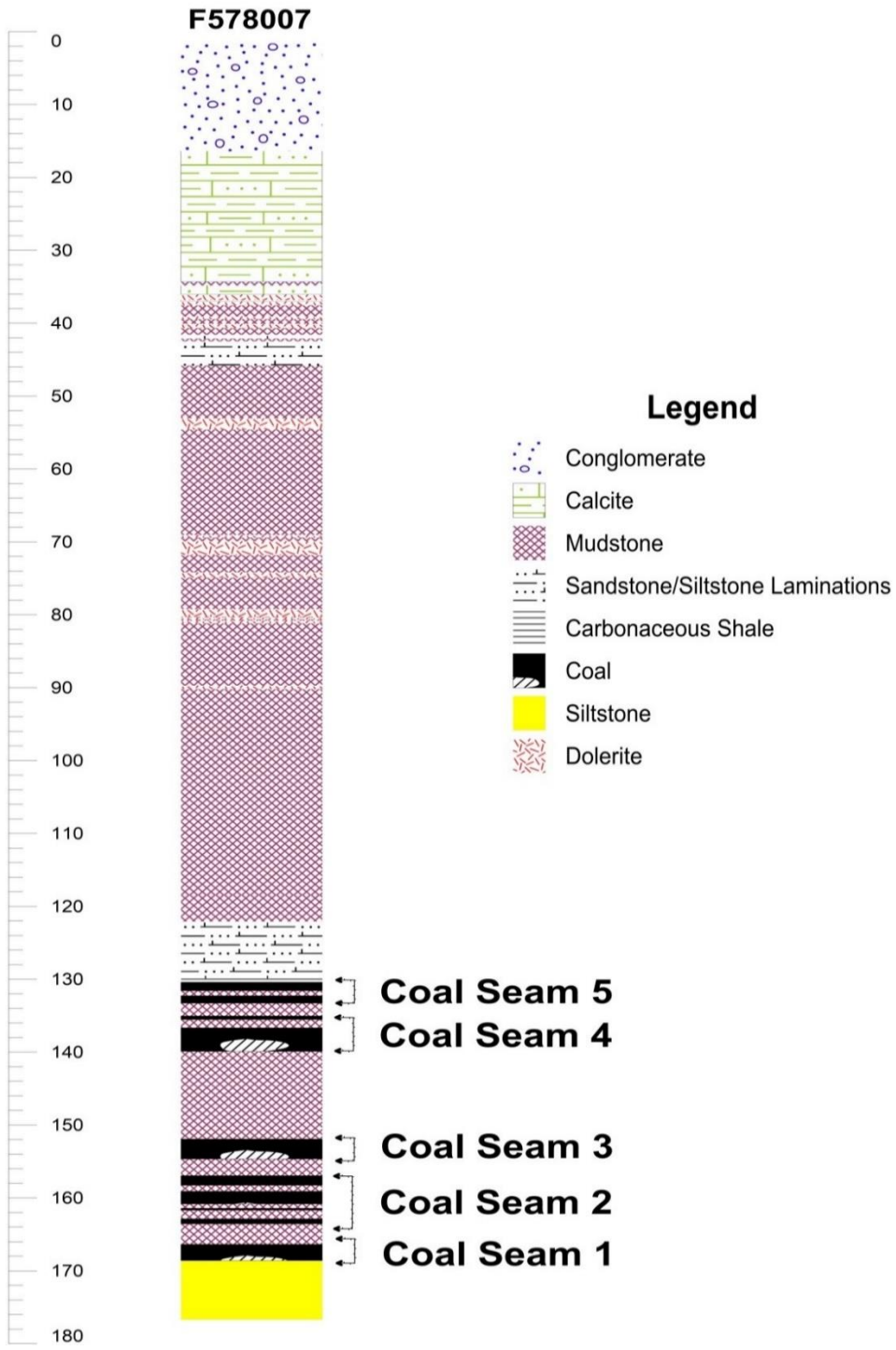

Figure 3.7: Borehole F578007 showing variation of lithologies, through the hanging wall, coal seams and footwall.

sandstone with siltstone laminations was intersected at a depth of 122.08 m whereby the sandstone was characterised medium to fine grained size particles and shiny quartz particles; the siltstone laminations were characterise by silt size particles (Fig. 3.7). From this study it was observed that the sandstone/siltstone laminations occurred at the upper part of the fining-upward sequences where sandstone, mudstone and

coal were present; and was characterised by deposition in floodplain conditions that formed deposits by unidirectional flow under fluvial conditions.

Borehole S658002

The borehole S658002 was drilled to a depth of 196.35 m and logging was done from 5.6 m due to surface weathering. The borehole intersected the hanging wall and coal seams, and was found to be 25.23 m less when compared to borehole R637002. Borehole S658002 has 3 coal seams, namely; coal seam1, coal seam 2 and coal seam 3 (Fig. 3.8).

Coal Seam 1

This coal seam 1 occur at a depth interval of 191.92 – 183.60 m, seam 1 was embedded within the mudstone and the entire coal seam has a maximum thickness of 8.32 m thick.

Coal Seam 2

Coal seam 2 was embedded within the mudstone with moderately thick and thin layers of coal being separated by intercalating bands of mudstones. The main coal layer was about 7.25 m thick with the entire coal seam having a maximum thickness of 27.88 m thick. This made coal seam 2 to be the thickest seam within the coal seam zone of borehole S658002. The coal in the coal seam was characterised by a very dark black colour, with a texture ranging from fine vitreous to porphoritic (ophitic); and fine to medium grain sizes. This coal seam has mudstone intercalations which were highly carbonaceous.

Coal distribution and thickness was largely controlled by a combination of factors namely; palaeoclimate, palaeography and palaeo-tectonics. All these influenced the environment of deposition which was fairly gentle and shallow causing underwater upliftment to occur thereby causing the sediments to be exposed when the seawater drop to become local sources of terrigenous clasts.

Coal seam 3

The coal seam 3 was embedded within a mudstone with a thin isolated layer of coal that was about 0.26 m thick, separated and embedded within the mudstone (Fig. 3.8).

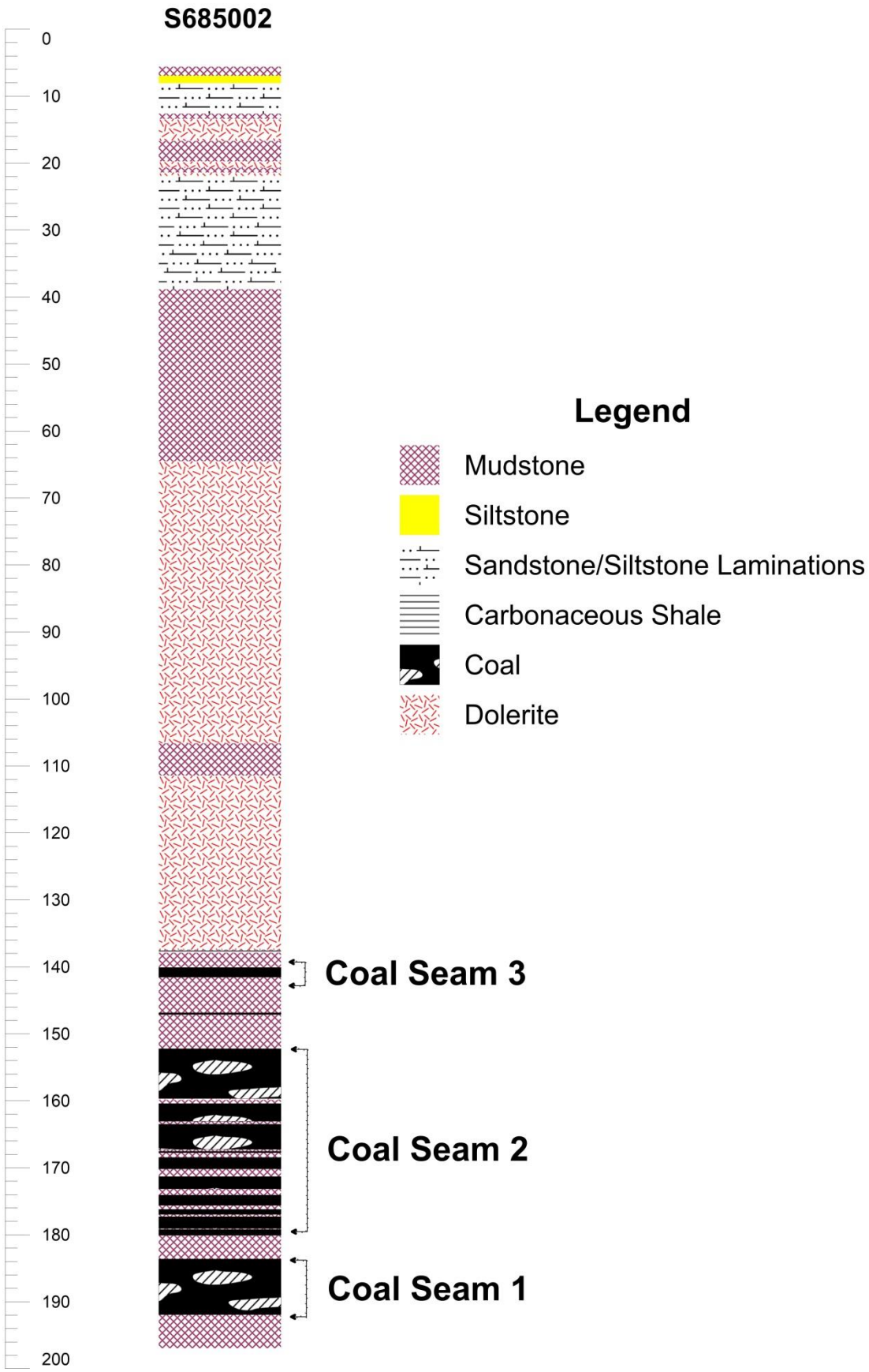

Figure 3.8: Borehole S658002 showing three coal seams with coal seam 3 being the thickest.

Coal seam 3 has no clear contact with the overlying layer and the degree of maturity of the mudstone within the different coal seams was directly proportional to the grain sizes of the rock ranging from silt size particles to vitreous texture depending on the carbonaceous content within the rock. The occurrence and distribution of the dolerite dyke influenced the occurrence of the carbonaceous below the mudstone of coal seam 3.

Borehole W661001

Borehole W661001 was drilled at Wildebeesthoek Farm up to a depth of 185.47 m. A summary log was done on this borehole and was found to have 2 coal seams, namely coal seams 1 and coal seam 2 (Fig. 3.9).

Coal Seam 1

Coal Seam 1 was embedded within the carbonaceous shale and dolerite dyke intrusion on the footwall of the coal seam; with a mudstone on the hanging wall. The dolerite dyke intrusion was found to have a thickness of 85.47 m thick, while the coal layers were found to be intercalated by bands of mudstone and carbonaceous shale with coal. The maximum thickness of the main layer of coal was about 4.22 m thick, with the entire coal seam having a maximum thickness of 22.35 m (Fig. 3.9).

The dolerite intrusion consisted of medium to fine grained particles, however the coal ranged in colour from shiny dark black to dull dark black and having a vitreous texture. Carbonaceous shale had a vitreous texture and was dark black in colour

Coal Seam 2

The footwall of coal seam 2 occurred at a depth of 57.45-77.65 m characterised by mudstone that was grey to dark colour with fine to medium grain sizes. This coal seam 2 has mudstone intercalations, with the coal being organic rich, having a dark black colour.

Coal seam 2 was embedded within the mudstone with moderately thick and thin coal layer being separated by intercalating bands of mudstone and carbonaceous shale. The entire coal seam was about 8.27 m thick with the main coal layer being characterised by a maximum thickness of about 2.27 m. The coal seam comprised

massive patches of pyrite and the dolerite dyke intrusion made the contact between the coal seams and the overlying lithologies to be clear (Fig. 3.9).

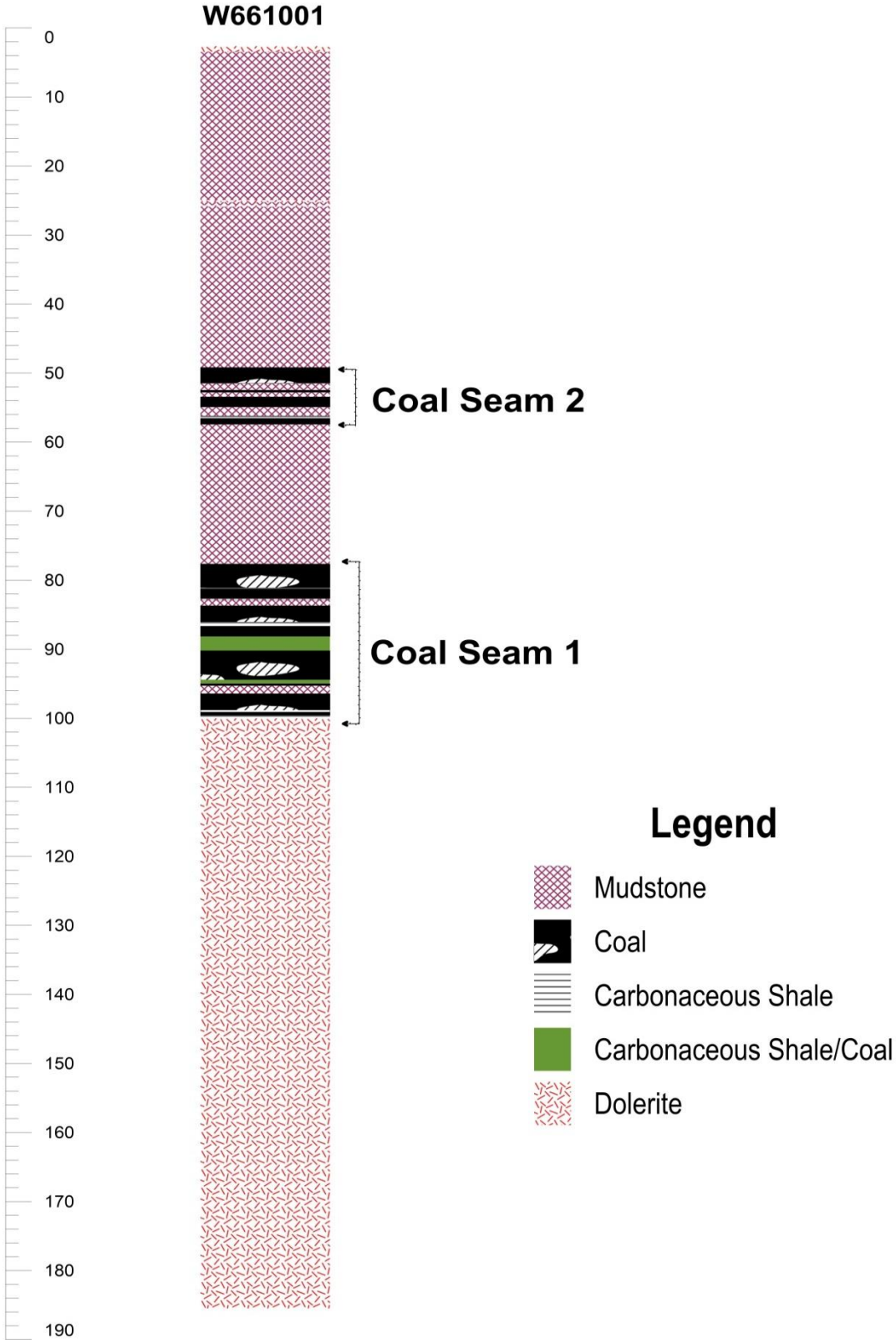

Figure 3.9: Borehole W661001 showing positions of coal seams and lateral distribution of the dolerite dyke.

Borehole F186001

Borehole F186001 was drilled to the depth of 150 m and comprised of 3 coal seams namely; coal seam 1, coal seam 2 and coal seam 3 (Fig. 3.10).

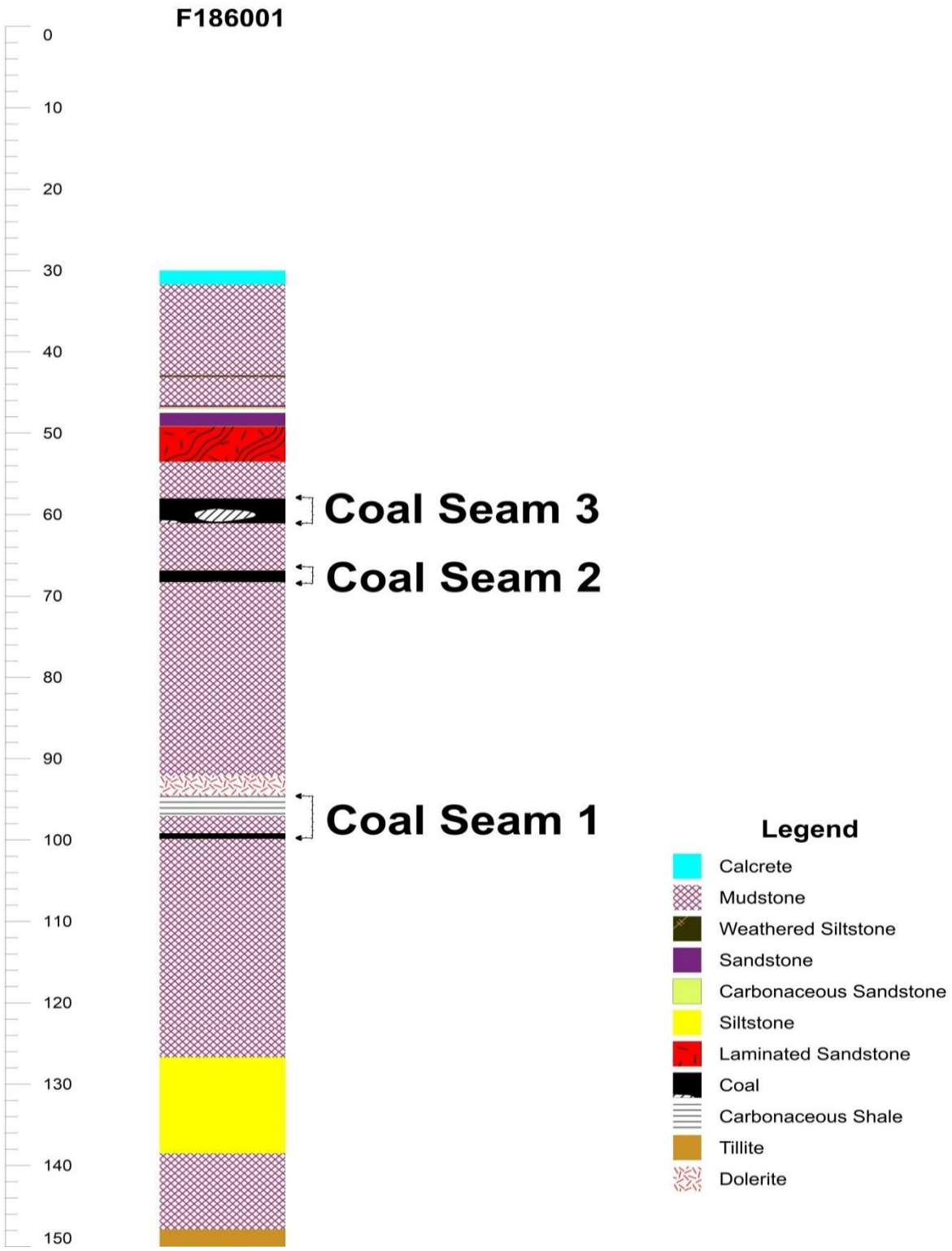

Figure 3.10: Borehole displaying the different lithologies at Fannie Farm within the Soutpansberg Coalfield.

Coal Seam 1

The footwall of coal seam 1 along borehole F186001 occurred at a depth interval of 150.00 – 99.83 and consisted of tillite, mudstone and siltstone. Coal seam 1 was embedded with the mudstone with the main seam having a thickness of 0.65 m, and the carbonaceous shale with coal having an entire thickness of 2.46 m.

Coal Seam 2

The footwall of coal seam 2 occurred at a depth interval of 94.58 m, and the coal seam was embedded with the mudstone with the entire coal seam having a thickness of 1.44 m. The coal was characterised by a dark black colour with a vitreous texture.

Coal Seam 3

Coal seam 3 was embedded within the mudstone and occurred at a depth interval of 61.05 – 58.00 m, having an entire thickness of 1.05 m. The mudstone above and below this coal seam was characterised by a dark grey colour with very fine (silt size particles) to fine grained particles.

Borehole F186002

Borehole F186002 was drilled at Fannie farm to a depth interval of 141.79 m and logging was done from 3.3 m due to surface weathering. The borehole intersected hanging wall, coal seams and footwall lithologies and comprised of 3 coal seams (Fig. 3.11).

Coal Seam 1

Coal seam 1 was interwoven within the mudstone with the main coal seam having a maximum thickness of 0.37 m, however this was recorded to be the thinnest coal seam within borehole F186001. The mudstone surrounding coal seam 1 was not competent and comprised of silt size particles with a dull black colour.

Coal Seam 2

This coal seam was embedded within a dolerite dyke intrusion on the footwall and mudstone on the hanging wall, however this seam recorded a maximum thickness of

about 1.54 m. The dolerite intrusion were characterised by medium grained size particles with a greenish grey colour.

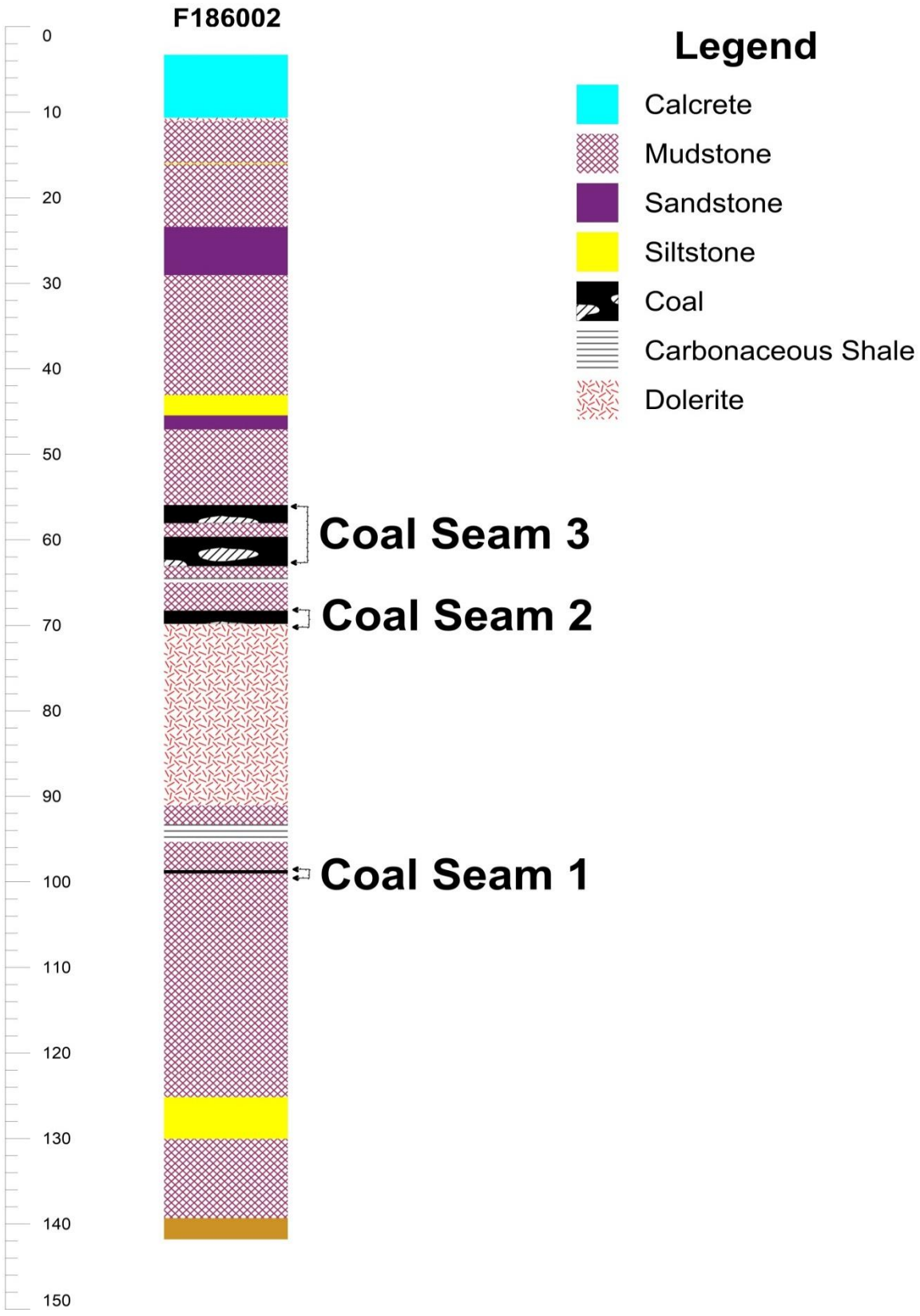

Figure 3.11: Borehole displaying the locations of various coal seams.

Coal Seam 3

The footwall of coal seam 3 occurred at a depth interval of 68.28 – 64.45 m; seam 3 was embedded within the mudstone with coal layers being separated by an intercalation of mudstone that was about 1 m thick. The main coal layer within the coal seam was about 3.42 m thick with the overall coal seam thickness of about 7.14 m; making coal seam 3 to the thickest the coal seam in borehole F186002.

Borehole F186003

Borehole F186003 was drilled to a depth of 147.85 m at Fannie farm; and intersected the hanging wall, coal seams and footwall lithologies (Fig. 3.12). Borehole F186003 comprised of 5 coal seams, namely; coal seam 1, coal seam 2, coal seam 3, coal seam 4 and coal seam 5. A summary log was done on this borehole.

Coal Seam 1

The footwall of coal seam 1 was characterised by mudstone and siltstone with this seam being embedded within the mudstone, thus having a thickness of approximately 2.14 m.

Coal Seam 2

The footwall of coal seam 2 was characterised by mudstone and carbonaceous shale, with the coal seam having a thickness of about 0.65 m.

Coal Seam 3

Coal seam 3 was embedded with the carbonaceous shale and mudstone and the seam was recorded to have approximately 2.52 m coal layer thickness.

Coal Seam 4

Coal seam 4 was characterised by 1.37 m thick of coal that was having a dark black colour with a glittering vitreous lustre.

Coal Seam 5

Coal seam 5 was the thickest coal seam attaining a maximum thickness of about 3.12 m and was embedded within the mudstone that was about 5 m thick.

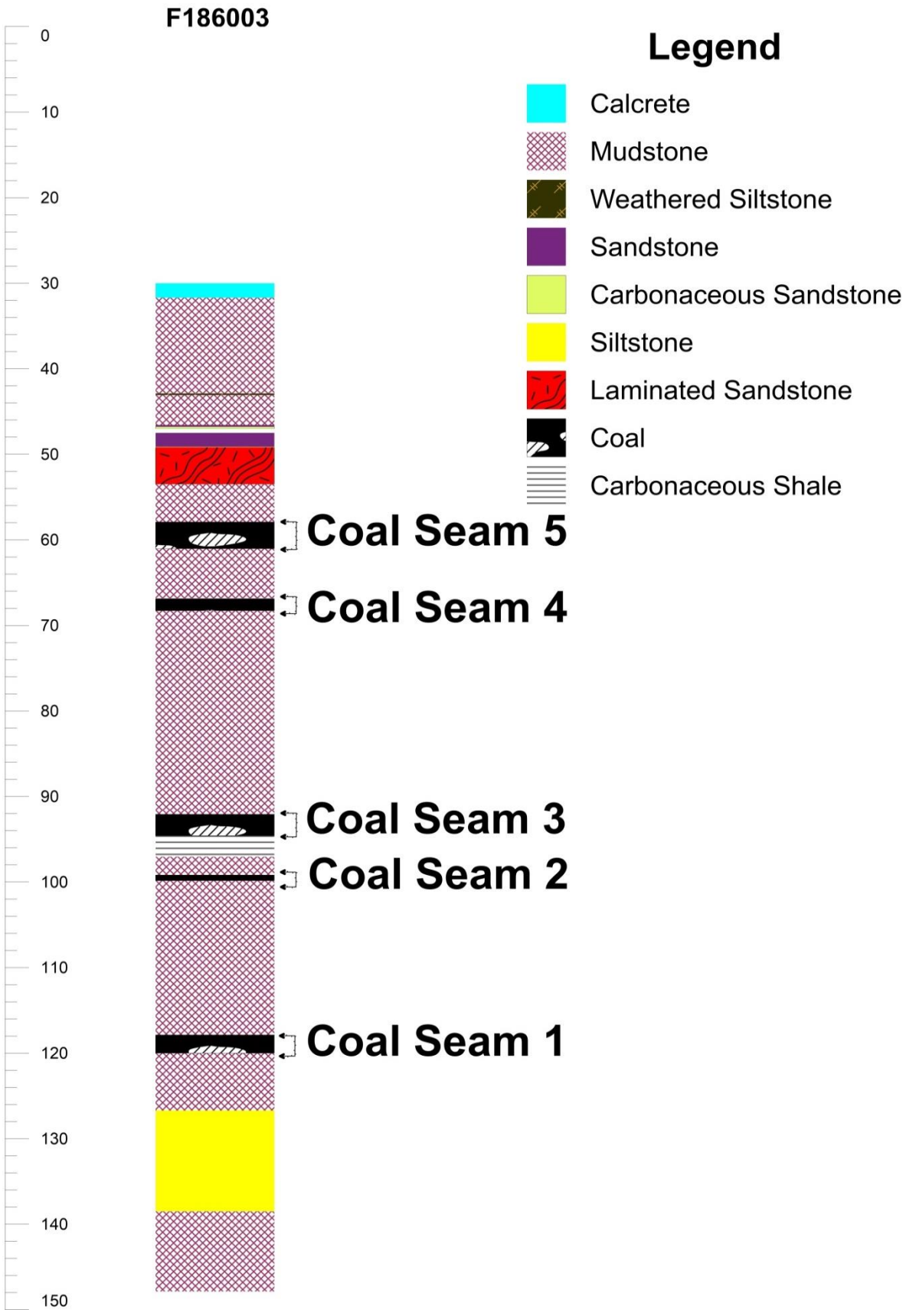

Figure 3.12: Borehole displaying the distribution of lithologies and various coal seams.

3.2.2 Core Sampling

Sampling was conducted simultaneously with borehole logging. Sampling was done along the coal seams, lithologies above and below the coal seams, and as well as along the contacts between the lithologies (Fig. 3.13). Sampling intervals varied according to variations in the lithologic units throughout the core and the total number of samples collected from each borehole was determined by the position and thickness of the lithologies.

Core samples were collected by splitting the core in half lengthways, sampling one half and storing the other as duplicate so that a continuous vertical portion of the core remained. Core sampling was conducted for the purposes of studying the rock mineralogy and chemistry. Sample bags made of thick polythene were used to collect samples and each sample was numbered accordingly.

During core logging, rock specimens were collected from 3 boreholes that were logged. All the collected rock samples were taken for laboratory work such as petrography, XRF geochemical analysis and coal tests analysis to study the general characteristics of coal. A total of 18 samples were collected from boreholes F186001, F186002 and F186003 (Table 3.1).

Table 3.1: Location and nature of samples collected.

F186001/ Depth	Sample	F186002/ Depth	Sample	F186003/ Depth	Sample
51.43	Laminated sandstone	47.10	Mudstone	56.03	Mudstone
57.90	Mudstone	55.45	Mudstone	80.01	Mudstone
58.00	Coal	60.50	Coal	92.08	Coal
61.05	Coal	91.06	Dolerite	118.06	Coal
124.00	Mudstone	91.98	Mudstone	120.00	Mudstone
125.00	Mudstone	118.95	Mudstone		
		138.85	Mudstone		

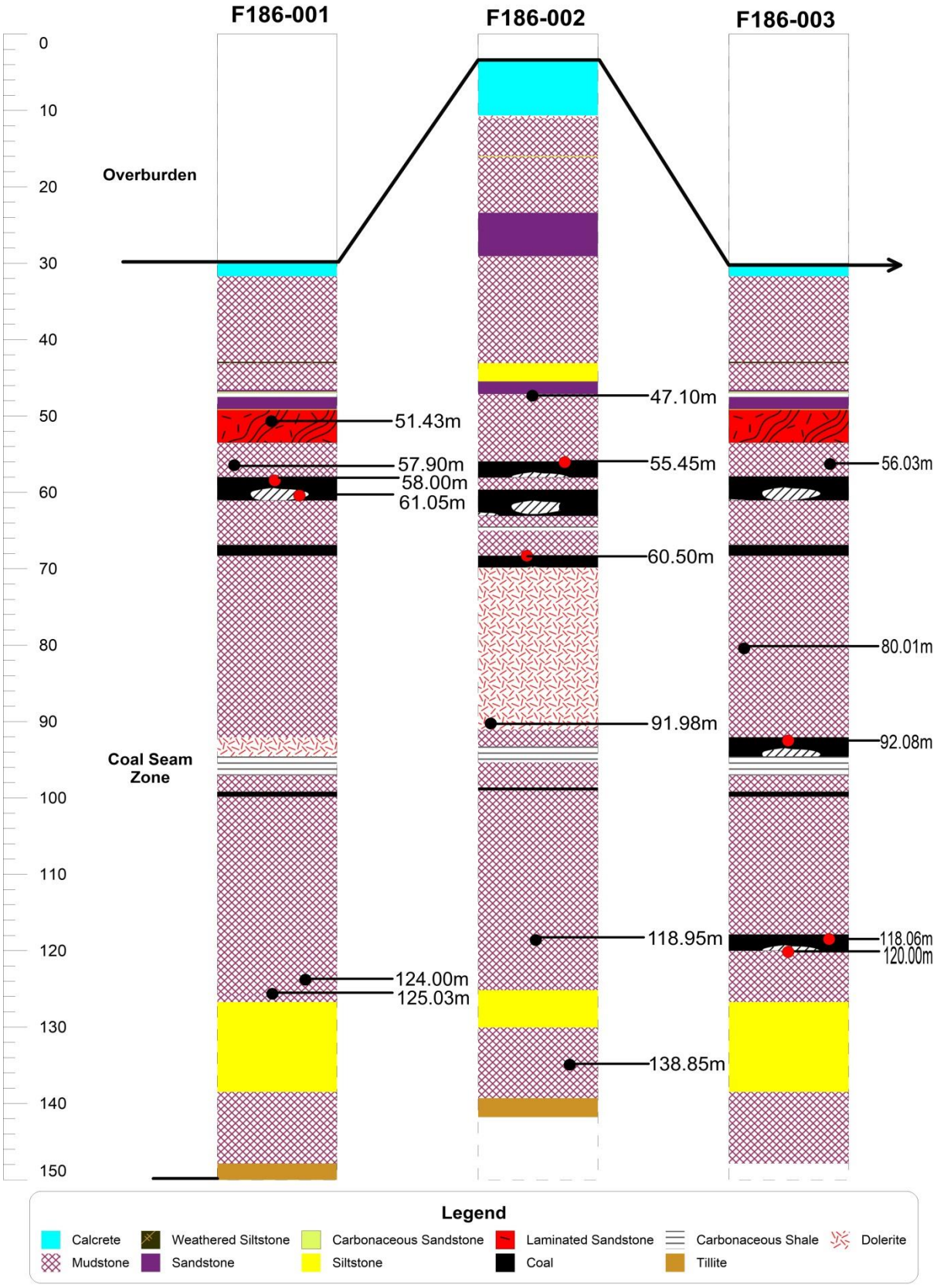

Figure 3.13: Sampling points along boreholes F186001, F186002 and F186003 within the hanging wall, coal seams and footwall.

3.2.3 Correlation of Core Logs

The correlation of different boreholes was done to delineate the boundaries of the coal seams and their thickness; as this is the productive zone hosting organic and inorganic macerals that produce the coal bed methane and coal, and to understand variations of the lithologies along the strike (Fig. 3.14).

The thickness of the coal seams of the 3 boreholes varied along the strike and with depth, in other instances, the same lithology was displaced or undulated. This was observed in borehole F578002 which was 74.65 m deep whilst borehole F578001 was 197.67 m deep in the same Rissik farm. This was attributed to geological phenomena such as folding and displacement. Moreover the floor topography of the different boreholes in different farms varied and played a crucial role in the thickness of the rocks.

It was further noted that boreholes drilled in areas where there was high topography the coal seam zones were thin, whilst boreholes drilled in low topography areas had thick packages of the coal seam zone (Fig. 3.4, 3.6, 3.8 and 3.9). During core logging, the 3 boreholes logged showed almost similar sequence/rock distribution pattern with tillite occurring at the base of the profile and calcite occurred on the top of the profile as overburden.

Coal Seam Zone

The coal seam zone was characterized by variations in lithologies along the strike and all boreholes had intersected this zone, making it possible to perform correlation. Due to this the coal seam zone was subdivided into 3 units namely, the Lower Unit (mainly coal and mudstone), Middle Unit (mudstone, carbonaceous shale, sandstone/siltstone laminations), and Upper Unit (mudstone, sandstone/siltstone laminations and sandstone). This subdivision was as a result of the different maturity levels of coal within the zone and was predominately composed of mudstone.

Coal Seam Beds

The coal seam beds showed significant paleographical basin infilling, whereby the thickness of the seam beds varied and increased from east to west; with the seam bed of borehole F578001 having a maximum thickness of 3.2 m and a minimum thickness

of 0.9 m; while borehole F578002 has a maximum thickness of 6.6 m and a minimum thickness of 0.3 m. The variation and changing pattern of sedimentary conditions within the basin were correlatable over long distances and showed a single discontinuous deposition cycles that were uniform in time and this was attributed to the gradual change in facies within the hanging wall of the coal seam beds.

Boreholes F578001 and F578007 were characterized by hanging walls made of sandstone with siltstone laminations. This indicated a change in depositional environment, whereby the rate and flow of the transporting agent had reduced. From this study, it was observed that the sandstone/siltstone laminations occurred at the upper part of the fining-upward sequences where sandstone, mudstone and coal were present; and was characterised by very fine grained, thin fining upward sequences that indicated lithologies deposited in floodplain conditions that were formed by unidirectional flow under fluvial conditions.

Correlation of the coal seam beds has shown that the thickness of each coal seam bed was not consistent, while the thickness of coal bearing rocks in the different boreholes changed from a few centimeters to several tens of meters. This was observed/evident by the occurrence of mudstone that was characterized by thickness changes displaying thin thickness where the coal seams were thick and thick mudstone occurrence where the coal seam beds were thin.

In conclusion borehole F578001 was characterized by thin coal seam beds indicating the location of occurrence to be that of a high topography region when compared to borehole F578002 occurring at a low topography. These correlated boreholes showed almost the same sequence/rock distribution pattern with tillite occurring at the base of the profile and calcrete occurring at the top of the profile as overburden.

The thickness of coal bearing rocks (mudstones) were directly proportional to the increase in coarse clastic material in the sediment, and this served as a reminder that the growth and development of the coal forming swamps that existed in the Soutpansberg Coalfield were that which formed during the Permian period where depositional cycles were characterized by fluvial and floodplain channel deposition. The regular alternation of less disturbed and more discontinuous accumulation of material of plants and flooding of areas by sediment bearing streams existed.

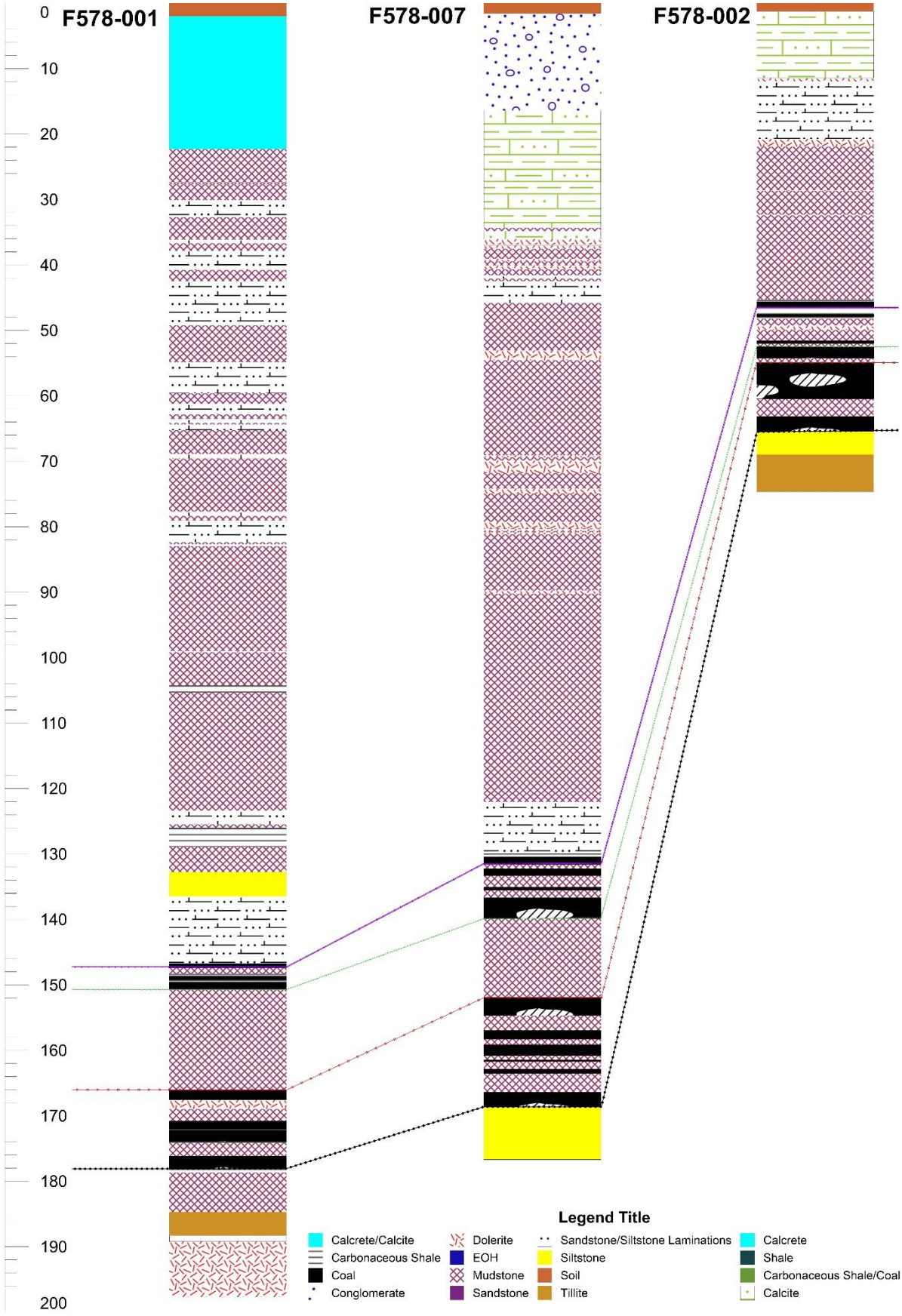

Figure 3.14: Correlation of coal logs to get the coal stratigraphy along boreholes F578001, F578007 and F578002 showing the coal seams.

General Stratigraphy of the Soutpansberg Coalfield

The Makhado Coal Project is not yet operational, although it has identified a number of coal prospects within the Soutpansberg Coalfield. However, only the Madzaringwe and Mikambeni prospects will be exploited as they have high economic potential. The generalized stratigraphy column of the coal bearing sequence in the Soutpansberg Coalfield is represented in Figure 2.3. The stratigraphy of the study area showed little deviation from that of the Soutpansberg Coalfield and the stratigraphic profile of the study area is shown in (Fig. 3.15).

A dolerite dyke cuts across the base of the Archaean granite gneiss. The pre-Karoo lithologies consisted of coarse-grained greyish brown diamictites, which formed an undulating pre-Karoo topography within which the Karoo sedimentary rocks were deposited on the floor of the Beit Bridge gneisses. Overlying unconformably, the pre-Karoo lithology was a conglomerate with sand matrix containing pebbles (tillite); this unit was up to 13 metres thick. This section is referred to as the Tshidzi Formation which is equivalent to the Dwyka Group of the Supergroup.

The Madzaringwe Formation which is equivalent to the Ecca Group rests conformably over the pre-Karoo diamictites surface (Tshidzi Formation). Having a dull greyish black colour to black containing very fine to fine-grained particles, this section of the mudstone has coal seams that are rich and shiny; the coal is intercalated with the mudstones. The coal seams were fully developed in some areas and attained a maximum thickness of about 6 meters.

The main seam consisted of coal, shale mudstone and some sandstone. While the lower seam consisted of shale, coal, coal with shale and a siltstone marker, the coal was associated/has a close relationship with mudstone. In the borehole a thin carbonaceous layer of siltstone occurred immediately after the sandstone, acting as a marker for the coal horizon (Madzaringwe formation-maximum thickness of the Ecca Group 69.08 m).

Overlying the Madzaringwe Formation was a unit of sandstone and mudstone with dolerite intrusions in certain farms within which the boreholes logged had physical and chemical changes to the lithologies depending on the depth of the lithologies and this

impacted on the overall mineralogical characteristics of the rocks. Thin layers of calcrete were found within the mudstone.

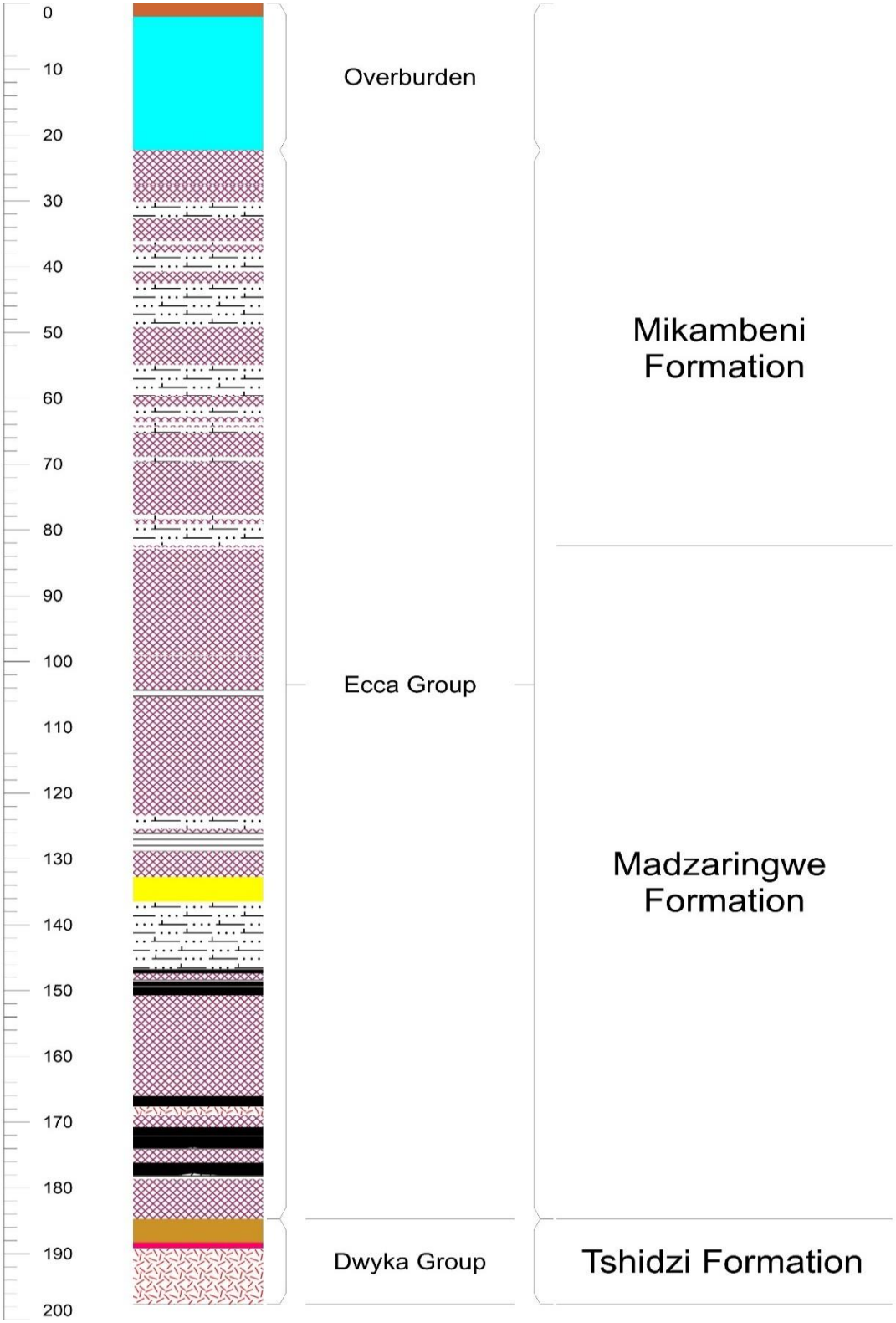

Figure 3.15: Stratigraphy of Soutpansberg Coalfield based on the core logs studied (modified after Sullivan *et al*., 1994).

Three (3) dolerite dykes were present in the footwall and at the base of the coal seam zone (lower parts of the stratigraphic profile). The basement dolerite dyke was characterized by fine to medium grains with a greyish green colour. The lower Madzaringwe Formation dykes were separated by a series of mudstones, carbonaceous shale and at times with sandstone/siltstone laminations. Dolerite occurrences were common within the Soutpansberg lithologic profiles cutting across different rock strata at different depths.

3.3 Laboratory Work

The rocks collected from the field were taken to the laboratory for preparation and laboratory investigation, using petrographic microscopy and a range of analytical techniques to investigate the regional variations of the Soutpansberg coal stratigraphy and characterisation. The work was undertaken at the Department of Mining and Environmental Geology, University of Venda; Siza Coal Services, and at Council for Geoscience.

3.3.1 Petrographic Study and Depositional Environments

Thin Section Preparation

The aim of petrographic study for this research work was to determine the variation of the coal stratigraphy on the eastern part of the Soutpansberg Coalfield so as to establish if there was any lithological influence on coal occurrence. Thin sections were prepared from the collected coal and rock samples.

Preparing thin sections from coal was more difficult than any other material due to coal's friability, and dangers of coal burning with the application of too much heat (Frank and Mergner, undated). The procedure for preparing thin sections is as follows (Frank and Mergner, Undated; Mining and Environmental Geology, University of Venda Laboratory Manual):

a) The coal sample is impregnated with paraffin overnight in an electric oven at a temperature of 70^0C. Then the sample is placed in a white enamelled pan with sufficient paraffin when melted to cover it. By doing this the coal sample is made strong enough to allow the sawing off of a piece for thin section preparation.

b) After 24 hours has elapsed, the coal sample is removed from the oven and placed on a mat of paper hand towel so as to drain off the excess paraffin and let it cool. After cooling a piece is cut from the coal sample with a hacksaw and mounted on a glass section. During mounting of the sample to the slide, moderate heat is required because the coal sample has a tendency to warp during impregnation when the heat is high.

c) Warping is prevented by cutting a thicker slice of about 5 mm or more. The first grinding takes place on the medium lap with silicon carbide for the removal of saw marks, after which grinding continues on a fine lap with 600 silicon carbide and this is followed by hand grinding with 600 optical alundum on the plate glass until a smooth scratch free surface is obtained.

d) Prior to mounting on the glass, the smoothly ground surface is polished on cloth-covered rotating lap with tin oxide until all traces of scratches and pits are removed. The cloth used in covering the lap should not be coarse, but a fine-grade cotton material. The tin oxide is placed in a container with water and applied to the revolving lap with a camel's hair brush. Manipulation by the fingers on the coal slice in a circular movement from the centre of the lap to the edge prevents furrows from developing.

e) Allowing the chip to dry thoroughly overnight, thus the tendency to form bubbles is reduced. However, after the coal chip has been firmly mounted on the slide and all bubbles eliminated, pressure was maintained on the slide with the mounting rod until the mounting substance (Balsam) has set/settled.

f) Grinding is resumed on the medium rotating lap with silicon carbide until the section became slightly translucent at the edges. When the section begins to be fray at the edges before it shows signs of translucency, then grinding is stopped, however grinding was continued by hand on the glass plate with 600 optical alundum until the desired thinness of the polished section was reached. Alundum and water were applied to the rotating lap with the fingers, this is done so as to prevent scorching of the section.

Sedimentary Facies

Sedimentary facies looked at the study of different strata, specifically the lithologic facies and characterization of stratigraphic intervals. These sedimentary facies were used to study and interpret depositional environments, to better understand the

regional variation of the coal stratigraphy (sequence stratigraphic framework), and source areas. Malaza *et al*. (2013), defined 10 lithofacies of the Soutpansberg and Tuli Coalfields based on detailed descriptions of cores and fieldwork from the Soutpansberg and Tuli Coalfields.

Facies is defined as the character of a rock expressed by its formation, composition and fossil content (it's a product of deposition). In this study, facies description includes texture, lithology and thickness, colour, composition, grain characteristics, bedding characteristics, sedimentary structures, nature of overlying and underlying contacts, and post depositional features (Johnson, 2004).

Two major groups of sedimentary facies exist and can be classified as lithofacies which deals with observable petrological features of sedimentary rocks, and biofacies which accounts for biological features such as different types of fossil contents (Miall, 1990 and 2000). In this study seven sedimentary facies were identified in the Soutpansberg Coalfield and the following depositional environments were deduced from the physical characteristics of the identified and studied facies (Table 3.2).

Table 3.2: Sedimentary facies characterisation

Facies	Formation	Depositional Environment
Siltstone	Mikambeni & Madzaringwe Formation	Channel & floodplain conditions
Coal	Madzaringwe Formation	Fluvial & braided channels
Mudstone	Mikambeni & Madzaringwe Formation	Floodplain environments
Carbonaceous shale	Mikambeni & Madzaringwe Formation	Fluvial meandering & braided channels
Shale	Mikambeni & Madzaringwe Formation	Fluvial meandering channels
Sandstone/siltstone laminations	Mikambeni Formation	Fluvial channel deposition
Sandstone	Mikambeni Formation	Fluvial channel
Calcrete	Overburden	Overburden

Calcrete

In hand specimen, calcrete was found to be fine to medium-grained with a reddish yellow colour, indicating moderate degree of alteration (Plate 3.1). Calcrete is a

calcium rich rock commonly found near the surface of the earth in most boreholes studied, consisting of hardened accumulation of silica, aluminium and iron oxides; formed as a result of climatic fluctuations in arid and semi-arid regions. In this case, at the Rissik Farm calcrete occurred at a depth of 14.20 m.

Plate 3.1: Hand specimen of calcrete showing moderate degree of alteration.

Mudstone

In hand specimen the mudrock was characterized by fine grains measuring up to 0.1 mm, with thin light grey quartz laminations and an overall dark grey colour which was attributed to the presence of carbonaceous material (Plate 3.2).

Plate 3.2: Hand specimen of mudstone showing thin light grey quartz laminations.

In thin section, mudstone was found to have a heterogeneous texture displaying fine grains of quartz, measuring up to 0.1 mm x 0.5 mm; with fine to medium-grained appearance of organic matter measuring up to 0.01 mm x 0.5 mm (Fig. 3.16a). A

random pyrite nodule was also observed under thin section. Furthermore, the mudstone was infiltrated with a single continuous hairline quartz vein filled with carbonaceous material and opaque minerals (Fig. 3.16b).

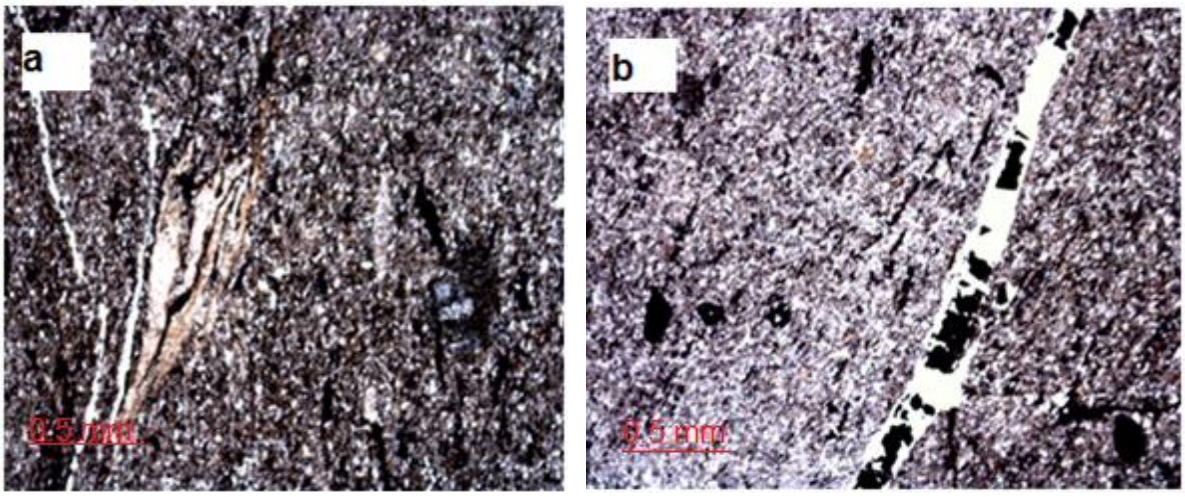

Figure 3.16: (a) Photomicrograph of mudstone displaying heterogeneous texture; (b) Photomicrograph of a hairline vein of quartz in mudstone.

Carbonaceous Mudstone

In hand specimen, the carbonaceous mudstone was found to be fine to coarse-grained, measuring up to 0.3 mm (Plate 3.3). The carbonaceous rock was poorly sorted with silt or clay forming matrix, the grain size and the degree of sorting may be set apart by separating the rock into gradational, but with discernible horizons. The pyrite patches measured up to 20 mm.

Plate 3.3: Hand specimen of carbonaceous mudstone with patches pyrite.

Carbonaceous mudstone mostly had dull to bright coal with banded appearance which was highly fissile, grey to black in colour and organic rich silt particles (Plate 3.3). This

colour was attributed to the presence of highly carbonaceous material, pyrite and iron oxides that indicated a reducing environment.

In thin section, the mudstone was characterised by fine to medium grains, organic matter cemented by very fine clay particles measuring up to 0.3 mm x o.5 mm; and medium to coarse-grained quartz laminations measuring up to 0.4mm x 0.5 mm (Figure 3.17a); while figure 3.17 (b) in thin section demonstrated coarse grained nodules of organic matter measuring up to 1.8 mm x 0.5 mm, that were slowly being chewed up by the clay cement, the presence of nodules within the mudstone was influenced by the maturity of the coal above and below the mudstone.

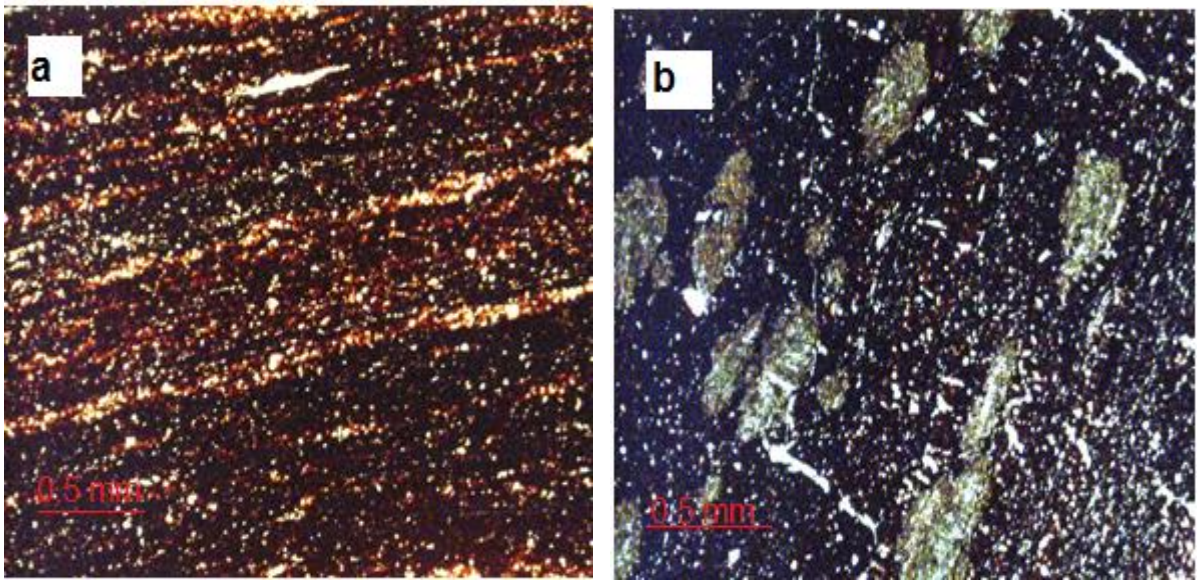

Figure 3.17: (a) Photomicrograph of fine to medium-grained mudstone; (b) Photomicrograph of coarse-grained nodules within the mudstone.

In thin section, the mudstone that occurred below the coal seam zone in borehole F186002 at a depth of 138.85 m consisted of heterogeneous/irregular oversized to angular quartz grains, cemented together by silt matrix and the occurrence of minor opaque minerals (Fig. 3.18). The fine to medium quartz grains within the mudstone measured up to 0.6 mm x 0.5 mm, while the medium to coarse grains measured up to 10 mm x 0.5 mm, and the massive/oversized quartz grains in thin section measured up to 45 mm x 0.5 mm; the average grain size of these quartz grains in mudstone measured to 18.33 mm x 0.5 mm.

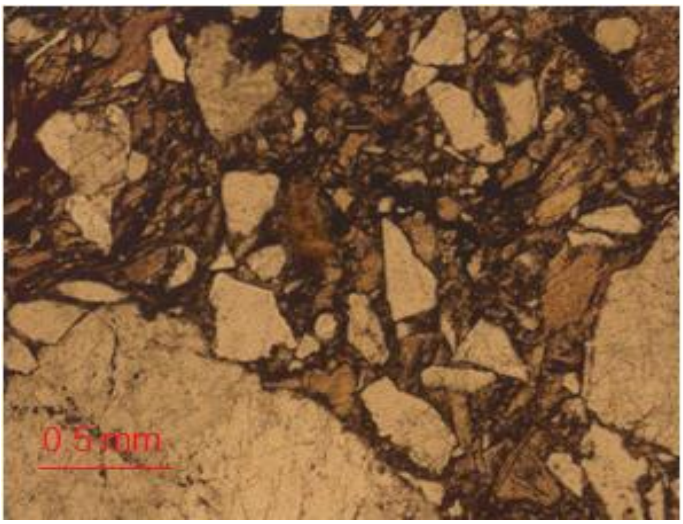

Figure 3.18: Photomicrograph of mudstone with heterogeneous quartz grains cemented by silt matrix.

Interpretation

Mudstone and carbonaceous mudstone are considered as lithologies (deposits) of wetlands, freshwater mires and floodplains. The mudstone grades vertically into a sequence of interbedded sandstones and mudstones, upward coarsening was reflected in the thickness of the intercalation units and transition into the coarser grained particles (Malaza *et al*., 2013).

Sandstone

In hand specimen, sandstone was found to be fine to coarse-grained, well to moderately sorted with the finer grains defining cross bedding measuring up to 0.2 mm (Plate 3.4a); while the coarse grains showed horizontal stratification measuring up to 1.9 mm (Plate 3.4b), displaying an equigranular texture.

Sandstone is a clastic sedimentary rock that consists of quartz, plagioclase and laminations of siltstone (Plate 3.4). The sandstone is light to dark grey black in colour. At a depth of 144.21 m the transition from sandstone to low mudstone coal bearing rocks started to show especially where intercalations of mudstone occurred.

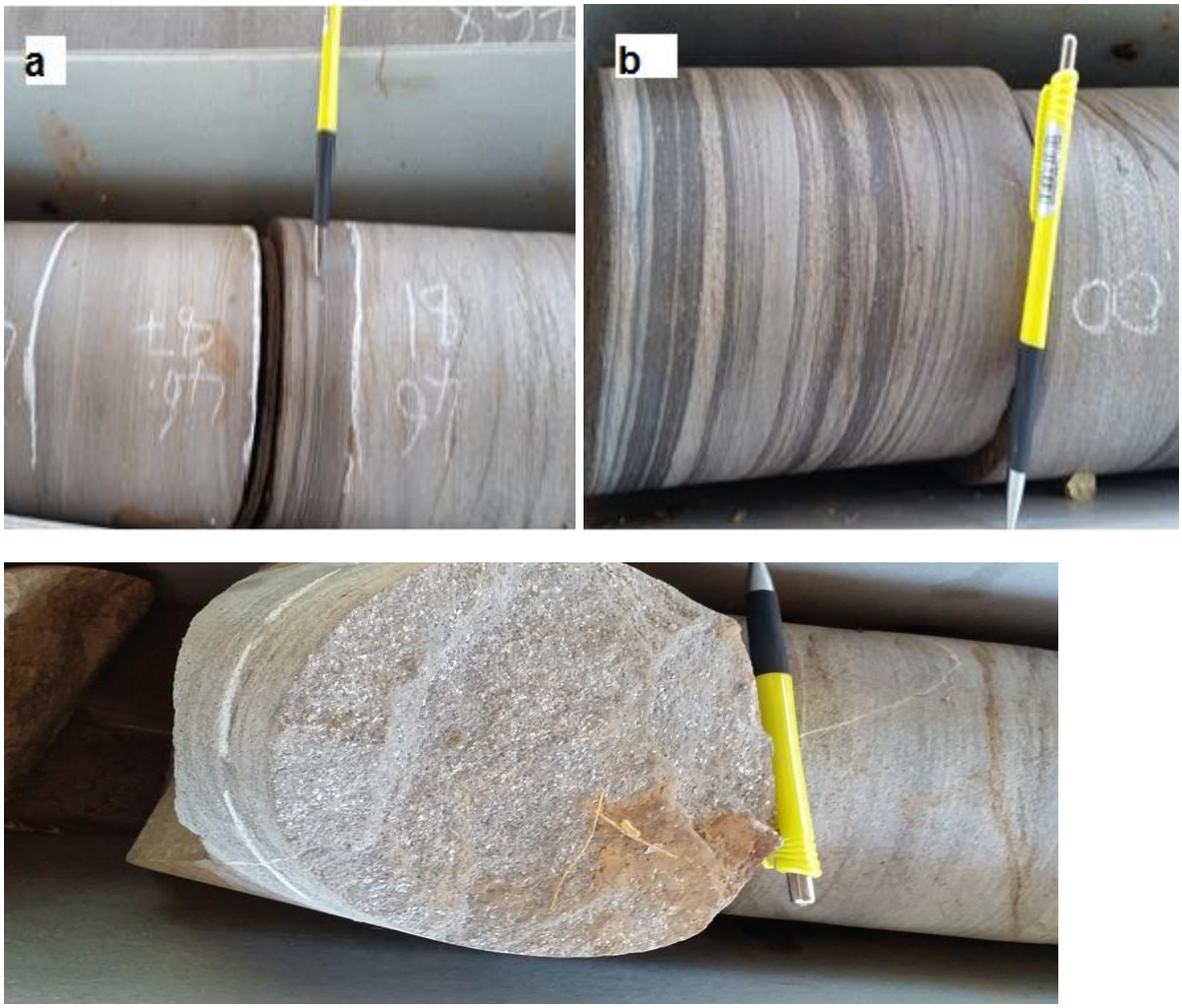

Plate 3.4: Hand specimen of sandstone: (a) laminated sandstone, (b) siltstone bands within the sandstone and; (c) fine to medium-grained sandstone.

In thin section, sandstone displayed moderate to well sorted, fine to coarse grains, which were sub-angular to sub-rounded measuring up to 1.2 mm x 0.5 mm and 1.9 mm x 0.5 mm; consisting mainly of quartz and opaque minerals (Fig. 3.19). The quartz grains were consolidated with siliceous cement into concretions of irregular form and were measuring up to 0.9 mm x 0.5 mm. The quartz cement appeared as continuous and discontinuous overgrowths in detrital grains.

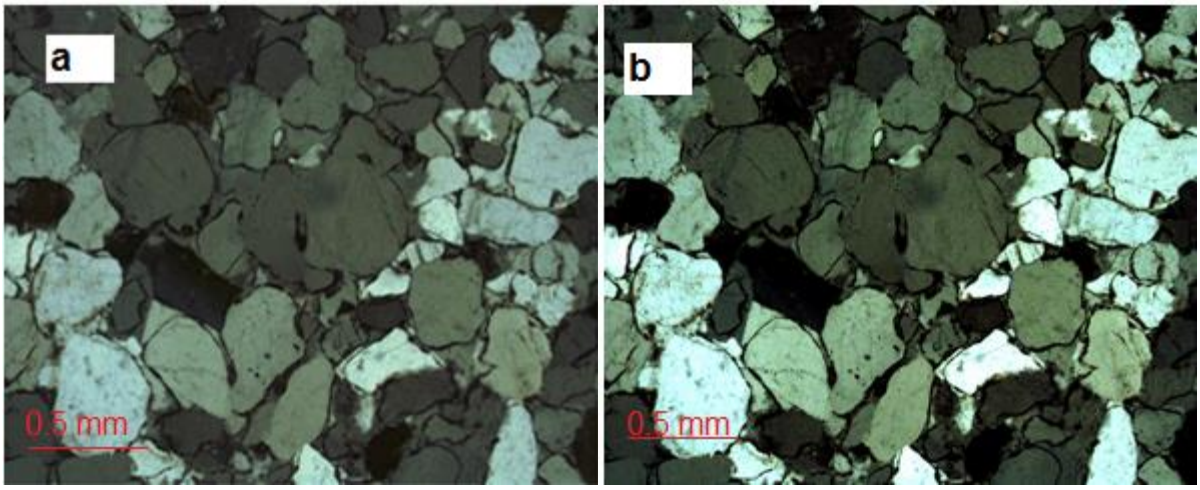

Figure 3.19: Photomicrograph of moderately sorted sandstone.

In thin section, the organic matter rich laminated sandstone was found to be fine-grained, consisting predominately of clay cement, with a single anhedral quartz grain measuring up to 0.8 mm x 0.5 mm and minor opaque minerals in the matrix (Fig. 3.20 (a) and (b)).

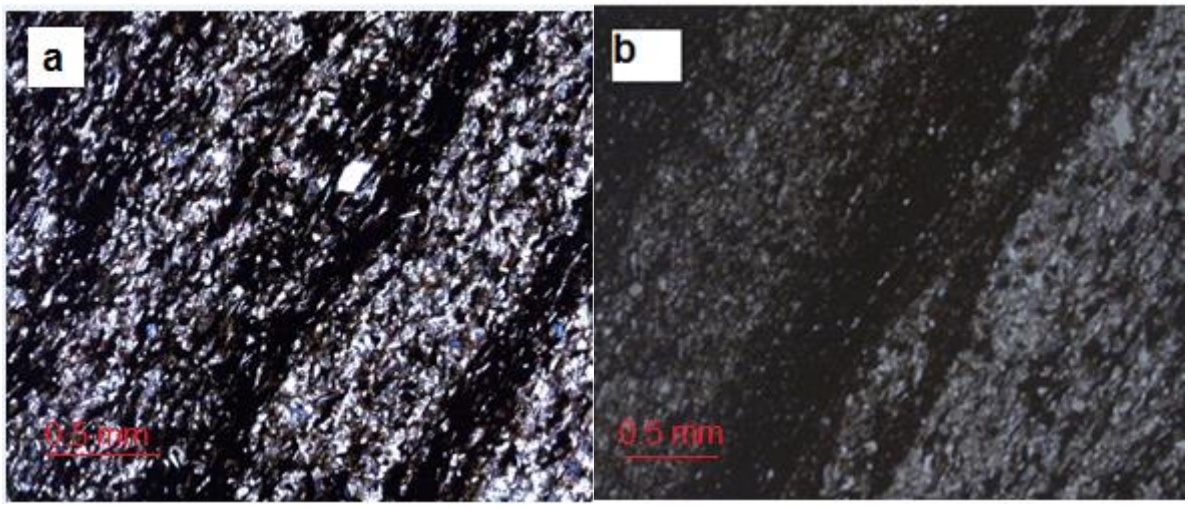

Figure 3.20: Photomicrograph of organic matter rich sandstone with laminations of light coloured quartz.

Interpretation

The intercalations of these sedimentary strata (sandstone with siltstone laminations) indicated low current velocity (Harms *et al*., 1982). Sandstones and laminated sandstones formed due to the alternating sedimentation of bedload and suspended load particles and can also occur in a variety of depositional environments, (for

example, downstream migration of sand as ripples. Deposition occurs under periodic alterations of low and very low energy conditions (Holland *et al*., 1989).

Coal

In hand specimen, the sample consisted entirely of coal and carbonaceous siltstone (Plate 3.5). The distribution of coal can be local or continuous, with individual seams measuring up to 0.4 mm in grain size of the porphyry coal. The coal was usually black to very black with vitreous lustre on cleat surfaces, but can also have a duller appearance when the silt content increases.

Plate 3.5: Hand specimen of dull coal with shiny coal bands.

Upper contacts were sharp with overlying grey or black shale. Lower contacts were either sharp or gradational with underlying clay. The coal in some of the studied cores contained abundant plant remains such as leaves. Post-depositional features included nodular pyritization as well as calcareous mineralization in cleat spaces.

In thin section, the mudstone was found to have very fine grains that could not be measured and displayed the thermal intrusion of a dolerite dyke that was characterised by a smooth glassy appearance (Fig. 3.21a), the texture of the rock was clastic to fine; however, in thin section the rock displayed breaking along the weak planes due to the thermal intrusion and consisting of about 95% carbonaceous and organic matter (Fig. 3.21b).

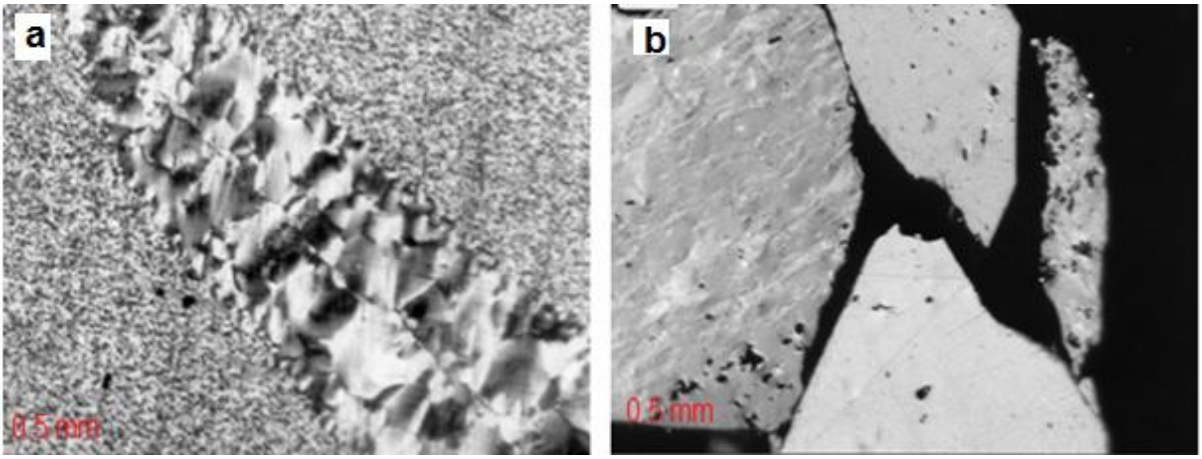

Figure 3.21: (a) Photomicrograph of igneous intrusion cutting across mudstone; and (b) Photomicrograph of coal breaking along weak planes.

Interpretation

The process of deposition and formation of coal is through peat accumulation, burial and coalification. This is evident by the high organic content, preserved plant remains, and laminated and compacted nature. Coal with higher sulphur content or pyritization and overlying black shale points to development in proximity to marine conditions, marine flooding highly influences the quality of underlying coal. Coal with higher ash indicates development in proximity to active marine or non-marine siliciclastic depositional environments (McCabe, 1984).

Thick coal seams to indicate long persistent, slowly subsiding moderately drained and densely vegetated back swamp (Diessel, 1992; Malaza *et al*., 2013). Thin coal seams contains abundant splits of carbonaceous mudstones that indicate short-lived flooding during the formation period. Carbon-rich seam exhibiting glittering vitreous lustre, massive bands of coal due to weak cohesion signifying that the rock was not competent (Plate 3.5). The lamination bands were shale bands showing different grades of maturity, the dark shiny laminations were the matured layer of coal comprising high carbon content, while the dull black layer was characterized by fine grains.

Dolerite

In hand specimen, dolerite was characterised by a greenish-grey colour, having coarse grains measuring up to 0.9 mm, and consisting of quartz, feldspar and

pyroxene (Plate 3.6). The rock has a medium grained (Ophitic) texture.

Plate 3.6: Hand specimen of dolerite showing coarse grained quartz crystals.

In thin section, the ophitic textured dolerite showed high content of pyroxene (about 60%) with moderate degree of alteration of this pyroxene, and moderate proportions of quartz about 15% and feldspar, about 25% and high content of pyroxene (about 60%) (Fig.3.22).

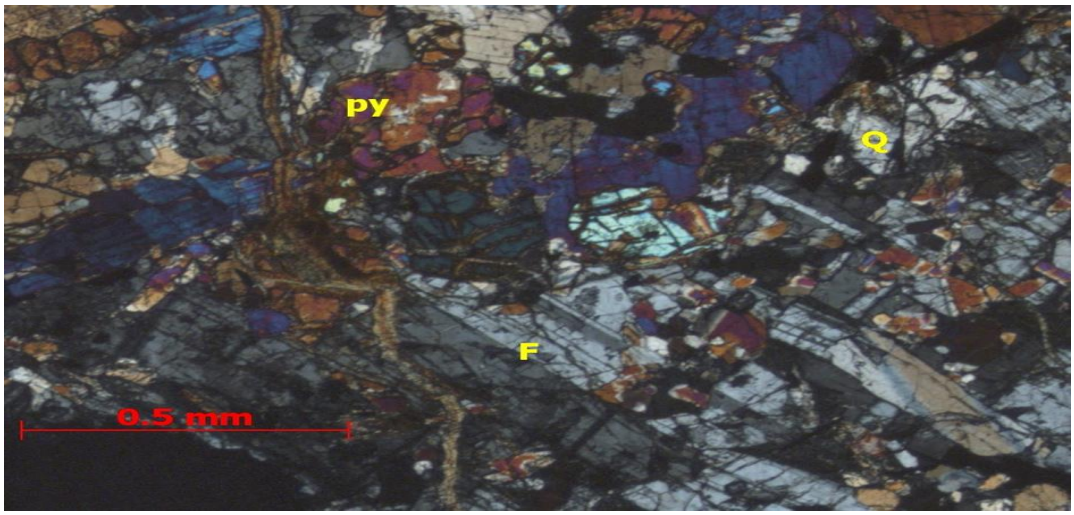

Figure 3.22: Photomicrograph of dolerite displaying fine to medium grains.

Interpretation

Depositional Environments

According to Boggs, (2001), sedimentary rocks are formed through 5 processes which are erosion, weathering, transport, deposition and diagenesis processes. The

properties of sedimentary rocks such as sediment textures and structures are formed by chemical, physical and biological processes. Depositional process and the properties of rocks have close genetic relationships. Tucker (2001) noted that stratigraphic record is made up of depositional sequences, and within them there is commonly a regular and predictable arrangement of sedimentary facies deposited at specific intervals.

The stratigraphy of the Karoo Supergroup (Fig. 2.2) records a transition from glacial period through fluvio-deltaic and swampy periods and turning arid before the extrusion of continental flood basalts (Smith *et al*., 1993; Williamson, 1996; Modie, 2008). The transition is represented dominantly by siliclastic sedimentary sequence ranging from glacial diamictites of the Dwyka Group to a succession of fluvio-deltaic sandstone and mudstone units with intercalated coal beds belonging to the Ecca Group that gives rise to fluvial and Aeolian red beds and the succeeding basalt lava flows of the Stormberg Lava Group (Williamson, 1996; Modie, 2008).

3.3.2 Whole Rock Geochemical Analysis

The main aim of conducting whole rock geochemical analysis was to establish the presence of the host rocks and their characteristic features, and to investigate compositional breaks of the hanging wall, coal seams and footwall lithologies from boreholes F186001, F186002, and F186003 in order to evaluate the depositional environment of coal and its characteristics. Whole rock geochemical analysis was done at the University of Venda, Mining and Environmental Geology Laboratory and at Council for Geoscience.

Sample Preparation

The 18 samples selected for whole rock geochemical analysis were crushed using the jaw crushers to pea size, then passed into a secondary crusher to particle size of about 0.25 cm, and then milled in the roller into powder form. The samples were prepared and heated to release volatile contents such as water and analysed by means of XRF for major and trace elements. A total of 9 major elements and 37 trace elements were analysed (Tables 3.3 and 3.4).

Table 3.3: Major oxides analysis of samples from borehole logs F186001, F186002 and F186003

Oxides	**Al_2O_3**	**CaO**	**Fe_2O_3**	**K_2O**	**MgO**	**MnO**	**P_2O_5**	**SiO_2**	**TiO_2**
Boreholes/Units	**%**	**%**	**%**	**%**	**%**	**%**	**%**	**%**	**%**
Hanging Wall									
F186001/51.43	26.11	0.20	3.86	2.36	0.56	0.06	0.05	61.75	0.84
T186LD01/57.90	6.34	0.15	8.4	0.86	0	0.043	0.13	28.8	0.489
Coal Seam									
F186001/58.00	39.1	0.21	0.92	0.83	0.25	0.004	0.24	45.12	1.744
F186001/61.05	23.81	0.43	1.47	1.76	0.56	0.015	0.18	62.52	0.923
Footwall									
F186001/124.00	35.58	0.11	0.83	2.43	0.09	0.01	0.07	54.94	1.37
F186001/125.00	37.03	0.14	0.72	2.07	0.04	0.01	0.29	56.01	2.09
Hanging Wall									
FF186002/47.10	20.12	0.57	11.54	2.43	0.91	0.21	0.07	43.70	1.13
F186002/55.45	23.67	0.81	13.01	1.97	0.47	0.24	0.11	47.05	1.01
Coal Seam									
F186002/60.50	5.76	0.66	14.37	0.54	0	0.30	0.18	23.25	0.53
Footwall									
F186002/91.98	39.31	1.23	6.25	1.94	0.94	0.05	0.05	43.84	1.07
F186002/118.95	31.61	0.16	0.58	0.47	0.06	0	0.16	56.00	1.50
F186002/138.85	35.79	0.09	1.01	1.13	0.37	0.003	0.032	50.02	1.74
Hanging Wall									
F186003/56.03	35.48	0.28	0.92	0.61	0.31	0.00	0.48	51.35	1.58
F186003/80.01	38.04	1.02	1.09	1.81	0.56	0.05	0.85	52.83	1.93
Coal Seam									
F186003/92.08	23.12	0.13	0.66	1.29	0.29	0.003	0.09	63.5	0.81
F186003/118.06	7.01	0.48	1.52	0.54	0.00	0.01	0.23	24.26	0.59
Footwall									
F186003/120.00	39.52	1.16	6.42	1.94	0.92	0.05	0.05	43.84	1.06
Dolerite	6.00	8.15	10.87	1.73	18.49	0.13	0.51	43.69	1.87

Table 3.4: Trace elements analysis

Elements	Ag	As	Ba	Bi	Ce	Co	Cr	Cs	Cu	Dy	Er	Eu	Ga	Gd	Ge	Hf	La	Mo
Borehole/Unit	ppm	ppm	ppm	ppm	ppm	ppm	Ppm	ppm	ppm	ppm	ppm	ppm	ppm	ppm	ppm	ppm	ppm	ppm
Hanging Wall																		
F186001/51.43	0.70	7.00	681.60	0.40	152.80	9.00	39.50	5.40	42.60	13.00	9.20	0.60	31.90	9.00	1.70	14.50	49.30	1.00
F186001/57.90	0.8	32.8	423.2	0.5	63.4	23.2	60.6	5.4	33.7	28.3	20.6	0.00	45	18.9	6.1	9	89.1	1.6
Coal Seam																		
F186001/58.00	0.5	18.7	1359.1	0.4	732.8	3.5	78.5	5.4	109.4	3.1	2.2	0.1	75.7	1.2	2.3	21.9	29.7	1.3
F186001/61.05	0.7	11.5	747.1	0.4	420.4	3.9	34.8	5.4	85.6	5	3.6	0.10	40.2	1.5	1.2	20.2	25.4	5
Footwall																		
F186001/124.00	0.70	7.10	1082.4	0.4	144.10	2.00	72.60	5.40	144	2.80	2.00	2.10	45.60	0.00	1.40	32.70	27.50	1.50
F186001/125.00	0.78	8.02	1125	0.40	150	2.75	74.03	5.4	151	2.96	2.89	2.54	48.15	0.35	1.67	33.82	31.90	1.89
Hanging Wall																		
F186002/47.10	0.60	10.3	900.80	0.40	150.80	19.70	130.6	5.40	42.10	38.90	26.9	3.10	28.00	38.3	2.10	10.40	137.5	0.60
F186002/55.45	0.72	8,6	579	0.4	138	24.09	116	5.4	38.31	41.76	30.01	0.00	37.98	41.2	2.07	7.09	142.8	0.69
Coal Seam																		
F186002/60.50	0.90	6.00	457.10	0.40	129.30	33.50	62.40	5.4	23.00	48.40	34.1	0.50	46.90	48.4	2.10	0.00	153.0	0.80
Footwall																		
F186002/91.98	0.30	83.0	857.10	0.40	97.80	14.80	96.80	5.4	129.3	21.10	14.9	0	45.30	16.6	1.40	25.00	80.60	2.60
F186002/118.95	0.70	8.20	1175.7	0.40	192.90	1.40	116.60	5.4	110.2	1.90	1.30	0	44.70	0.20	1.20	24.90	26.60	1.20
F186002/138.85	0.6	3.5	1372.2	0.4	212.1	3.1	115	5.4	266.1	3.4	2.4	0	52	0	1.5	42.6	30.9	4
Hanging Wall																		
F186003/56.03	0.60	27.2	1235.2	0.40	762.70	2.60	83.80	8.20	98.80	3.10	2.20	0.00	63.40	1.70	1.70	22.30	40.50	1.40
F186003/80.01	0.69	18.0	957.5	0.40	582	2.01	69.0	8.35	86.23	2.98	1.74	0	58.21	0.97	1.42	20.8	27.91	1.79
Coal Seam																		
F186003/92.08	0.7	12.1	661	0.4	331	1.7	19.4	7.6	78.7	2.2	1.6	0	31.8	0	1.2	16	15.1	2.9
F186003/118.06	1.30	17.6	501.60	0.40	155.90	4.60	64.40	5.40	80.10	5.10	3.70	0.10	90.60	0.50	4.50	14.60	22.60	2.00
Footwall																		
F186003/120.00	0.40	73.0	852.10	0.40	93.00	15.30	93.30	5.40	204.7	21.60	15.4	0.50	45.80	16.7	1.30	23.00	81.00	2.40
Dolerite	21.68	-	-	-	13.4	50.20	18.33	-	5.23	-	-	-	-	-	-	-	-	-

Table 3.4: Trace element analysis continued

Elements	Nb	Ni	Rb	S	Sb	Sn	Sr	Ta	Th	Ti	U	V	Y	Yb	Zn	Zr	Pb
Borehole/Unit	ppm	ppm	ppm	ppm	ppm	ppm	ppm	ppm	ppm	ppm	ppm	ppm	ppm	ppm	ppm	ppm	Ppm
Hanging Wall																	
F186001/51.43	16.30	38.10	96.30	237.50	0.20	2.80	83.20	0.80	14.10	1.10	3.30	184.10	42.20	19.50	202.20	440.30	65.00
F186001/57.90	19.2	170.4	37.2	1251.8	0.3	2.8	40.7	0.7	4.5	9.6	0.9	149.3	39.5	74.6	414.10	396.4	305.6
Coal Seam																	
F186001/58.00	28	224.1	81.1	284.9	0.5	3.7	1311	1.5	18.3	4	6	355.6	70.2	83.5	487.7	572.6	174
F186001/61.05	20.3	35.7	130.9	597.8	0.5	2.9	551.5	1.3	17.2	2.5	4	208.5	68.7	15.2	237.4	459.1	107.2
Footwall																	
F186001/124.00	17.80	104.2	32.70	114.70	0.20	2.80	146.8	1.90	29.40	2.50	1.10	276.10	30.80	39.40	212.10	652.20	65.80
F186001/125.00	19.77	106.9	33.0	120.05	0.29	3.01	149	2.15	32.75	2.62	1.67	283	32.45	45.12	220	687.01	70.00
Hanging Wall																	
F186002/47.10	12.30	19.70	78.70	1999.70	0.70	2.20	75.20	0.85	51.80	1.30	3.80	275.50	37.30	23.80	305.80	284.10	96.00
F186002/55.45	12.07	24.61	62.07	4294	0.96	2.45	89.53	0.71	51.0	1.62	3.17	194.0	33.01	28.95	294	252	66.05
Coal Seam																	
F186002/60.50	12.20	56.10	27.90	7819.70	1.30	2.90	291.9	0.60	51.80	1.80	2.80	143.40	32.10	41.30	108.90	158.60	56.10
Footwall																	
F186002/91.98	11.80	428.5	78.80	160.90	0.20	2.20	30.60	2.60	20.70	2.30	3.20	261.20	38.00	166.1	129.30	204.80	772.9
F186002/118.95	20.00	128.6	34.10	221.10	0.00	3.00	222.9	1.50	23.10	2.40	1.40	349.20	34.40	48.00	293.20	552.50	76.00
F186002/138.85	14.3	230.1	58.6	103.60	0.3	2.6	67.70	3.2	5.9	2.8	0.7	394.5	50.2	85.8	146.6	305.8	32.6
Hanging Wall																	
F186003/56.03	31.20	195.6	55.50	262.70	0.00	3.10	951.1	1.40	30.70	3.70	4.00	369.70	42.60	73.00	179.70	646.70	253.1
F186003/80.01	32.5	148.0	61.01	289.03	0.00	2.30	493	1.39	23.41	2.78	3.69	235.08	43.18	13.69	50.03	454.78	205.9
Coal Seam																	
F186003/92.08	16.9	40.5	106.4	829.6	0.00	2.8	275.8	1.2	14.3	1.7	2.7	166.4	46.7	15.8	47.9	259.9	113.1
F186003/118.06	21.10	197.6	44.60	7616.20	0.00	3.80	497.30	1.20	15.10	3.80	12.1	179.10	72.30	74.60	322.30	481.30	163.6
Footwall																	
F186003/120.00	12.40	378.8	78.50	128.70	0.00	3.10	29.60	2.50	21.50	2.00	2.90	244.40	36.00	148.1	108.70	198.90	679.9
Dolerite	19.2	26.52	25.6	-	-	-	758	-	22.8	-	-	444.2	-	-	81.8	29.8	8.12

3.3.3 Physical and Chemical Coal Analysis

Proximate analysis of coal was used to characterize coal. The coal rank was determined through the analysis of the fixed carbon and ash, moisture content and volatile matter as well as to quantify and study variations in gas emissions from the samples. These characteristics were investigated as stated below:

Fixed Carbon and Ash

Fixed carbon and ash are the solid combustible residue that is left behind when coal is burned and the volatile matter is expelled. It normally contains some amounts of nitrogen and hydrogen, while ash is the residue that is left behind when coal is completely incinerated and it represents the bulk mineral matter after carbon, sulphur, oxygen and water have been given off during combustion (Snyman, 1998). The ash remaining after coal or coke has been incinerated in air is derived from inorganic complexes in the original coal substance and from associated mineral matter, the amount of sulfur retained in the ash is partly dependent on conditions of ashing and the results of determination are reported on a air-dried basis.

Three coal samples were selected for physical and chemical coal analysis. The sample was prepared in accordance with ISO1171, where the sample were crushed and milled to pass a sieve of 212 microns aperture. One gram of the coal sample was weighed in a clean dry silica dish that was 8 mm to 15 mm deep and spread accordingly in the dish and reweighed. The weighed samples were placed in an air drying room with a controlled temperature and dried over a period of 24 hours.

The fixed carbon and ash samples in the dish were placed in a furnace at room temperature, raising the furnace temperature to 500ºC over a period of 1 hour and hold at this temperature for 30 minutes; for brown coals a holding period of 60 minutes at 500ºC was required.

The coal sample was further heated at a temperature of 815ºC±10ºC in the same furnace, however, this temperature was maintained for 1 hour; then the dish with the coal sample was removed from the furnace and allowed to cool on a thick metal plate for 10 minutes then transferred to a desiccator to let the sample further cool down at room temperature, after the cooling the sample was further weighed. The controlled

furnace temperature of 780ºC to 815ºC was used because this is the temperature where all volatiles found in coal burn.

The container with the sample dish should be covered with a lid before flushing the container with dry gas in order to reduce the pick-up of moisture during cooling. The temperature was always maintained until a constant mass of the sample was reached. The ash content was then calculated from the mass of the residue after incineration.

Fixed carbon content was determined by calculation through acquired results information of inherent moisture, volatile matter and ash content obtained from the tested samples during proximate analysis using the equation below (USCOR, 1967):

Fixed Carbon = 100% – [(Moisture + Volatile Matter + Ash)%]

Moisture Content

The sample was prepared in accordance with SANS 10135-2, where the coal sample was crushed to a point that it passes through a test sieve of 212 microns, the sample was further exposed in a thin layer for at least 30 minutes to allow the moisture content of the sample to attain an equilibrium with the laboratory atmosphere (air drying room with a controlled temperature ranging from 30-35ºC). The sample was thoroughly mixed for 1 minute and 1 gram of the sample was uniformly spread in the weighing vessel, the cover of the weighing vessel was replaced, then the initial mass of the sample contents and vessels was determined.

A weighing vessel is a shallow cylindrical vessel of a diameter 30 mm having a well-fitted cover was used to weigh the sieved coal; this weighing vessel and its cover shall be heat resistant, non-corrodible, clean, dry and accurately weighed. The cover was then placed in a desiccator, the test sample and the uncovered vessel was then placed in an air oven with a maintained temperature of 105ºC - 110ºC and heated to a constant mass, and the atmosphere was changed at a rate of at least 5 times per hour to avoid contamination and spoiling of the sample (Table 3.6).

By maintaining a temperature of about 110^0C in the oven, the moisture laden air at that temperature was swept out and replaced by fresh air. The cover was then replaced and the vessel was let to cool on a metal plate for 10 minutes; it was then transferred to the desiccator then let to cool for another 10 minutes, after which the

mass was determined after heating. The purpose of drying was to reduce the moisture in the sample to approximately equilibrium with the air in the laboratory, thus minimize changes in the moisture content during sample analysis (USOCR, 1967).

Volatile Matter

Volatile matter consists of hydrocarbons, and sulphur; viz; gas, vapour that are released during combustion. Furthermore, volatile matter is defined as the inherent moisture which is given off when air dried coal samples are heated at a temperature of 900^0C in the absence of air.

The coal sample used for volatile matter determination was crushed and grounded to pass a sieve of 212 microns, then thoroughly mixed and in moisture equilibrium with the laboratory atmosphere. A test portion from the same test sample was separated for determination of moisture in parallel with the determination of volatile matter. A platinum crucible with tight fitting lid was used involving a sample of 1 gram of 60 mesh air dried coal and heating the sample for approximately 7 minutes at a temperature of 925^0C to $\pm 25^0$C.

This temperature was maintained by opening the door of the oven to cause the temperature of the oven to fall (USCOR, 1967). The crucible from the furnace was removed, cooled rapidly by placing it on an air cooled steel plate and weighed. The percentage of volatile matter was calculated from the loss in mass of the test portion after deducting the loss in mass due to moisture (Table 3.6).

At this specified temperature, clay minerals present in the coal will lose their hydroxyl groups in the form of water vapour, carbonate minerals will dissociate into carbon dioxide, while the basic oxides and pyrite lose their general mass as sulphurous gas especial in low grade coal (Synman, 1998).

Sulphur and Carbon Analysis

The analysis of sulphur and carbon concentrations in coal samples used the same procedure and it was done by using high temperature combustion with infrared absorption detection. The sample was placed in a combustion system where it was burnt in a stream of pure oxygen at a temperature of 1350^0C. The sample goes

through the processes that cause the sulphur and carbon bearing compounds to break down and free the sulphur which forms sulphur dioxide.

From the combustion system, the gas passes through an anhydride tube where moisture particles are removed by traps filled with anhydrous magnesium perchlorate. The sulphur dioxide flows to the infrared detection cells where the gas is passed through a cell where sulphur is measured by infrared adsorption detector. The energy that is radiated enters the cell body through a window and travels through a second window at precise wavelength filter (Table 3.7).

Nitrogen and Oxygen Tests

To determine the nitrogen and oxygen in a coal sample, the coal is decomposed catalytically using sulphuric acid to form aluminium sulphate from which the nitrogen and oxygen content is titrated. During coal combustion various nitrous oxides are formed. Nitrogen occurs almost exclusively in the organic matter of coal (Speight, 2005); the original source of nitrogen might have been formed from both plant and animal protein (Table 3.8).

Three samples were analysed for proximate and ultimate coal analysis. The samples were collected from 3 different boreholes in the study area (Soutpansberg Coalfield) along different borehole depths where coal occurred. The purpose of this was to establish the coal quality along with depth as well as the coal stratigraphy of the Soutpansberg Coalfield. Below in Table 3.5 is the standard classification of coal by ranks.

Table 3.5: Standard classification of coals by rank (ASTM D388-05)

Type	Fixed Carbon (wt %)	Volatile Matter (wt %)	Ash (wt %)	Moisture (wt %)
Anthracite	75-85	2-12	4-15	3-6
Bituminous	50-70	15-45	4-15	2-15
Sub-Bituminous	30-57	28-45	3-10	10-25
Lignite	25-30	24-32	3-15	25-45

In this research the American Society for Testing Materials (ASTM) and the International Standardisation Organisation (ISO) standards were applied in the analysis of coal. This was based on 2 coal properties, namely; fixed carbon values and calorific values where higher rank coals are classified according to fixed carbon on air dry basis, and the lower rank coals are classified according to gross caloric value on the moist basis. Below are the proximate and ultimate results of the 3 coal samples analysed from the Soutpansberg Coalfield.

Table 3.6 Results of proximate and ultimate analysis of the Soutpansberg Coal.

Proximate Analysis					**Ultimate Analysis**		
Sample No	Fixed Carbon	Moisture	Volatile Matter	Ash Content	Hydrogen	Nitrogen	Carbon
S2B1	5.9	0.7	11.8	81.6	1.49	0.22	5.3
S2B2	50.4	0.8	27.4	21.4	4.02	1.63	70.3
S3B3	42.5	0.7	25.2	31.6	3.62	1.41	60.1

Table 3.7: Average coal gas concentrations of borehole F186001, F186002 and F186003

Gases	**Gas Concentrations (ppm)**	**Combustion Time (Min)**
CO_2	1.70	1.43
H_2	0.40	3.58
O_2	0.70	3.79
N_2	0.55	4.09
CH_4	1.75	4.55
CO	0.50	5.72

Table 3.8: Physical characteristics of coal

Character-istics	**Air dried**										
Samples	Calorific Value	Relative Density	Sulphur	Swelling Index	Total Carbon	Hydrogen	Nitrogen	Oxygen	Carbon Dioxide	Mercury	Thermal Conductivity
	ISO 1928		ASTM D4239	FSI	ASTM D5373						
F186001	5.18	2.15	0.24	1.1	11.59	1.56	-0.94	3.07	2.51	0.28	213.0
F186002	24.67	1.52	1.35	0.0	67.19	4.77	2.70	3.84	1.06	0.18	210.0
F186003	22.45	1.56	1.42	0.5	59.61	4.01	2.47	3.93	1.71	0.11	209.0
TOTAL/AVE	**17.43**	**1.7**	**1.00**								

CHAPTER 4: DATA ANALYSIS AND INTERPRETATION

4.1 Stratigraphic Analysis

The Soutpansberg Coalfield is situated to the north of the Soutpansberg Mountain Range in the Limpopo Province and forms part of the Tshipise Basin. This basin consists of coal-bearing rocks of Permian age that were deposited during the periods of marine transgression and regression (SACS, 1980). The depositional setting included periods of marine, fluvio-glacial to fluvial palaeo-channel sediment deposition, where coal formation occurred in the back swamp areas of this environment.

The Mikambeni and Madzaringwe Formations hosted multiple coal seams that were of economic potential and measured a maximum thickness of about 6.6m coal seam beds. A simplified stratigraphic column of the Soutpansberg Coalfield is shown in Figure 4.1. There were a number of igneous intrusions in the form of dykes and sills within the study area. Through petrographic studies these intrusions were confirmed to be doleritic due to their composition and they vary significantly in the degree of alteration and character.

From the study of core logging and analysis of the lithological features on the cores with stratigraphic depth; deducing the environment of deposition of the studied cores, it was concluded that the rock sequence represented a single continuous depositional event, it was evident by the occurrence of a single strata that was part of a given sequence that was correlated over a long distance from borehole to borehole to be isochronous horizons (Fig. 3.14). Furthermore, the thickness of coal seam beds were consistent and do highly fluctuate when compared to the coal bearing rocks (mudstones).

The location of channel inflows into peat swamp stages has been shown by the maximum thickness of mudstone interlayers and with each interlayer being associated with 1 inflow channel of deposition. The stratigraphic profile has shown a distinguishing tendency characterised by an increase in the proportion of coal-bearing rocks (mudstones and siltstones) in the bottom filling that increases downstream with depth, with the gradual filling of the channel as the stream speed decreased.

Stratigraphic Profile	Facies/Rock Units	Depositional Environment
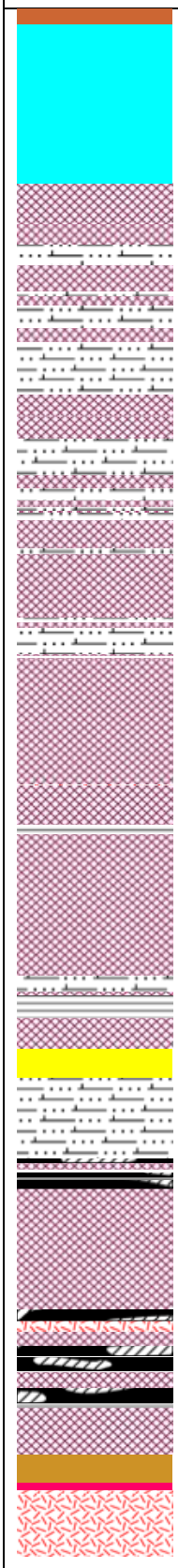	Soil Calcrete	
	Mudstone	Floodplain Environments
	Sandstone/ Siltstone Laminations	Fluvial Channel Deposits (Fluvial Meandering Channels)
	Mudstone	Floodplain Environments
	Carbonaceous Shale	Fluvial Channel Deposits
	Mudstone	Floodplain
	Siltstone	Channel and Floodplain Conditions
	Mudstone with Coal	Fluvial and Braided Channels
	Coal with Dolerite Intrusion	Fluvial and Braided Channels
	Mudstone	
	Tillite	Fluvioglacial (Braided) Depositional Environment
	Granite Gneiss	
	Dolerite	

Figure 4.1: Stratigraphic profile of the Soutpansberg Coalfield.

These processes repeat one after another with short periods of flooding followed by the deposition of an interlayer.

4.1.1 Textural and Grain Size Analysis

Texture and Grain Size Analysis

Grain size analysis is a statistical evaluation of the size distribution of rock-forming minerals in different rock types as studied under the microscope. Grain size serves as the most important physical aspect of a rock which provides information about the surface processes of a rock related to the dynamic conditions of transportation and deposition. The grains of the rock in the field were studied using the naked eyes and a hand lens, at times together with a ruler to measure the size of the grains if big enough.

The main purpose of undertaking textural and grain size analysis of the different lithologies within the coal stratigraphy of the Soutpansberg Coalfield was to determine the lithological characteristics of rocks constituting the stratigraphy, and to determine whether the igneous intrusions and coal seam had any influence on the texture and grain size of these lithologies (Tables 4.1, 4.2 and 4.3).

Furthermore, these parameters were used to compare and contrast the relationship between the coal seam zones with its host rocks. The texture and grain arrangements of rocks differed depending on the mode of formation and transportation (Table 4.1).

Table 4.1: Textural and grain size analysis of the coal and host rocks

Characteristics		**Footwall**	**Coal Seams**	**Hanging Wall**	**Dolerite**
Grain Size	Mudstone	0.01 mm			
	Coal		0.2-0.01 mm		0.45 mm
	Mudstone			0.005 mm	
Grain Shape		sub-euhedral to anhedral	rounded-sub rounded	rounded-sub rounded	angular-sub angular
Grain Arrangement		heterogeneous	homogeneous	heterogeneous	heterogeneous
Texture		medium-coarse	very fine-coarse	fine-medium	fine-medium

The coal seam zone was made up of rounded to sub-rounded grain shapes with very fine and at times coarse-grained texture. Mineralogically the coal seam zone was dominated by abundant organic matter. Mineral compositions of the coal seams of borehole F186001, F186002 and F186003 of the Soutpansberg Coalfield had similar characteristics (Table 4.2).

The hanging wall was made up of sandstones that had rounded to well-rounded grain sizes, with a medium to coarse-grained texture; and the mudstone was made up of medium sized grains (Table 4.3). Mineralogically the mudstones within the hanging wall were dominated by quartz, having sub-rounded to rounded patches of coal, and feldspars.

Table 4.2: Mineralogical characteristics of the coal and host rocks

Characteristics		**Footwall**	**Coal Seams**	**Hanging Wall**	**Dolerite**
Colour	Mudstone	greyish black	black	greyish black	grey
	Coal				
Major Minerals	Mudstone		organic matter		Plagioclase pyroxenes
	Coal				
Minor Minerals		feldspar	-	feldspar	quartz
Degree of Devolutization		low-moderate	moderate	low-moderate	none
Alteration Products			coal rank increased due to igneous intrusions		none
Sulphide Enrichment		low-moderate	moderate	moderate-high	none

Table 4.3: Sedimentological characteristics of coal stratigraphy

Characteristics	Thickness (m)		Colour	Texture	Grain Size	Grain Shape	Matrix	Sorting	Sedimentary Structures	Depositional Interpretation
Rock Type	Max	Min								
Siltstone	4.26	1.1	light grey	fine	very fine	rounded	matrix supported	well sorted	pyrite inclusions	channel & floodplain
Coal	6.2	1.8	dark black	fine	silt size	not visible	matrix supported	well sorted	pyrite mineralisation	fluvial
Mudrock	11.75	1.17	greyish black	clastic – medium	medium	rounded	matrix supported	well sorted	bedding, and authegenic pyrite	floodplain environments
Coal	6.2	1.8	dark black	coarse	medium-coarse	rounded-sub-rounded	clast supported	poorly – medium sorted	stratifications and minor joints	fluvial
Carbonaceous shale	2.57	0.34	dull black	fine-medium	fine (silt size particles)	not visible	matrix supported	well sorted	bedding, breaks along plane, pyrite mineralisation	floodplain environments
Shale	2.6	n/a	greyish black	medium	clastic medium	not visible	matrix supported	poorly-well sorted	minor joints, stratifications and disseminated pyrite	floodplain environments
Laminated sandstone	8.77	0.23	light grey	coarse	medium-coarse	rounded-sub-rounded	clast supported	poorly sorted	minor joints and pyrite mineralisation	fluvial channel
Sandstone	10	0.84	white	equigranul	very fine	rounded	matrix supported	well sorted	stratifications	Fluvial channel deposit
Calcrete	12.35	0.73	yellowish	medium	medium	rounded	-	well	-	-

4.2 Geochemical Analysis

4.2.1 Analysis of Major Oxides

Silica was used as base oxide to study the tectonic setting, variation patterns and maturity of sedimentary facies with all major oxides, as it undergoes little or no changes during diagenesis when compared to other major oxides which undergo substantial changes chemically.

Al_2O_3 vs SiO_2

The chemical contents of silica ranged from 23.25 to 63.5 wt% with an average of 46.64 wt%. While the chemical contents of aluminium oxide ranged from 5.76 to 39.52 wt% with an average of 26.33 wt%. This showed silica to be an oxide which has the greatest range of chemical contents as compared to aluminium oxide (Fig. 4.2).

This finding confirmed paragenetic relationship between aluminium oxide and silica, furthermore, from the Al_2O_3 and SiO_2 graph; the evidence showed that the ratio of aluminium to silica oxide was 6:11 based on their averages, hence suggesting strong geochemical relationship that was influenced by the environment of deposition (Fig 4.2). This demostrates a paragenetic significance and their modal abundance as the occurrence of one element can commonly suggest or even require the presence of the other.

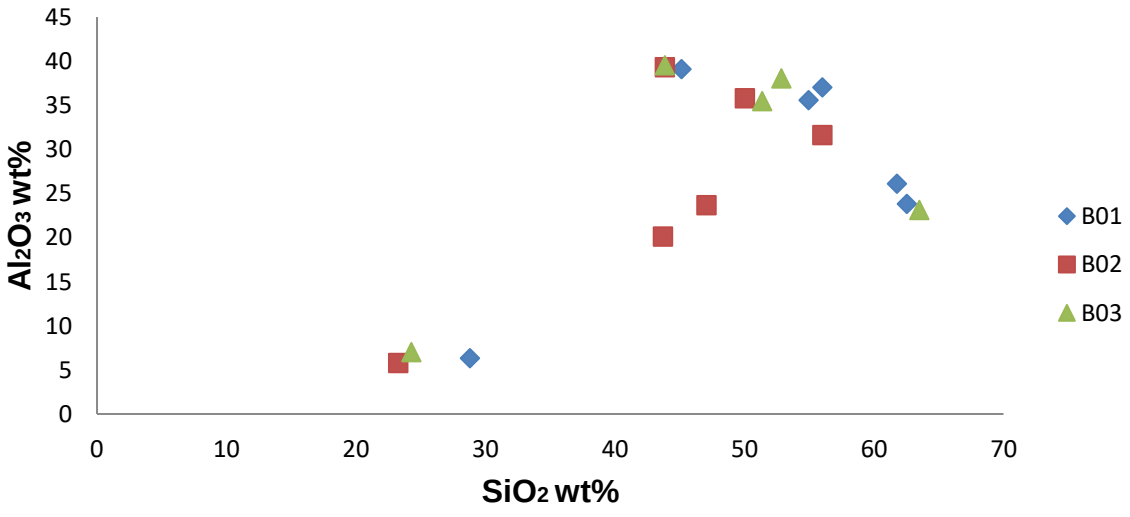

Figure 4.2: Plot of Al_2O_3 and SiO_2 showing correlation of the oxides.

It may further be deduced that there was high amount of primary detrital contents of both silica and aluminosilicates within the portion. This was shown by a strong positive

correlation that existed between these two major oxides. High values of Al_2O_3 and SiO_2 also indicated the prevalence of quartz and clay minerals (Kaolinite), representing a common source of environmental deposition and origin which was a marine environment.

CaO vs SiO_2

The analysis of CaO vs SiO_2 showed that the concentration of CaO was erratic with depth and coal seam zone recording the lowest value of 0.09 wt% in borehole 3 (B03) and the highest value of 1.23 wt% in the footwall of borehole 2 (B02). Furthermore, in borehole 1 (B01) at a depth of 51.43 and 57.90 m respectively, the contents of calcium oxide showed low values ranging from 0.20 to 0.15 wt%. These variations indicated that calcium oxide (CaO) was derived from weathering and diagenesis of plagioclase feldspar minerals and the enrichment of quartz particles, while the concentration of silica oxide (SiO_2) was 61.75 and 28.8 wt% respectively. This suggested high contents of silica, which could be due to felsic environment from which the rocks might have been derived from (Fig 4.3).

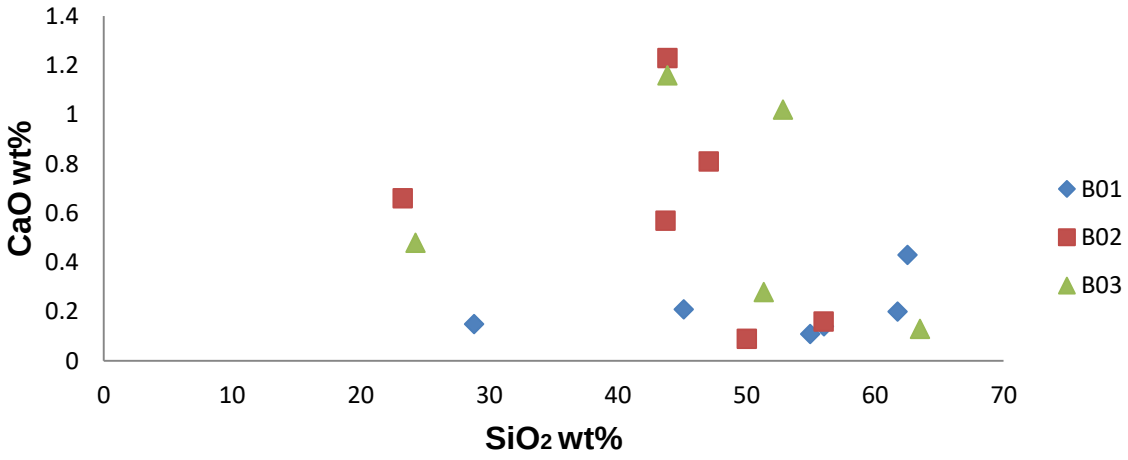

Figure 4.3: Plot of CaO Vs SiO_2 showing variation and distribution of oxides.

Additionally, in borehole F186001 at a depth of 61.05 m there was an increase in concentration of CaO, doubling the content of the top contact which was 0.43 wt%. The same applied to silica content that increased from 45.12 wt% in borehole F186001 at a depth of 58.0 to 62.52 wt% (Table 3.3). This was a clear indication that CaO content decreases with an increase in silica content (SiO_2), reflecting that these silica contents were mainly derived from silica-rich sediments or sand grains with less

calcium oxide being incorporated into the portion (calcium oxide was being altered and depleted during diagenesis), as a result of the mixing of chemically distinct components which contributed to the composition of the sediment (Fig. 4.3).

P_2O_5 vs SiO_2

Based on geochemical results plotted in Figure 4.4, potassium pentoxide (P_2O_5) showed a minimum value of 0.05 with a maximum value of 0.29 wt% while the values of silica ranged from 28.8 to 61.75 wt%. The lower content of potassium pentoxide was as a result of depletion in clay mineral content (Kaolinite) during the transportation, mixing and the deposition of rocks within the basin. Additionally, the compositional relationships of these fluids from the two major oxides (P_2O_5 and SiO_2) reflect that the chemical constituents were simply locally distributed during silification hence resulting in negative correlation. The high content of silica suggests that the environment of deposition was of felsic origin, in which quartz was the most dominant mineral.

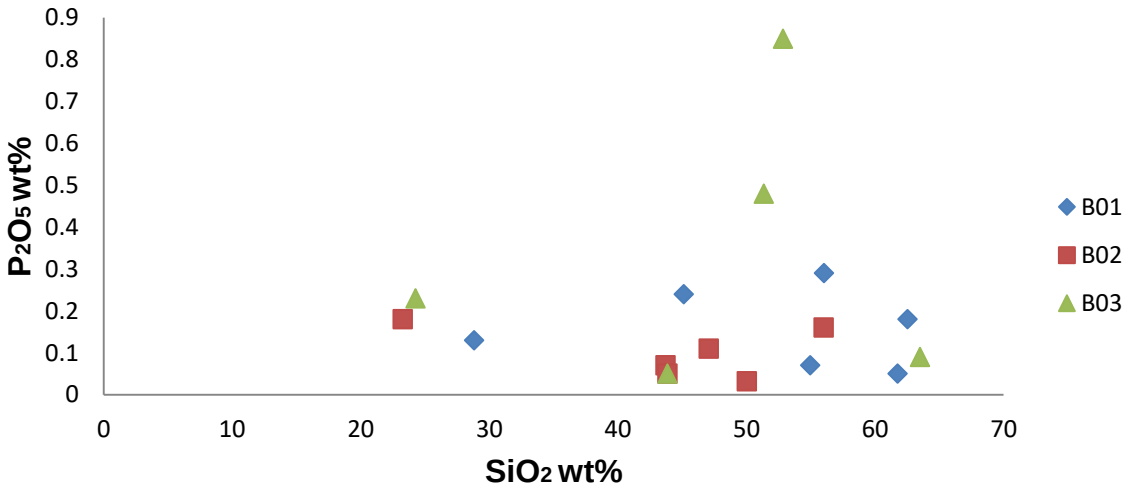

Figure 4.4: Plot of P_2O_5 and SiO_2 showing the distribution of the oxides.

MgO Vs SiO_2

The concentration of magnesium oxide was relatively low, resembling that of calcium oxide as shown in Figure 4.5; suggesting that ferromagnesian minerals seeped from iron-rich fluids and got trapped in felsic environment, but in very low concentrations. The ferromagnesian fluids were further redistributed within the silica, thus resulting in negative correlation. Felsic rocks were rich in silica (SiO_2), hence the high

concentrations of SiO_2 and low values of MgO were attributed to the close relationship and association that MgO has with carbonates such as calcite and dolomite (Fig 4.5).

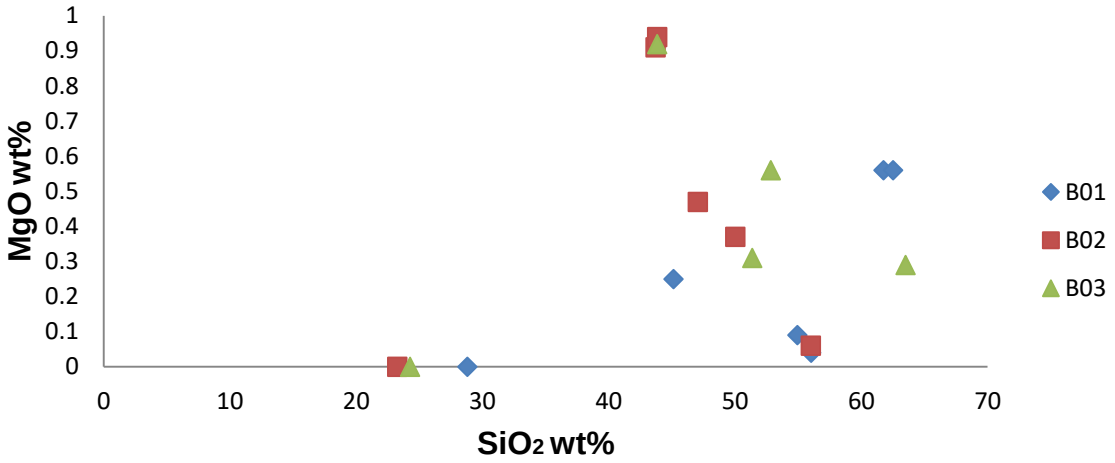

Figure 4.5: MgO Vs SiO_2 Plot showing distribution.

K_2O vs SiO_2

The graph below shows the relationship between potassium oxide (K_2O) and silica (SiO_2), and from the graph it was evident that the contents of silica were quite high while the contents of K_2O were low, ranging from 0.47 to 2.43 wt% with an average of 1.23 wt%. This suggested that the K_2O particles were encapsulated within the silica-rich particles emanating from terrigenous sediments derived from land as a result of weathering and diagenesis as see the figure below of major oxides (Fig. 4.6).

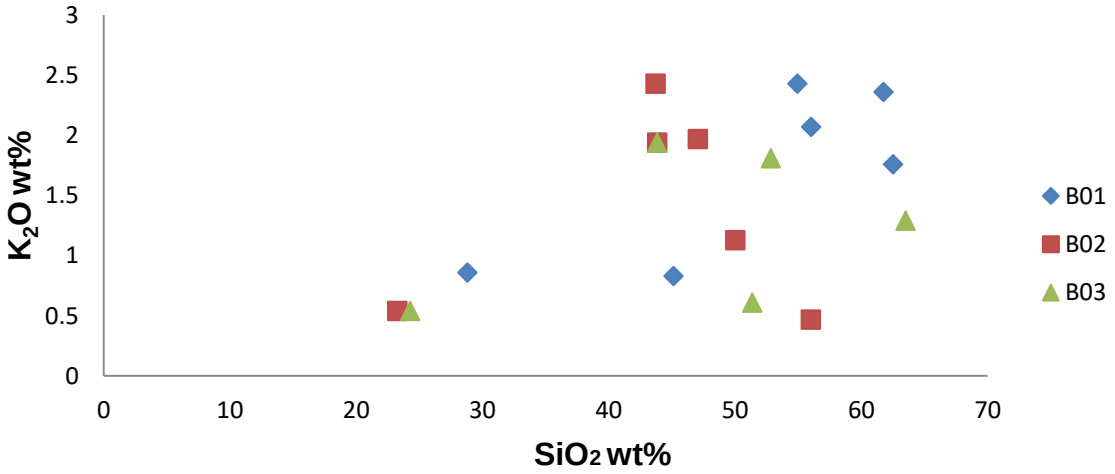

Figure 4.6: Plots of major oxides K_2O and SiO_2 showing the distribution of oxides.

Al_2O_3 vs TiO_2

Oxides such as titanium dioxide (TiO_2) showed relatively low values, ranging from 0.49 to 2.09 with an average of 1.24 wt%; a positive relationship was observed; this suggested that a portion of titanium oxide was incorporated into the silica fluids resulting from silica-rich sediments and sand grains resulting in low concentrations of titanium oxides as it was partially depleted during diagenesis (Fig. 4.7).

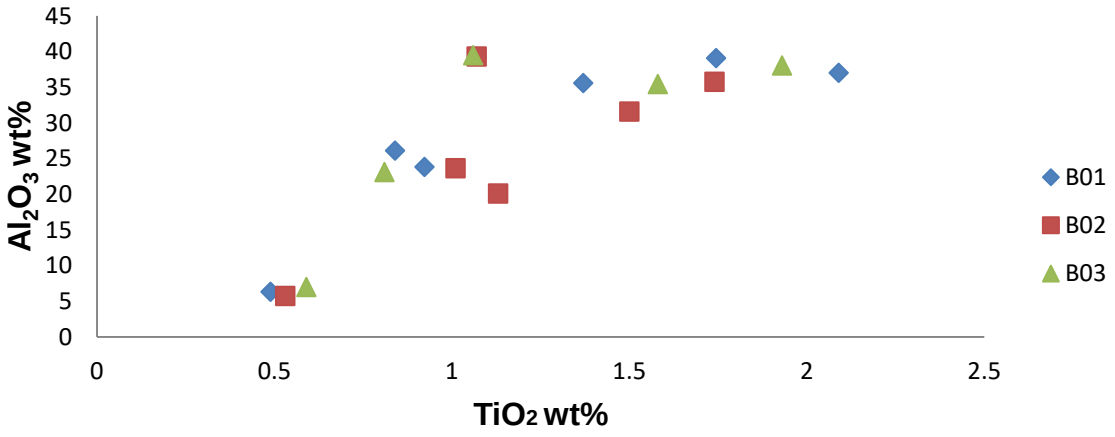

Figure 4.7: The relationship of major oxides Al_2O_3 and TiO_2 showing a positive correlation of the oxides.

Depth vs Fe_2O_3 + SiO_2 + CaO

The contents of calcium oxide (CaO) has shown values ranging from 0.21 to 15.58 wt% indicating variations of calcium oxide content within the hanging wall of the coal seam zone. From the graph below (Fig 4.8), it can be observed that the concentrations of Fe_2O_3 and CaO were constant confirming the same depositional environment, in the same manner, the concentration of SiO_2 ranged from 23.25 and 61.75 wt% respectively reflecting that the silica concentrations increased with an increasing depth.

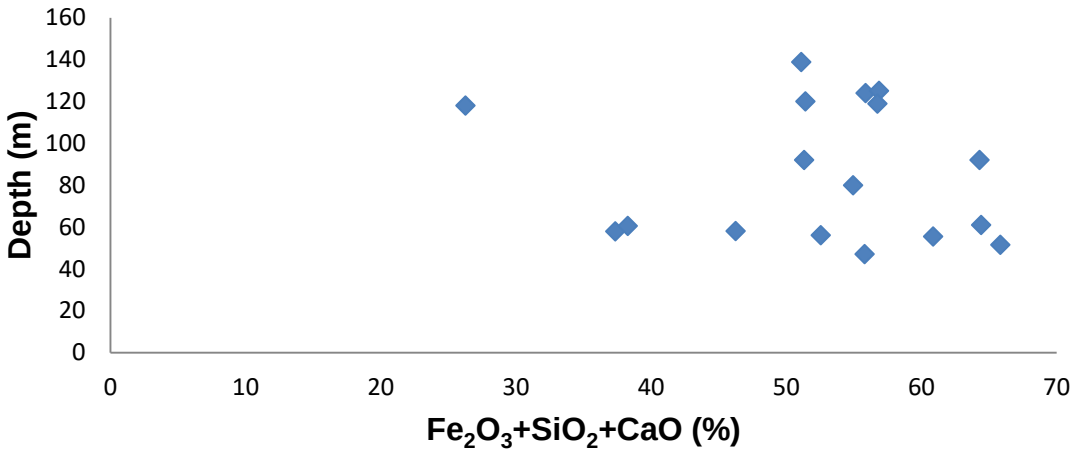

Figure 4.8: Relationship between depth and major oxides (Fe_2O_3+SiO_2+CaO).

4.2.2 Analysis of Trace Elements

Different concentrations of trace elements present in the coal samples were analysed in order to determine the organic matter input, origin of the coal, maturity and mineralogical significance of the coals within the Soutpansberg Coalfield. A comparison of the distribution of sulphur showed that for the first 40 m there was no sulphur within the different lithologies (Fig 4.9). It was further noted that low values of sulphur, about 1000 ppm were distributed at a depth between 40 and 140 m.

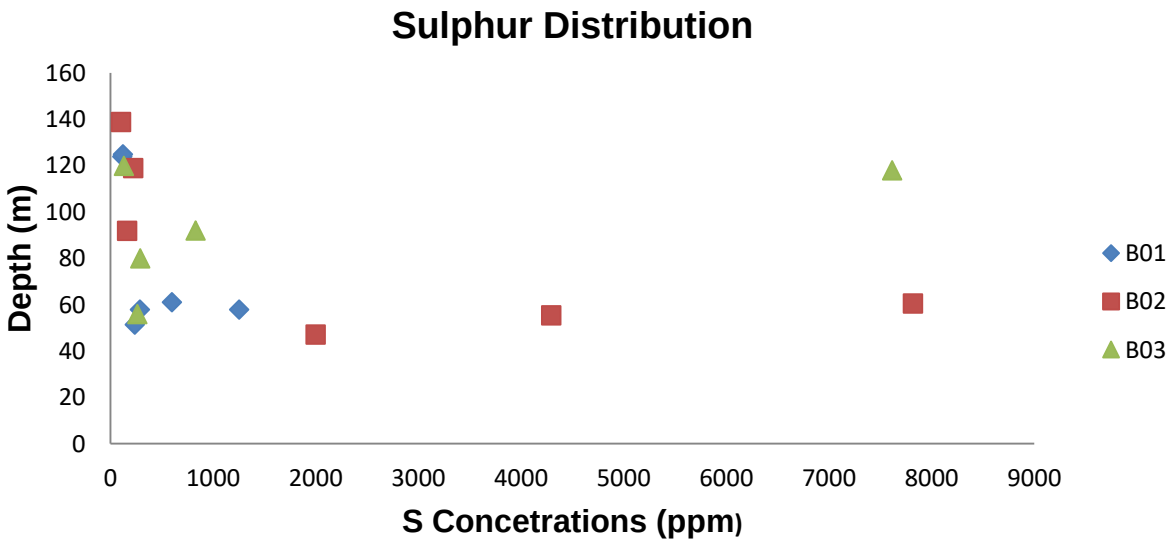

Figure 4.9: Concentrations of S with depth.

The close relationship between Chromium and Nickel content within the analysed coal samples suggested that the organic matter within the coal was derived from terrestrial/marine environment and that the coal was of low to moderate maturity (Fig 4.10).

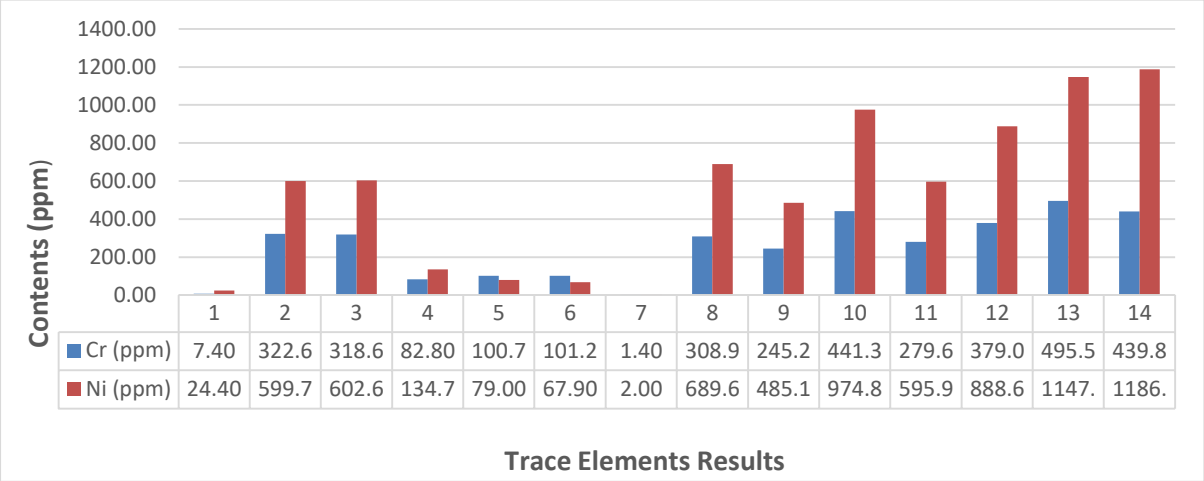

	1	2	3	4	5	6	7	8	9	10	11	12	13	14
Cr (ppm)	7.40	322.6	318.6	82.80	100.7	101.2	1.40	308.9	245.2	441.3	279.6	379.0	495.5	439.8
Ni (ppm)	24.40	599.7	602.6	134.7	79.00	67.90	2.00	689.6	485.1	974.8	595.9	888.6	1147.	1186.

Figure 4.10: Geochemical graph of Cr and Ni.

Trace elements Arsenic (As), Lead (Pb), Zinc (Zn) and Stibnium (Sb)

Concentrations of As, Pb, Zn and Sb were determined, and the results are presented in Table 3.4. This indicated that these elements share common origin within the analysed coal samples. These elements were found in very low concentrations and their contents (Fig. 4.11).

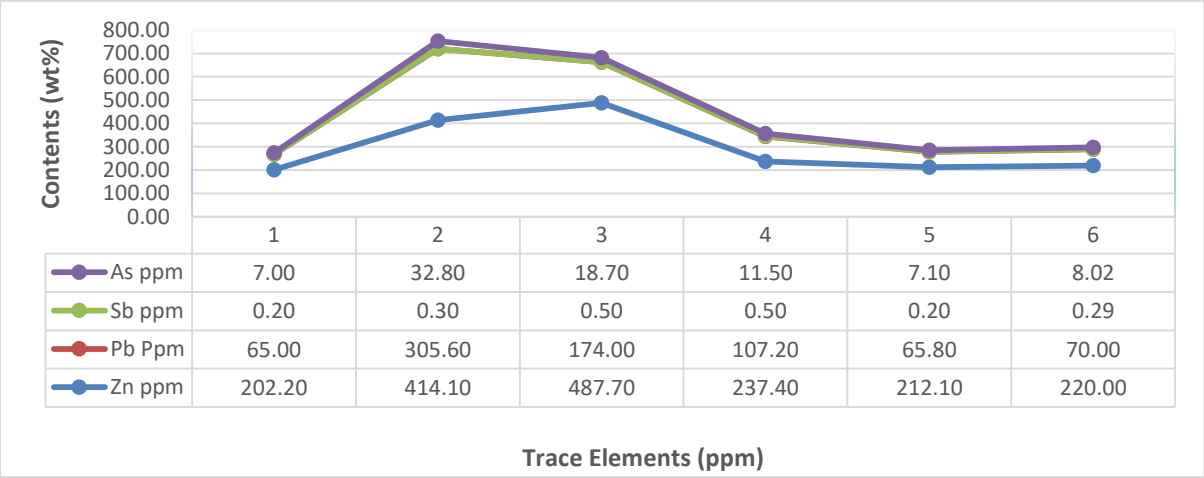

	1	2	3	4	5	6
As ppm	7.00	32.80	18.70	11.50	7.10	8.02
Sb ppm	0.20	0.30	0.50	0.50	0.20	0.29
Pb Ppm	65.00	305.60	174.00	107.20	65.80	70.00
Zn ppm	202.20	414.10	487.70	237.40	212.10	220.00

Figure 4.11: Geochemical graph of trace elements As, Sb, Pb and Zn.

This indicated that trace elements associated with sedimentary rocks might have been derived from silica-rich sediments during deposition.

Plot of V/Ni vs Depth

From Figure 4.12 it was evident that the ratio of V/Ni has a positive correlation with depth suggesting biological degradation during coalification. The high concentration of V and the low concentrations of Ni are indicative of the distance travelled and the rate of transportation, as well as the rate of accumulation and degradation of the coal and host rocks (mudstones); the concentration of V/Ni ranged from 0.61 to 13.9 ppm. From the figure below note that the plotted histograms of V/Ni against depth from 1-6 represent borehole 01, V/Ni against depth from 7-12 represent borehole 02; and the histogram of V/Ni against depth from 13-17 represent borehole 03.

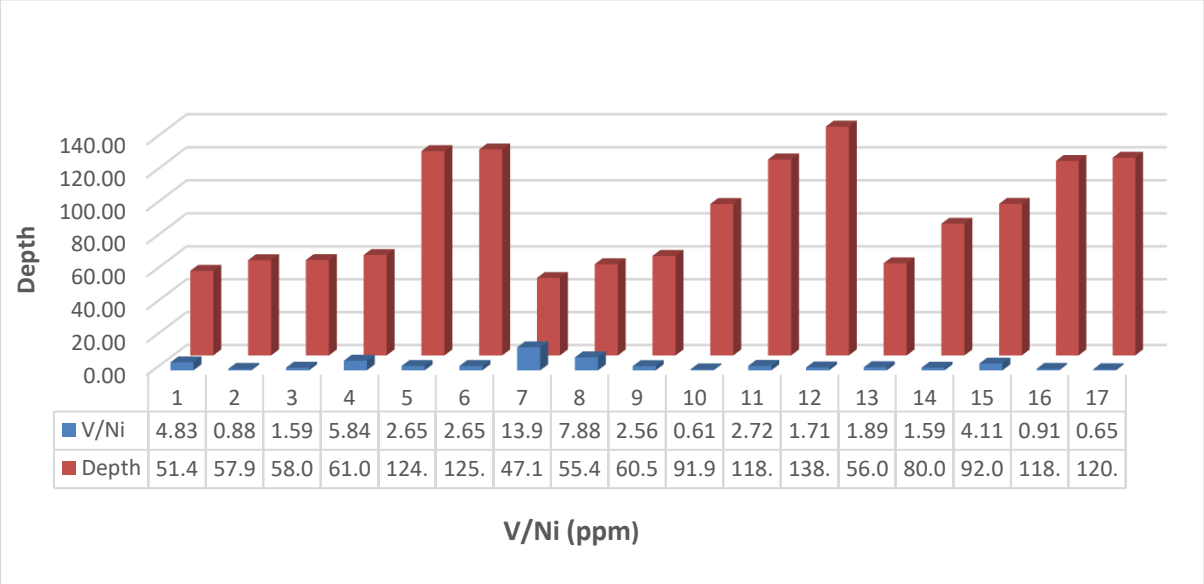

	1	2	3	4	5	6	7	8	9	10	11	12	13	14	15	16	17
V/Ni	4.83	0.88	1.59	5.84	2.65	2.65	13.9	7.88	2.56	0.61	2.72	1.71	1.89	1.59	4.11	0.91	0.65
Depth	51.4	57.9	58.0	61.0	124.	125.	47.1	55.4	60.5	91.9	118.	138.	56.0	80.0	92.0	118.	120.

Figure 4.12: Geochemical ratios of V/Ni with depth

Variations in the distribution of elements in coal seam zones represented different factors in geochemical environments during coal formation as well as changes and differences in pH and plant species of coal that accumulated in the peat swamp environment (Table 4.4). Concentrations of the trace elements within the coal samples varied and it was noted that the mineral content of F186001 coal is the highest.

The presence and distribution of trace elements such as Cr, Cu, Fe, Mn, Ni, Ti, V and Zn; and their use as geochemical parameters to establish the origin of coal has been

presented in Table 4.3 and 4.4. The high vanadium content in coal (143.40-355.6 ppm) suggests a moderate to high mature and marine/terrestrial sourced coal.

Mean= $\frac{\Sigma X}{n}$

= (2.76 + 210.6 + 51.9 + 0.0664 + 3.79 + 110.8 + 75.36 + 240.84) / 8

= 696.116/8

= 87.015

Standard Deviation (σ) = $\frac{\sqrt{\Sigma(X-\mu)^2}}{n-1}$

= √ [1/(8-1)] * [(2.76-87.015)² + (210.6-87.015)² + (51.9-87.015)² + (0.0664-87.015)² + (3.79-87.015)² + (110.8-87.015)² + (75.36-87.015)² + (240.84-87.015)²

= √ (1/7) * (7098.91 + 15273.25 + 7560.13 + 6926.40 +565.73 + 135.84 + 23662.13)

= √0.143 * 61222.39

= √8754.80

σ = 93.57

Coefficient of Variation of all Coal Seams (CV) = Standard Deviation/ Mean

= 93.57/87.015

CV = 1.07533

The value of V/Ni ranges from 0.9 to 5.840 (Table 4.5), the source rock depositional environment determines the proportionality of vanadium to Ni. The concentration of iron ranged from 0.66 to 14.37 ppm with an average of 3.79, while that of sulphur ranged from 284.9 to 7819.70 ppm with an average of 3429.64; iron was the least abundant metal in coal samples, the significant concentrations of iron and sulphur in coal samples indicated the presence of iron bearing minerals such as iron pyrite (FeS_2) and siderite.

Table 4.4: Concentrations of trace elements and major oxides in the Soutpansberg Coalfield.

Coal Seam Samples	Cr ppm	Cu ppm	Fe %	Mn %	Ni ppm	Ti ppm	V ppm	Zn ppm
F186001/58.00	78.5	109.4	0.92	0.004	224.1	4	355.6	487.7
F186001/61.05	34.8	85.6	1.47	0.015	35.7	2.5	208.5	237.4
F186002/60.50	62.40	23.00	14.37	0.30	56.10	1.80	143.40	108.90
F186003/92.08	19.4	78.7	0.66	0.003	40.5	1.7	166.4	47.9
F186003/118.06	64.40	80.10	1.52	0.01	197.6	3.80	179.10	322.30
Mean	**51.9**	**75.36**	**3.79**	**0.0664**	**110.8**	**2.76**	**210.6**	**240.84**
Range	**59.1**	**86.4**	**13.71**	**0.297**	**188.4**	**2.3**	**212.2**	**439.8**
CV	**0.563**	**0.442**	**1.564**	**1.973**	**0.831**	**0.394**	**0.401**	**0.726**
CV= Coefficient of Variation								

Vanadium (V) and Zn were the most abundant elements in this coal, with V concentrations ranging from 143.40 to 355.6 ppm with an average of 210.6; while Zn has concentrations ranging from 47.9 to 487.7 ppm with an average of 240.84. The highest concentration of vanadium and Zn were both recorded in borehole 1.

Titanium occurred in low concentrations when compared to chromium with trace element concentrations ranging from 1.7 to 4 ppm with an average of 2.76; 19.4 to 78.5 ppm with an average of 3.79 respectively. The least concentration of titanium and chromium were recorded in borehole 3 (Table 4.4); the highest concentration of manganese was found in borehole 2 having 0.30 ppm, while the highest concentration of copper was found in borehole 1.

The distribution of trace elements such as Ni and V provides information about the environment of deposition and maturity of the different samples analysed. These elements were strongly correlated with depth and the ratio of Ni and V appears not to be disturbed by post diagenetic processes (Table 4.5).

The closeness in the Cr, Cu and Ni contents as well as V/Ni ratios for all the analysed coal samples suggested the same depositional environments (Table 4.5). V/V+Ni ratio can be related to redox reaction condition in source rocks and low ratio reflected oxicity

while high ratios of (≥0.9) reflected anoxic condition in the depositional environment of coal (Killops and Killops, 2005). The moderately high V/V+Ni ratio (0.48-0.85) showed that the coals were deposited under oxic conditions where the oxygen capacity was limited, however this was the typical coal depositional environment; furthermore, this was in agreement with other work done on the coals of the Soutpansberg Coalfield.

Table 4.5: Trace Metals Ratios in the Soutpansberg Coalfield.

Coal seam samples	Ni (ppm)	V (ppm)	V/Ni (ppm) ()	V/(V+Ni)
F186001/58.00	224.1	355.6	1.587	0.61
F186001/61.05	35.7	208.5	5.840	0.85
F186002/60.50	56.10	143.40	2.556	0.72
F186003/92.08	40.5	166.4	4.109	0.80
F186003/118.06	197.6	179.10	0.906	0.48

A good measure of the degree of weathering was obtained using the following equation to calculate the chemical index of alteration (CIA) using molecular proportions Nesbitt and Young (1982):

$$CIA = [\frac{Al_2O_3}{(Al_2O_3 + CaO + Na_2O + K_2O)X100}]$$

From the calculation using the above equation, the CIA values of coal from the sampled borehole 1 up to borehole 3 ranged from 94%, 82% and 91% respectively. The main trend in the major oxides in the coal used for this study indicates that the coal is of low-ash content which is enriched with elements associated with detrital minerals. The Soutpansberg Coal samples were both calsic and ferrocalsic in chemical composition (Fe, Ca, Al and Si). This indicates that the coal seams consisted of coal layers of average to low quality bituminous coal, intercalated with mudstone and at times with non-coal material such as shale and minor sandstones (Fig. 4.13).

It was also established that the coal studied in this research comprise low moisture content, medium to high volatile matter, medium to high ash content (about 81.6% for S2B1). The fixed carbon ranges from 5-9% to 50% and based on this the coal may be ranked as low bituminous coal. The composition of ash from different coal varies

widely depending on the quantities of clay, shale, pyrite, calcite and other minerals present in the coals; the source of iron oxide is normally pyrite and it commonly occurs in coal.

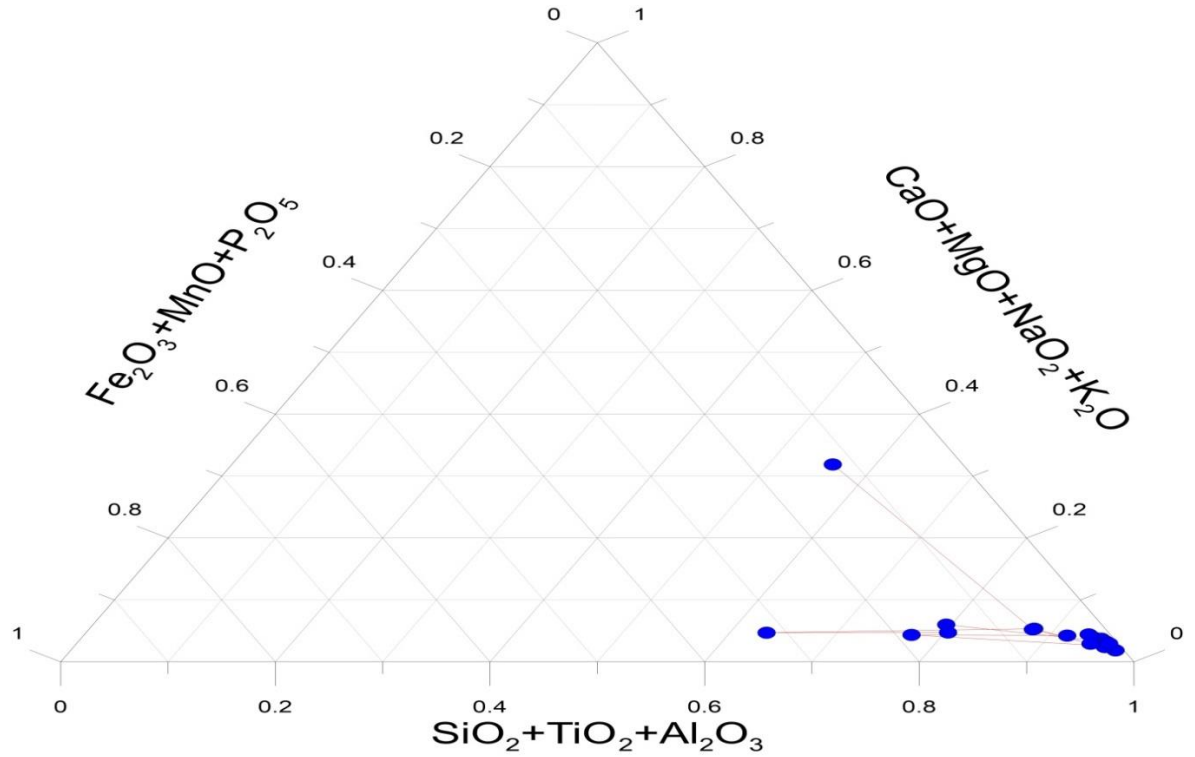

Figure 4.13: Ternary oxide plots of coal ash analysis classification of the Soutpansberg Coal.

4.3 Physical and Chemical Coal Analysis

Coals have been classified according to their physical and chemical properties, by referring to parameters such as fixed carbon and volatile matter, and calorific value. Coals have been classified either for scientific purposes or for coal use (Thomas, 2013). Carbon-hydrogen correlations have been used for scientific purposes.

Coal properties/quality influences the behaviour and use of coal in modern society. Lignite has the lowest calorific values and highest moisture content. The proximate and ultimate results of coal analysis showed that the Soutpansberg coal is lignite to bituminous coal because it has high amounts of carbon and fixed carbon with low moisture content. Bituminous coal can also be used for electric power generation and can be converted to coke for use in the metallurgical industry. Coal with high fixed

carbon can be used for domestic heating fuel and do not ignite easily, however; it does burn slowly for some time (Fig. 4.14).

The proximate parameters from 3 different boreholes in the Soutpansberg Coalfield are given in Table 3.6. One of the important methods of characterising coal is the ultimate analysis which involves the chemical approach to characterising coal by determining the amounts of the principal chemical elements in coal samples. Carbon and hydrogen are the main principal combustible elements in coal, however; carbon is the predominant one based on weight, constituting about 5.3% (the lowest) to 70.3% (highest) of the total.

In this research, coals having a high percentage of carbon (70.3%), generally have high hydrogen content in the range of 4.02% and this drops as the value of carbon content drops (Fig. 4.15). Where the value of carbon was low the sample was in clear contact with sandstone that has shale laminations (shallow stratigraphic depth), conversely the nitrogen content of almost all coals was in the range of 1-2% (Table 3.6).

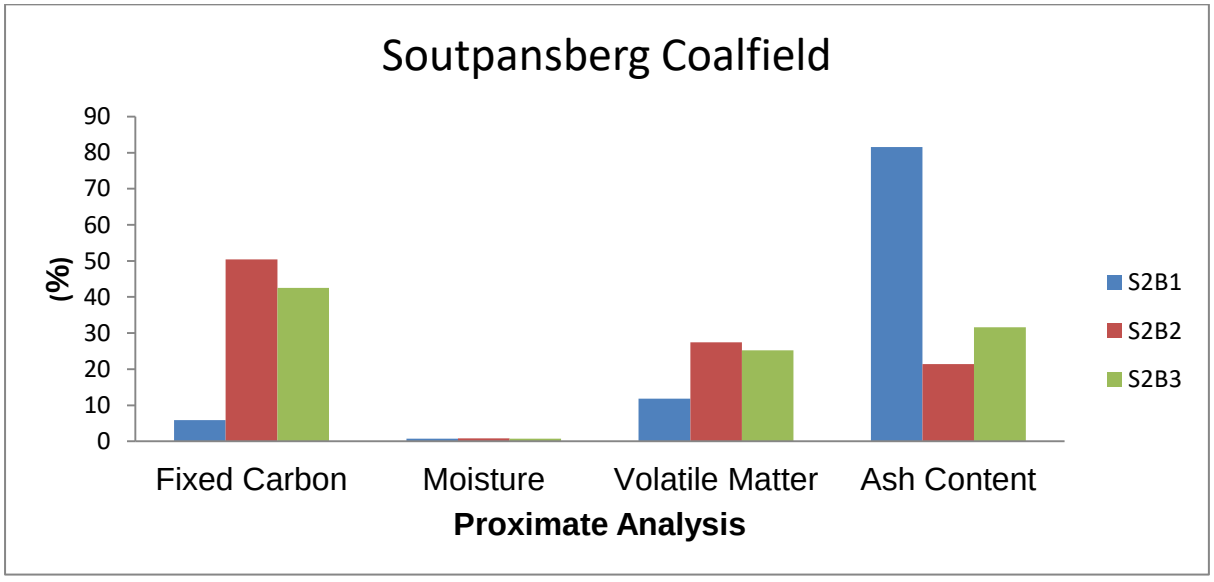

Figure 4.14: Distribution of the coal parameters in Fannie Farm within Soutpansberg Coal.

By using the standard classification of coals by rank S2B2 and S2B3 can be assigned to the sub-bituminous to bituminous coal rank class (medium-volatile bituminous coal rank class). The fixed carbon, volatile matter, moisture and ash were calculated to the

mineral matter air dry basis (ASTM). The coals have low moisture content ranging from 0.7-0.8%, and ash content ranging from 21.4-32%. The fixed carbon and volatile matter values of the coal samples ranged from 42.5 to 50.4% and from 25.2 to 27.4% respectively.

The above analysis shows a clear relation between moisture, ash and carbon values and the stratigraphic position of the coal beds, as the depth increases, the coal rank increases (the carbon content increases with depth hence coal maturity increases). The amount of sulphur in the analysed samples was high with a minimum value of 103.6 ppm and a maximum value of 7819.70 ppm (Table 3.4). The sulphur was determined to be a combination of organic and pyritic sulphur, but predominately pyritic sulphur.

Coal Rank Variations with Depth

The current study established that the coal rank increases as the stratigraphic depth of burial increases (Fig. 14). This is demonstrated by the general increase in fixed carbon and decrease in volatile matter from younger to older coal beds. The ash content also decreases with depth; however, the moisture content remains relatively low with varying stratigraphic depths.

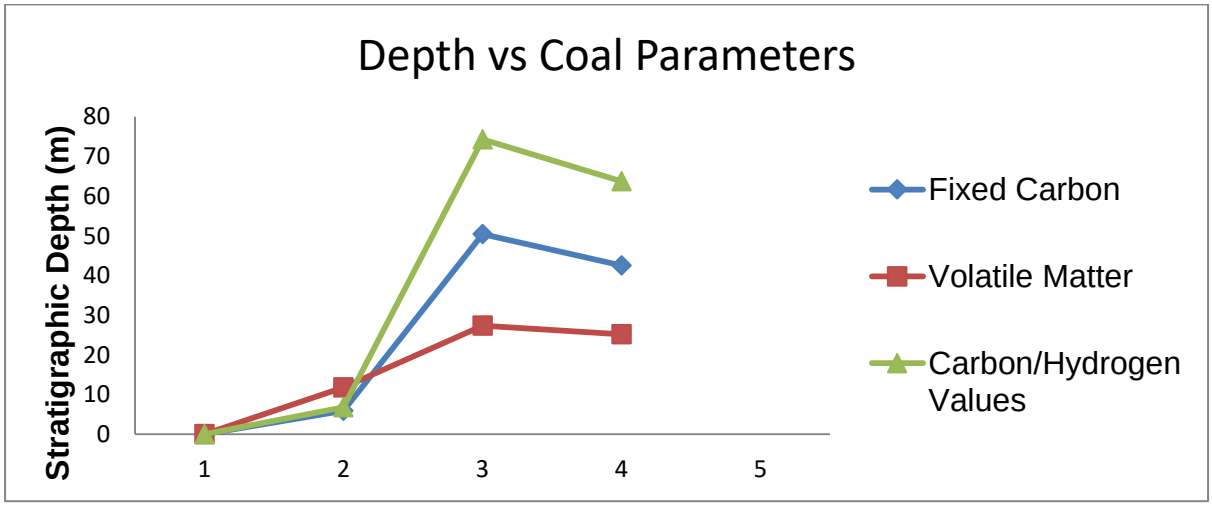

Figure 4.15: Graph showing the relationship between stratigraphic depth and coal rank.

The increase in coal rank in the Soutpansberg Coal results from stratigraphic depth of burial and structural deformations as variations in fixed carbon values indicate spatial variation or differences in the maceral composition of the coal.

Coal Chemical Properties and Carbon Emissions

A graph of coal gas concentrations over combustion time showed great average variations of coal gases, with hydrogen having the least percentage amount of 0.40% and carbon monoxide having a percentage amount of 0.50%. High gas concentrations were observed for methane (CH_4) and carbon dioxide (CO_2) amounting to 1.75% and 1.70% respectively (Fig. 4.16). The average gas concentrations of coal from the 3 boreholes namely; Borehole F186001 (B01), F186002 (B02) and F186003 (B03) as observed on the graph supported the findings by William and Tailakov (undated) that the amount of methane released during coal mining and combustion depend on the coal rank and coal seam depth. Take note that for the 1st minute the machine was being calibrated. At 0.6 seconds to 1.0 minutes calibration of the machine was undertaken.

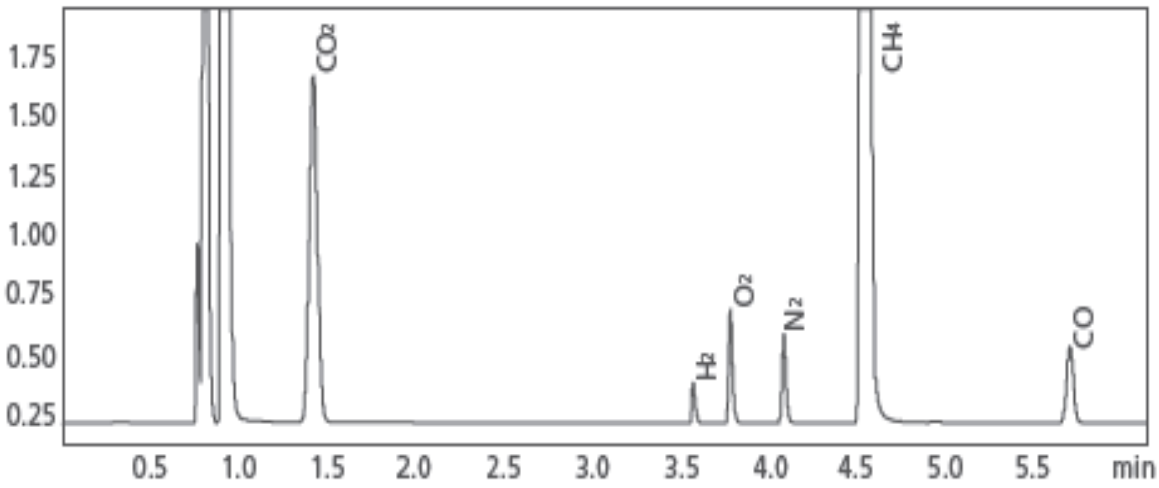

Figure 4.16: Release of greenhouse gases on burning coal against timeframe.

It has been argued that the burning of oil, coal and natural gas releases large quantities of CO_2, CH_4 and NO_2 gases to the atmosphere, and a rise in these gases result in global warming (Ogola and Awuor, 1997). This increase in heat has led to the greenhouse gas effect which results in climate change. This has been confirmed in this study that the two main greenhouse gases, namely; carbon dioxide and methane were found to be released on burning coal after 1.5 and 4.5 minutes respectively. The study concurs with Goldblatt et al. (2002) that coal mining produces negative externalities primarily in the form of air pollution, global warming from greenhouse gases emissions, accidents, biodiversity impacts and water pollution.

CHAPTER 5: DISCUSSION, CONCLUSIONS AND RECOMMENDATIONS

5.1 Discussion

South Africa has one major sedimentary basin that contains thick, organic rich shales, the Karoo basin in Central and Southern Africa. The Karoo Supergroup is known as the host of coal and other base metals in Limpopo Province. The Limpopo Province has 4 coal basins and 6 coalfields namely; the Springbok flats, Waterberg, Mopane, Tuli, Tshipise and Venda-Pafuri of which the Mopane, Tshipise and Venda-Pafuri constitute the Soutpansberg Coalfields representing one basin.

Core logging and analysis have revealed that coal distribution and thickness vary greatly at different core logs studied in the Soutpansberg Coalfield (Figs. 3.4-3.8. Furthermore, the coal seam zone was characterised by various lithologies ranging from laminated sandstone, dull grey to black mudstone, carbonaceous shale to bright black coal. This supports the argument by Sparrow (2012) that the coal-bearing strata in the Soutpansberg Coalfield are inconsistently developed with coal occurrences being that of typical bright coal/carbonaceous mudstones associations, forming composite coal zones.

Core logging has further revealed the sedimentary facies/structures found within the lithologies and the depth at which different lithologies were intersected during borehole drilling. From these sedimentary structures, it was possible to deduce the environment of coal deposition. The following structures stratifications, beddings, breaks along plane, pyrite mineralisation and pyrite inclusions demonstrated different depositional modes and characteristics; as well as variations in the nature and distribution geochemical elements. This was supported by the analysis of the distribution of major oxides and associated trace elements. The conclusion from this study therefore supported findings by Brandl (2002), that coal quality and thickness of seams vary markedly from place to place in this coalfield due to varying local depositional environments.

Stratigraphic analysis showed the occurrence, distribution and thickness of different lithologies with depth (Figs 3.8 and 3.13). The main rock types were sandstone/siltstone laminations and mudstone, as well as dolerite dykes. From geochemical analysis it was observed that dolerite influenced coal quality with depth.

More so stratigraphic analysis revealed little deviation from the previous stratigraphy of the Soutpansberg Coalfield Stratigraphy by (Sullivan *et al*., 1994) that noted two main coal zones the Mikambeni and Madzaringwe Coal Formations. Two main coal seams, were identified in the study area, the upper or main seam and the lower seam that are separated by a vertical distance of 95 m.

Brandl and McCourt (1980) found that, in the Main Karoo Supergroup, coal occurs in the sandstone rich Madzaringwe Formation that overlies the Mikambeni Formation. In this study core logging and analysis found that sandstone/siltstone laminations act as a marker into the coal seam zone where the transition of coal-bearing rocks occur with depth in the Soutpansberg Coalfield.

According to the Tshikondeni Mine Report (1993), the Fripp Sandstone Formation overlies the coal-bearing strata in the Tshikondeni area and the thickness of the layers varies between 100 and 120 m. The colour varies from white to greenish in places and is fine to coarse-grained with various conglomerate bands.

The South African basins containing the Karoo Supergroup strata that appear in different tectonic settings, but the overall climatic overprinting resulted in similar vertical lithological profiles (Groenewald *et al*., 1991; Johnson *et al*., 1996).

In the main Karoo Basin in South Africa, the intrusions have manifested themselves as extensive cross cutting dykes or displacing sills. Where the intrusions interacted with the country rock, thermal contact metamorphism occurred. The intrusions not only affected the quality and characteristics of coal (Van Alphen, 2012), but they also had direct influence on mining processes (Du Plessis, 2008).

The Mikambeni and Madzaringwe Formation are the principal mineralised zones hosting the carbonaceous shale, coal, sandstone with siltstone laminations. This coal horizon is often initiated by sandstone which act as an indicator/transition to a mineralised zone in the Soutpansberg Coalfield, hence these formations are exploration targets in this Coalfield.

The rock specimen studied showed high variations in concentrations of SiO_2, Al_2O_3, and Fe_2O_3 in major oxides and V, Cr, Ni, Cu, Zn, B and S in trace elements. Trace elements are of great significance in determining the environment of deposition and maturity of coal within the Soutpansberg Coalfield. Killops and Killops (1993, 2005)

noted that the nature and quality of trace elements/metals in coal depends on its location and geological history, therefore quantitative study of the metal content can give information concerning the origin, depositional environment, organic matter content and maturation of coal.

High concentrations of sulphur content make the coal unsuitable for making of coke for metallurgical purposes and have been recognised as a source of air pollution resulting in acid rain. Much of the sulphur in coal is derived from the sulphur content in plant material making up the original peat. High sulphur concentrations in coal are derived from the depositional environment such as sea water that contains sulphates.

Hancox and Geotz (2014) noted that the Ecca Group which is divided into Mikambeni and Madzaringwe Formations experienced variable mineralisation associated with geological structures and varying rock types, degree of alteration combined with high levels of coal maturity with increasing depth. The analysis done on coal sample from borehole 2 (S2B2) proved this to be true.

The methane content in coal seams increases with depth and age of the seam (as depth of the coal seam increases, so does the pressure level), thereby reducing the level of permeability causing methane to be tightly bounded to coal and surrounding rock strata (www.worldcoal.org, February 2017).

The composition of the atmosphere is important because some gases and aerosols affect the flow of incoming solar radiation and outgoing infrared radiation. Greenhouse gases include carbon dioxide (CO_2), methane (CH_4) nitrous oxide (N_3O), Ozone (O_3), Chlorofluorocarbons (CFCs), Hydrofluorocarbons (HFCs) and sulphur dioxide (SO_2) to mention a few, and an increase in these gases has caused a rise in the amount of heat from the sun withheld in the earth's atmosphere, heat that would be radiated back into space (Ogola and Awuor, 1997). This increase in heat has led to the greenhouse gas effect which results in global warming.

5.2 Conclusions

Based on this study, the following conclusions have been made:

- Coal seams within the Soutpansberg Coalfield occurs within the Madzaringwe Formation. Three coal basins have been identified in this coalfield, the Venda-

Pafuri, Tshipise and Mopane. These coal basins run from east to the west and the quality of coal increases westwards.

- The depositional environment of coal in the Soutpansberg coalfield was found to be that of fluvial and braided channels (Marine environment).
- Within the Madzaringwe Formation, core logging revealed the occurrence of coal zones where coal seams are intercalating with mudstones, but in places, siltstone forms the footwall of coal. Rarely is coal intruded by dolerite dyke as is the case along borehole W661001. Most of the drill holes intersected mainly 3 coal seams, although in some cases either 2 or 5 seams were intersected. The thickest coal seam was intersected by borehole F578002, coal seam 2 at an interval of 52m-60m (8m thick); however, the multiple coal seams were measured to have a maximum thickness of 6.6m coal seam beds.
- From the results and observations of core logging and correlation, it was noted that the coal horizon was characterised by different coal-bearing lithologies such as mudrock, shale, carbonaceous shale, siltstone and bright coal; and these lithologies ranged from medium to very fine-grained, coal horizon was characterised by very fine to silt size grains of shale to carbonaceous shale and siltstone;
- Correlation of boreholes along the strike showed that shale and mudrock were the predominant rocks within the coal horizon;
- Textural and grain size analysis showed that the footwall often comprises tillite, granite gneiss and at times dolerite dykes and sills as observed in boreholes R637002, F578001 and F578002;
- The boreholes analysed were composed of large to medium-grain sized rocks at the top, which gradually transitioned to fine to very fine grain rock as the coal horizon progresses downwards. The carbonaceous shale and siltstones were characterised by very fine grains to silt size particles respectively, while the bright shiny coal had a vitreous texture, the dull black coal is characterised by very fine grains, with this in mind it was concluded that the coal bearing rocks in the coal horizon ranged from heterogeneous to homogenous grain packing.
- From core logging and interpretation of lithological features it was deduced that the rock sequence represented a single continuous depositional event that was

supported by the occurrence of a single strata that can be correlated over a long distance from borehole to borehole.

Geochemical analysis of coal bearing rocks using XRF showed that:

- Silica was used as a base oxide and the silica content ranged from 23.25 to 63.5 wt%; while the chemical contents of aluminium oxide ranged from 5.76 to 39.52 wt%, this geochemical analysis of major oxides showed a positive correlation existed between these 2 major oxides where in the high levels of these 2 major oxides indicated the prevalence of quartz and clay minerals representing a common source of environmental deposition and origin which was marine environment.
- Trace elements, namely; Cu, Cr, Ti, Fe, V, Mn, Ni and Zn had high concentrations in coal, and they serve as geochemical indicators for coal occurrence and maturity along the stratigraphic depth; for example. High concentration of sulphur in coal was due to the occurrence of pyrite in coal seam;
- Geochemical analysis of major oxides and trace elements does show that variations in the environment of deposition and stratigraphic depth do influence the overall coal quality.

Physical and chemical analysis of coal showed that:

- The studied coal was concluded to be sub-bituminous to bituminous coal rank class (medium-volatile bituminous coal rank class). The coals have low moisture content ranging from 0.7-0.8%, and ash content ranged from 21.4-32%. The fixed carbon and volatile matter values of the coal samples ranged from 42.5 to 50.4%; and from 25.2 to 27.4% respectively. Carbon and hydrogen were the main principal combustible elements in coal, however; carbon is the predominant one based on weight, constituting about 5.3% (the lowest) to 70.3% (highest) of the total.
- The relationship between moisture, ash and carbon values; and the stratigraphic position of the coal beds, showed that as the depth increases, the coal rank increases (the volatile matter decreased while the fixed carbon content increased with depth hence coal maturity increases).

- Coal gas concentrations over combustion time showed great average variations of coal gases, with hydrogen having the least percentage amount of 0.40% and carbon monoxide having a percentage amount of 0.50%. High gas concentrations were observed for methane (CH_4) and Carbon Dioxide (CO_2) amounting to 1.75% and 1.70% respectively

5.3 Recommendations

- The study has established that the Soutpansberg coal studied here is of low bituminous rank and it is considered to be of economic value. Therefore, it was recommended that the coal can be used for economic purposes such as electricity generation and cement.
- Further studies should be undertaken to investigate trace elements and igneous intrusions within the coal seam zone as the current study was limited in scope due to limited fresh boreholes. The study should incorporate logging of more borehole cores and undertake comprehensive geochemical analysis of core samples.
- Further studies should be undertaken to investigate the behaviour of macerals and their relationships with igneous intrusions within the Soutpansberg Coalfield.
- Further research work should be done on the analysis of coal cleats, organic and geochemical compositions of coal and how these factors relate to gas content, composition and recoverability.
- More coal boreholes should be studied in order to develop a geological and geochemical model for interpreting coal quality and relating it to the stratigraphic and sedimentological framework. This is recommended as less boreholes of coal were available for this study to develop a model for coal occurrence within the Soutpansberg Coalfield.

REFERENCES

Aarnes, I., Svensen, H., Polteau, S. and Planke, S., 2010. Contact Metamorphic Devolutilisation of Shales in the Karoo Basin, South Africa and the Effects of Multiple Sill Intrusions, Chemical Geology 281 (3-4), pp. 181-194.

Adriano, D. C., Page, A. L., Elseewi, A. A., Chang, A. C., and Straughan, I., 1980. Utilisation and Disposal of Fly Ash and Other Coal Residues in Terrestrial Ecosystems: A Review. Journal Environmental Quality 9. pp. 333-344.

Akinyemi, S. A., Akinlua, A., Gitari, W. M., and Petrik, L. F., 2011. Mineralogy and Mobility Patterns of Chemical Species in Weathered Coal Fly Ash. Energy Sources Part A: 33, pp. 768-784.

Annehburg Foundation, 2016. Accessed online on the 09th February 2017. http://www.learner.org/courses/envsci/unit/text.php?unit.

Ashton, P. J., 2002. Avoiding Conflicts over Africa's Water Resources. Ambio 31 (3): pp. 236-242.

Barker, O. B., 1976. Discussion of Paper by Jansen, H.: The Soutpansberg Trough (Northern Transvaal) an Aulacogen Transactions of the Geological Society of South Africa, 79 (1), pp.146-148.

Barker, O. B., 1999. A Techno-Economic and Historical Review of the South African-Coal Industry in the 19th and 20th Centuries. In: Pinheiro, H. J., (Ed.), A Techno-Economic and Historical Review of the South African Coal Industry in the 19th and 20th Centuries and Analyses of Coal Product Samples of South African Collieries 1998-1999. Part 1. Bulletin 113 South African Bureau of Standards, pp. 1-63.

Barker, O. B., 2012. CBM in the Springbok Flats Coalfield- A Major Untapped Source of Energy. Accessed Online on the Internet http://www.fossilfuel.co.za/conference/2012/Oliver_Barker.pdf. Accessed on the 26 December 2016.

Bell, K., Spurr, M.R., 1986a. The Klip River Coalfield of Northern Natal. In: Anhaeusser, C.R., Maske, S. (Eds.), Mineral Deposits of Southern Africa, II. Geological Society of South Africa, pp. 2023-2032.

Boggs, S., 2001. Principles of Sedimentology and Stratigraphy. 3rd Ed., New Jersey, Prentice-Hall, 726pp.

Boko, M., Niang, I., Nyong, A., Vogel, C., Githeko, A., Medang, M., Osman-Elasha, B., Tabo, R., and Yanda, P, 2007. Africa. Climate Change 2007: Impacts, Adaptation and Vulnerability. Contribution of Working Group II to the Fourth Assessment Report of the Intergovernmental Panel on Climate Change, Parry, M. L., Canziani, O. F., Palutikof, J. P., Van der Linden, P. J., and Hanson, C. E. (eds.). Cambridge University Pres, Cambridge, UK, pp. 433-467.

Bordy, E. M., 2000. Sedimentology of the Karoo Supergroup in the Tuli Basin (Limpopo River Area, South Africa). PhD Thesis, Rhodes University, South Africa (Unpublished).

Brandl, G. and McCourt, S., 1980. A Lithostratigraphic Subdivision of the Karoo Sequence in the north-eastern Transvaal. Annual Geological Survey of South Africa, 14, pp. 51-56.

Brandl, G., 1981. The Geology of the Messina Area. Exploration Sheet 2230, Messina, Geological Survey of South Africa, 35pp.

Brandl, G., 2002. The Geology of the Alldays Area. Exploration Sheet 2228, Alldays, Geological Survey of South Africa, 71 pp.

Bryers, R. W., 1996. Fireside Slagging, Fouling and High-Temperature Corrosion of Heat Transfer Surface due to Impurities in Steam-Raising Fuels. Progress in Energy and Combustion Science, 22, pp. 120-129.

Budavari, S., Oneil, M. J., Smith, A., and Heckelman, P. E., 1989. Carbon Dioxide, P274 in the Merck Index: An Encyclopedia of Chemicals, DMGs and Biologicals, 11th Ed. Rahway N. J: Merck and Co.

Cadle, A. B., Cairncross, B., Christie, A. M. D., and Roberts, D. L., 1990. The Permo-Triassic Coal Bearing Deposits of the Karoo Basin. Southern African Economic Geology Research Unit, Information Circular No 218, University of Witwatersrand, South Africa.

Cadle, A. B., Cairncross, B., Christie, A. D. M., and Roberts, D. L., 1993. The Karoo Basin of South Africa: Type Basin for the Coal-Bearing Deposits of Southern Africa. International Journal of Coal Geology, 23, pp. 117-157.

Cairncross, B., Anderson, J. M., and Anderson, H. M., 1995(a). Paleoecology of the Triassic Molteno Formation, Karoo Basin, South Africa- Sedimentological and Paleontological Evidence. South Africa Journal of geology, 98, pp. 452-478.

Cairncross, B., 2001. An overview of the Permian (Karoo) Coal Deposits of Southern Africa. Journal of African Earth Science, Vol 33 (3-4), pp. 529-562.

Catuneanu, O., Hancox, P. J., and Rubidge, B. S., 1998. Reciprocal Flexural Behaviour and Contrasting Stratigraphies: A New Basin Development Model for the Karoonretroarc Foreland System, South Africa Basin Res. 10. pp. 417-439.

Catuneanu, O., Hancox, P. J., Cairncross, B. and Rubidge, B. S., 2002. Foredeep Submarine Fans and Forebulge Deltas: Orogenic Off-loading in the Underfilled Karoo Basin. Journal of African Earth Science Vol 35, 489-502.

Catuneaunu, O. H., Wopffner, P. G., Errikson, B., and Cairncross, B. S., 2005. The Karoo Basins of South Central Africa. Journal of African Earth Sciences, Vol 43, pp. 211-253.

Chabedi, C. K., 2013. Analysis of Technical Factors for Underground Mining of Deep Waterberg Coal Resources. Unpublished Master of Science Dissertation, University of Witwatersrand.

Crelling, J., and Dutcher, R. R., 1968. A Petrologic Study of a Thermally Altered Coal from the Purgatorie River Valley of Colorado, GSA Bulletin, 79 (10), pp. 1375-1386.

Cruz, R. V., Harasawa, H., Lal, M., Wu, S., Arokhin, Y., Punsalmaa, B., Honda, Y., Jafari, M., Li, C., and Huu Ninh, N. 2007. Asia. Climate Change 2007: Impacts, Adaptation and Vulnerability. Contribution of Working Group II to the Fourth Assessment Report of the Intergovernmental Panel on Climate Change, Parry, M. L., Canziani, O. F., Palutikof, J. P., Van der Linden, P. J., and Hanson, C. E. (eds). Cambridge University Press. Cambridge, UK, pp. 469-509.

De Jager, F. S. J., 1976. Coal In: Coetzee, C. B., (Editor), Mineral Resources of the Republic of South Africa, 5th Edition. Department of Mines, Geological Survey of South Africa, Government Printers, Pretoria 289-330.

De Jager, F. S. J., 1983. Coal Reserves of the Republic of South Africa- An Evaluation of the End of 1982. Pretoria: Geological Survey of the Department of Mineral and Energy Affairs.

De Wit, M., and Jacek, S., 2006. Changes in Surface Water Supply across Africa with Predicted Climate Change -AEON- Africa Earth Observatory Network, University of Cape Town. Rondebosch 7701. South Africa Science Express Report.

Diessel, C. F. K., 1992. Coal-Bearing Depositional Systems, Springer, Berlin, Germany, 1992.

Dreyer, C., 1999. Total Utilization of the Coal Resources: The Grootegeluk Experience. In: C. Anhaeusser (ed), Proceedings XVth CMMI Congress, Johannesburg, South African Institute of Mining and Metallurgy, pp. 153-164.

Duncan, A. R., and Marsh, J. S., 2006. The Karoo Igneous Province. In: Johnson, M. R., Anhaeusser, C. R., and Thomas, R. J. (Eds.). The Geology of South Africa, Geological Society of South Africa, Johannesburg/ Council for Geoscience Pretoria, 461-520.

Du Plessis, G. P., 2008. The Relationship between Geological Structures and Dolerite Intrusions in the Witbank Highveld Coalfield, South Africa. Masters Thesis. Department of Geology, University of Free State (Unpublished).

Du Toit, A. L., 1954. Geology of South Africa. 3rd Edition: Oliver and Boyd, Edinburgh and London, 611pp.

Eberhard, A., 2011. The Future of South African Coal: Market, Investment, and Policy Changes. Accessed from the Internet 2016. www.google.co.za/Soutpansberg/Coalfields/

Fabianska, M. J., and Kruszewska, K. K. J., 2003. Relationship between Petrographic and Geochemical Characterisation of Selected South African Coals. International Journal of Coal Geology, 54, pp. 95-114.

Falcon, R., and Ham, A. J., 1988. The Characteristics of Southern African Coals. Journal of South African Institute of Minerals and Metallurgy. Vol. 88 (5), pp. 145-161. Accessed online: www,saimm.co.za/journal/vo88no5p145.pdf.

Falcon, R., 2012. Coal in South Africa: Coal Qualities (Types) Related to Combustion, Presented at the Coal Quality Course, University of Witwatersrand, Johannesburg, 13-17 February 2012.

Feris, J., 2015. The Future of Underground Coal Gasification in South Africa. Accessed from the internet: www.cliffedekkerhofmeyr.com/en/news/publications/2015/mining-and-minerals/mining-and-minerals-alert-24.

Fischer, G., Mahendra Shah, and Harrij van Velthuizen., 2002. Climate Change and Agricultural Variability. A Special Report on Climate Change and Agricultural Vulnerability, Contribution to the World Summit on Sustainable Development. Johannesburg 2002 (Global, Agriculture).

Fitch, F. J., and Miller, J. A., 1971. Potassium Argon Radio Ages of Karoo Volcanic Rocks from Lesotho: Bulletin of Volcanology, 35, pp. 64-84.

Fourie, C. J. S., Henry, G., and Mare, L. P., 2014. The Structure of the Karoo-Age Ellisras Basin in Limpopo Province, South Africa, In the Light of New Airborne Geophysical Data. The South African Journal of Geology, Vol 117 (2), pp. 207-224.

Frank, S. R., and Mergner, J. L. Preparation of Rock Thin Sections. United States Geological Survey. Washington, D. C, pp. 1201-1207.

Gaigher, G. L., 1980. Mineral Matter in Some South African Coals, Masters Thesis, University of Pretoria, South Africa (Unpublished).

Gilligan, R.H., 1986. Orange Free-State-Vierfontein Coalfield. In: Anhaeusser, C.R., Maske, S. (Eds.), Mineral Deposits of Southern African, Vol. II. Geological Society of South Africa, Johannesburg, 1929-1937pp.

Goldblatt, M., Gelb, S., and Davies, G. 2002. Macroeconomics and Sustainable Development in Southern Africa: Synthesis Report of South African Study. Development Bank of South Africa. Midrand. South Africa. Accessed 30 June 2018.

Groenewald, P. B., Grantham, G. H., and Watkeys, M. K., 1991. Geological Evidence for a Proterozoic to Mesozoic Link Between South Eastern Africa and Dronning Maud Land, Antarctica. Journal of the Geological Society of London 148, pp. 1115-1123.

Guernier, V., Hochberg, M. E., Guegan, J. F., 2004. Ecology Drives the Worldwide Distribution of Human Diseases. PLOS Biology. Oxford. 2 (6), pp. 740-746.

Hancox, P. J., and Gotz, A. E., 2014. South Africa's Coalfields: A 2014 Perspective. International Journal of Coal Geology 132, pp. 170-254.

Harms, J. C., Southard, J. B., and Walker, R. G., 1982. Structures and Sequences in Clastic Rocks. Society of Economic Paleontologists and Mineralogists Short Course Notes, 9, Calgary, 240pp.

Harris, S., and Baneth, G., 2005. Drivers for the Emergence and Reemergence of Vector-Borne Protozoal and Rickettsial Organisms. International Journal for Parasitology. 35, pp. 1309-1318.

Haskins, D. R., and Bell, F. G., 2005. Drakensburg Basalts: Their Alteration, Breakdown and Durability. Quarterly Journal of Engineering Geology and Hydrogeology, 28 (3), pp. 287-302.

Hayhurst, A. N., and Lawrence, A. D, 1992. Progress in Energy and Combustion Science: Emissions of Nitrous Oxide from Combustion Sources. Elsevier, Science Direct Journal, Vol 18 (6), pp. 529-552.

Henderson, R. E., 1986. South Rand Coalfield. In: Anhaeusser, C. R., Maske, S. (Eds.), Mineral Deposits of Southern Africa, Vol. II. Geological Society of South Africa, pp. 1953-1961.

Hendrikson, T. A., 1975 (Ed.), Synthetic Fuels Data Handbook, Cameron Engineers, INC., Denver, C.O., pp. 19-75.

Holland, M. J., Cadle, A. B., Pinheiro, R., and Falcon, R. M. S., 1989. Depositional Environments and Coal Petrography of the Permian Karoo Sequence: Witbank Coalfield, South Africa. International Journal of Coal Geology, II, pp. 143-169.

IPCC., 2007. Fourth Assessment Report Intergovernmental Panel on Climate Change Secretariat. Geneva, Switzerland. http://www.ipcc.ch/>. Accessed 15 May 2017.

Isbell, J. L., Cole, D. I., Catuneanu, O. 2008. Carboniferous-Permian Glaciation in the Main Karoo Basin, South Africa: Stratigraphy, Depositional Controls, and Glacial Dynamics. Geological Society of America Special Papers 441, pp. 71-82.

Jeffrey, L.S., 2005. Characterisation of the Coal Resources of South Africa. The Journal of the South African Institute of Mining and Metallurgy, pp. 95-102.

Johansson, T. B., Kelly, H., Reddy, A. K. N., and Williams, R. H. (Eds), 1992. Renewable Energy: Sources for Fuels and Electricity. Island Press, Washington, 1160pp.

Johnson, H., 1976. The Waterberg and Soutpansberg Groups in the Blouberg Area, Northern Transvaal Transactions of the Geological Survey of South Africa, 79 (2), pp. 281-297.

Johnson, M. R., 1994. Thin Section and Grain Size Analysis Revisited. The Journal of the International Association of Sedimentologists. Vol, 41 (5), pp. 985-999. Accessed from https://doi.org/10.1111j.1365-3091.1994.tbo1436.x. Accessed 10 May 2017.

Johnson, M. R., Van Vuuren, C. J., Hegenberger, W. F., Key, R., and Show, U., 1996. Stratigraphy of the Karoo Supergroup in Southern Africa: An Overview. Journal of African Earth Sciences, Volume 23, Issue 1, pp. 3-15.

Johnson, M. R., Anhaeusser, C. R. and Thomas, R. J., 2006. The Geology of South Africa. Geological Society of South Africa and the Council for Geoscience, pp. 461-495.

Johnson, M. R., Van Vuuren, C. J., Visser, J. N., Robets, D. L., and Brandl, G. 2006. Sedimentary Rocks of the Karoo Supergroup: In Johnson, M. R., Anhaeusser, C. R., and Thomas, R. J. (eds.): The Geology of South Africa and Council of Geoscience. Geological Society of South Africa, Pretoria, pp. 461-495

Kerkkonen, O., 1997. Influence of Ash Reaction on Feed Coke Degradation in the Blast Furnance. Coke Making International, 9, pp. 34-41.

Killops, S. D., and Killops, V. J. 1993. An Introduction to Organic Chemistry. Longman Group Ltd, UK.

Killops, S. D., and Killops, V. J. 2005. Introduction to Organic Geochemistry. 2nd Ed. Blackwell Publishing Ltd.

Klaus, K. E. N., 2005. Glossary of Geology. American Geological Institute, Springer Science and Business Media, pp119-126. Accessed from the Internet on the 03 March 2019; https://books.google.co.za/books.

Kosminski, A., Ross, D. P., and Agnew, J. B., 2006. Reactions between Sodium and Kaolin During Gasification of Low Rank Coals. Fuel Processing Technology, 87, pp. 1051-1062.

Le Treut, H., Somerville, R., Cubasch, U., Ding, Y., Mauritzen, C., Mokssit, A., Peterson, T., and Prather, M., 2007. Historical Overview of Climate Change. In: Climate Change 2007: The Physical Science Basis. Contribution of Working Group I to the Fourth Assessment of the Intergovernmental Panel on Climate Change [Solomon, S. Qin, D. Manning, M. Chen, Z. Marquis, M. Averyt, K. B. Tignor, M. and Miller, H. L. (ed.)]. Cambridge University Press. Cambridge, United Kingdom and New York.

Liu, G., Vassilev, S. V., Gao, L., Zheng, L., and Zicheng Peng, Z., 2005. Mineral and Chemical Composition and Some Trace Element Contents in Coals and Coal Ashes from Huaibei Coalfield, China, Energy Conversion and Management, 46, pp. 2001-2009.

Lohe, E. M., 1990. Geological Parameters in Coalbed Methane Generation and Exploration. In: Paterson, L. (Ed.), Methane Drainage from Coal. CSIRO Division of Geomechanics, Syndal, Victoria, pp. 4-11.

Malaza, N., Liu, K., and Zhao, B., 2013. Facies Analysis and Depositional Environments of the Late Palaeozoic Coal-Bearing Madzaringwe Formation in the Tshipise-Pafuri Basin, South Africa. Hindawi Publishing Corporation, ISRN Geology, Vol. 2013. (Accessed 03 October 2013).

McCabe, P. J. 1984. Depositional Environments of Coal and Coal-Bearing Strata, Special Publications of the International Association of Sedimentologists, Vol. 7, pp. 13-44.

McCarthy, J., and Rubidge, B., 2005. The Story of Earth and Life. A Southern African Perspective on a 4.6 Billion Year Journey. Struik Publishers, Cape Town, 334 pp.

Meehl, G. A., Stocker, T. F., Collins, W. D., Friedlingstein, P., Gaye, A.T., Gregory, J. M., Kitoh, A., Knutti, R., Murphy, J. M., Noda, A., Raper, S. C. B., Watterson, I. G., Weaver, A., and Zaho, Z. C, 2007. Global Climate Projections. In: Climate Change 2007: The Physical Science Basis, Contribution of Working Group I to the Fourth Assessment of the Intergovernmental Panel on Climate Change [Solomon, S. Qin, D. Manning, M. Chen, Z. Marquis, M. Averyt, K. B. Tignor, M. and Miller, H. L. (eds)]. Cambridge University Press. Cambridge, United Kingdom and New York.

Melenevsky, V. N., Fomin, A. N., Konyshev, A. S., and Talibova, O.G., 2008. Contact Coal Transformation under the Influence of Dolerite Dyke (Kaierkan Deposit, Nril'sk District), Russian Geology and Geophysics, 49, pp. 667-672.

Miall, A. D., 1990. Principles of Sedimentary Basin Analysis. 2nd Edition, Springler-Verlag. New York Inc, 668pp.

Miall, A. D., 2000. Principles of Sedimentary Basin Analysis, 3rd Edition, Updated and Enlarge Edition. Springer 616pp.

Mintek, 2007. Assessment of Kwazulu-Natal Provinces Coal Mining and Coal Resources. Trace and Investment Kwazulu-Natal. Accessed online: www.tikzn.co.za/resources/doc/research. Accessed 18 August 2016.

Modie, B., 2008. The Palaeozoic Palynostratigraphy of the Karoo Supergroup and Palynofacies Insight into Palaeoenvironmental Interpretations, Kalahari Karoo Basin, Botswana. Unpublished Doctor of Philosophy, 20pp.

Myburg, C., 2012. Basin Analysis of Springbok Flats. Coaltech 2020 Presentations, Johannesburg.

Mussett, A. E., and Khan, M. A., 2000. Looking into the Earth: An Introduction to Geological Geophysics, Cambridge University Press, Cambridge, 470pp.

Naledzani, A. T., 1992. Farmers Support Programme and Agricultural Development in Venda. Unpublished Master's Thesis, University of Pretoria.

National Energy Council (N.E.C) 1991. Coalbed Methane Resource Development Industrial and Petrochemical Consultants (Pty) Ltd, 51pp.

Nesbitt, H. W., and Young, G. M., 1982. Early Proterozoic Climate and Plate Motion Inferred from Major Element Chemistry of Lutites. Nature, Vol. 299, pp. 715-717.

Neuendorf, K. K. E., Mehl Jr, J. P., and Jackson, J. A. (eds), 2005. Glossary of Geology, Geological Magazine 145 (01). Berlin, Heidelberg, New York: Springer-Verlag.

Ogola, J. S., 1997. Sources and Sinks of Greenhouse Gases. In Ogola, J. S. Abira, M. A. and Awuor, V. O. (eds.): Potential Impacts of Climate Change in Kenya. Climate Network Africa, Nairobi, pp. 17-29.

Ogola, J. S., and Awuor, V. O., 1997. The basic Scientific Issues of Climate Change. In Ogola, J. S., Abira, M. A. and Awuor, V. O. (eds.): Potential Impacts of Climate Change in Kenya. Climate network Africa, Nairobi, pp. 3-15.

Ogola, J. S., Abira, M. A., and Awuor, V. O. (eds), 1997. Potential Impacts of Climate Change in Kenya. Climate Network Africa, 199pp.

Prockop, L. D., and Chichkova, R. I. 2007. Carbon Monoxide Intoxication. An Update Review Journal of Neurological Science 262 (2007) 122-130. Accessed online on 09 February 2017: http://arlweb.msha.gov/illness_prevention/carbonmonoxide.

Roberts, D. L., 1992. The Springbok Flats Basin: A Preliminary Report. Unpublished Report, Council of Geoscience, 1992-0197, 23pp.

SACS: South African Committee for Stratigraphy, 1980. Stratigraphy of South Africa: Part 1. Kent: Lithostratigraphy of the Republic of South Africa, South West Africa/Namibia and the Republic of Bophutatswana, Transkei and Venda. Handbook of the Geological Survey of South Africa, 8, 690pp.

Saghafi, A., Pinetown, K. L., Grobler, P. G., and Van Heerden, J. H. P., 2008. CO2 Storage Potential of South African Coals and Gas Entrapment Enhancement due to Sills. International Journal of Coal Geology, 73, pp. 74-87.

Sanderson, A., 1997. A Review of the Coal Bed Methane Potential of South Africa's Coal Deposits and a Case Study from the North Eastern Karoo Basin. Unpublished Master's Thesis, Rand Afrikaans University, Johannesburg, 182pp.

Sharma, A., Kyotani, T., and Tomita, A., 2000. Direct Observation of Raw Coals in Lattice Fringe Mode Using High-Resolution Transmission Electron Microscopy. Energy and Fuels, 14, pp. 1219-1225.

Smith, R. M. H., Errikson, P. G., and Botha, W. J., 1993. A Review of the Stratigraphy and Sedimentary Environments of the Karoo-Aged Basin of Southern Africa. Journal of African Earth Sciences, Vol 16, pp.143-169.

Snyman, C. P. 1998. Coal: In the Mineral Resources of South Africa, By Anhaeusser, C. R., and Wilson, M. G. C. Pretoria, Council of Geoscience, 145-146pp.

South African Weather Service, 2008. Climatic Conditions Information 2008. Accessed from the Internet in 2013.

Sparrow, J., 2006. An Independent Competent Person's Report of the Overvlakte Project, Prepared for the Shareholders Zingaro Trade 39 (Pty) Ltd by Gemecs (Pty) Limited, 23pp.

Sparrow, J., 2012. The Soutpansberg Coalfields: The Forgotten Basin. Proceedings of the Limpopo Conference, Coal of Africa Limited.

Speight, J. D. 2005. Handbook of Coal Analysis, A Series of Monographs of Analytical Chemistry and its Applications (1st ed.). New Jersey: John Willey and Sons, INC. 227pp.

Stratten, T., 1968. The Dwyka Glaciation and its Relationship to the Pre-Karoo Surface. Unpublished PhD. Thesis, University of the Witwatersrand, Johannesburg 196 pp.

Sullivan, J., Brink, V., and Sullivan, D., 1994. The Soutpansberg Coalfields, Johannesburg. The Geological Society of South Africa, pp. 165-170.

Thomas, L., 2013. Coal Geology, 2nd Edition. Wiley-Blackwell (A John Wiley and Sons Ltd Publication).

Tshikhudo, P. P., 2005. Irrigation and Dryland Fruit Production: Opportunities and Constraints faced by Small-Scale Farmers in Venda. Unpublished Master's Thesis. University of Pretoria.

Tshikondeni Mine Report (EDMS)., 1993. Unpublished and Untitled Report, ISCOR Group, 11pp.

Tucker, M. E., 1992. Sedimentary Petrology- An Introduction to the Origin of Sedimentary Rocks. 2nd Edition. Blackwell Scientific Publication, 260pp.

Tucker, E. M., 2001. Sedimentary Petrology: An Introduction to the Origin of Sedimentary Rocks, 3rd Edition, Blackwell Sciences, 354pp.

UNDP., 2006. Human Development Report 2006. Beyond Scarcity: Power, Poverty and the Global Water Crisis, United Nations Development Programme. http://hdr.undp.org/hdr2006/report.cfm.>. 29 March 2016.

UNFCCC. 2007. United Nations Framework Convention on Climate Change-Climate Change: Impacts, Vulnerabilities and Adaptation in Developing Countries, Climate Change Sectretariat. Germany. http://unfccc.int/resources/doc/publications/impacts.pdf. November 2016.

United States Office of Coal Research (U.S.O.C.R)., 1967. Methods of Analyzing and Testing Coal and Coke by Staff, Office of the Director of Coal Research. U. S. Department of Interior, Bereau of Mines, 82 pp. TN23. U4No: 638 622.06173.

Van Alphen, C., 2012. Coal Quality Impact, Presented at the Coal Quality Coarse, University of Witwatersrand, Johannesburg, pp. 13-17; February 2012.

Van de Walt, B., 2012. The Petrology, Petrography and Geochemistry of Anomalous Borehole Core Sequences in the Highveld Coalfield, South Africa: A Case Study for Diatreme Activity. Unpublished Master's Thesis, University of Johannesburg.

Van Niekerk, D., Pugmire, R. J., Solumn, M. S., and Mathews, J. P. 2008. Structural Characterisation of Vitrinite Rich Permian-Aged South African Bituminous Coals. International Journal of Coal Geology, 76, 290-300.

Visser, J. N. J., Lock, J. C., and Collison, W. P., 1978. Subaqueous Outwash Fan and Esker Sandstones in the Permo-Carboniferous Dwyka Formation of South Africa. Journal of Sedimentological Petrology 57 (3), 467-478.

Visser, J. N. J., and Kingsley, C. S., 1982. Upper Carboniferous Glacial Valley Sedimentation in the Karoo Basin, Orange Free State Transvaal Geological Society of South Africa 85, 71-79.

Visser, D. G. L., 1989. The Geology of the Republic of South Africa, Transkei, Bophuthatswana, Venda and the Kingdomship of the Lesotho and Swaziland. Department of Mineral and Energy Affairs, Government Printers, Pretoria 494pp.

Wagner, N. J., and Hlatswayo, B. 2005. The Occurrence of potentially Hazardous Trace Elements in the Five Highveld Coals, South Africa. International Journal of Coal Geology, 63, pp. 228-246.

Wheeler, A. T., 2015. Palaeoenvironmental and Palaeclimatic Reconstruction of the Witbank Coal Deposits (Karoo Basin, South Africa). Unpublished Master's Thesis. University of Pretoria.

William, I., and Tailakov, O. V., (Undated). CH4 Emissions: Coal Mining and Handling. Good Practice Guidance and Uncertainity Management in National Greenhouse Gas Inventories, Energy Sector Journal, pp. 129-144.

Williamson, I. T., 1996. The Geology of the Area around Mmamabula and Dibete: Including an Account of the Greater Mmamabula Coalfield District. Memoir Geological Survey of Botswana 6, 239pp.

WHO, 2004. The World Health Report 2003- Shaping the Future. World Health Organisation. Geneva. Accessed online http://www.who.int/whr/2003/en/index.html.

XMP Consulting CC, 2014, South African Coal, Desktop Study. www.xmpconsulting.com/documents/sa%20desktop%20study.

Yao, Y., Lui, D., and Huang, W., 2011. Influence of Sills on Coal Rank, Coal Quality and Adsorption Capacity in Hongyound, Handan and Huaibei Coalfields, North China, International Journal of Coal Geology, 88 (2-3), pp.135-146.

South African Gas Emissions (www.google.co.za/gasemissions/s.a), Accessed from the Internet on the 28 July 2018.

Coal Mining in the Vhembe District (www.Eskom.co.za/coalmining2010), Accessed from the Internet on the 02 February 2016.

http://www.fossilenergy.gov/education/energy lessons/coal/coal-cct$_3$html. Accessed from the Internet on the 19 of September 2016.